TREATMENT OF CUTTING OILY WASTEWATER BY ELECTROCOAGULATION/ FLOTATION (ECF): REACTOR CONFIGURATIONS AND OIL CONCENTRATION

Miss Jittrapa Mongkolnauwarat

A Thesis Submitted in Partial Fulfillment of the Requirements
for the Degree of Master of Science Program in Environmental Management
(Interdisciplinary Program)
Graduate School
Chulalongkorn University
Academic Year 2014

การบำบัดน้ำเสียปนเปื้อนน้ำมันตัดด้วยกระบวนการรวมตะกอนด้วยไฟฟ้า : ลักษณะถังปฏิกรณ์ และ ความเข้มข้นน้ำมัน

นางสาวจิตราภา มงคลเนาวรัตน์

วิทยานิพนธ์นี้เป็นส่วนหนึ่งของการศึกษาตามหลักสูตรปริญญาวิทยาศาสตรมหาบัณฑิต
สาขาวิชาการจัดการสิ่งแวดล้อม (สหสาขาวิชา)
บัณฑิตวิทยาลัย จุฬาลงกรณ์มหาวิทยาลัย
ปีการศึกษา 2557

Thesis Title	TREATMENT OF CUTTING OILY WASTEWATER BY ELECTROCOAGULATION/ FLOTATION (ECF):REACTOR CONFIGURATIONS AND OIL CONCENTRATION
By	Miss Jittrapa Mongkolnauwarat
Field of Study	Environmental Management
Thesis Advisor	Associate ProfessorPisut Painmanakul, Ph.D.

Accepted by the Graduate School, Chulalongkorn University in Partial Fulfillment of the Requirements for the Master's Degree

.....Dean of the Graduate School
(Associate ProfessorSunait Chutintaranond)

THESIS COMMITTEE

.....Chairman
(Assistant ProfessorChantra Tongcumpou)

.....Thesis Advisor
(Associate ProfessorPisut Painmanakul, Ph.D.)

.....Examiner
(Dr.On-anong Larpparisudthi)

.....Examiner
(Dr.Seelawut Damrongsiri)

.....External Examiner
(Dr.Srayut Rachu)

จิตราภา มงคลเนาวรัตน์ : การบำบัดน้ำเสียปนเปื้อนน้ำมันตัดด้วยกระบวนการรวมตะกอนด้วยไฟฟ้า : ลักษณะถังปฏิกรณ์ และ ความเข้มข้นน้ำมัน (TREATMENT OF CUTTING OILY WASTEWATER BY ELECTROCOAGULATION/ FLOTATION (ECF):REACTOR CONFIGURATIONS AND OIL CONCENTRATION) อ.ที่ปรึกษาวิทยานิพนธ์หลัก: รศ. ดร.พิสุทธิ์ เพียรมนกุล{, 144 หน้า.

วัตถุประสงค์ของงานวิจัยนี้คือการแยกและบำบัดน้ำเสียปนเปื้อนน้ำมันตัดที่มีความคงตัวสูงด้วยกระบวนการรวมตะกอนและลอยตัวด้วยไฟฟ้าโดยใช้ขั้วอลูมิเนียม ปัจจัยที่ทำการศึกษา ได้แก่ ความหนาแน่นของกระแสไฟฟ้า ระยะห่างระหว่างขั้วไฟฟ้า ความเข้มข้นของน้ำมัน (0.5 1.0 และ 1.5 กรัมต่อลิตร) และรูปแบบถังปฏิกิริยาที่เหมาะสม ถังปฏิกิริยาที่ใช้ในงานวิจัยนี้ คือ ถังปฏิกิริยาแบบคอลัมน์ฟองอากาศ และถังปฏิกิริยาแบบอากาศยกที่มีการไหลเวียนภายนอกที่มีลักษณะส่วนไหลเวียนภายนอก (Downcomer) ที่แตกต่างกัน โดยการทดลองจะเดินระบบแบบกะและนำสภาวะการเดินระบบที่เหมาะสมไปทดสอบในการเดินระบบแบบต่อเนื่อง

จากการทดลองพบว่า กระบวนการรวมตะกอนและลอยตัวด้วยไฟฟ้าสามารถบำบัดน้ำเสียปนเปื้อนน้ำมันตัดได้ประสิทธิภาพสูงถึงร้อยละ 99 โดยมีสภาวะการเดินระบบที่เหมาะสม คือ ระยะห่างระหว่างขั้ว 2.5 เซนติเมตร และความหนาแน่นของกระแสไฟฟ้า 100 แอมแปร์ต่อตารางเมตร ส่วนความเข้มข้นของน้ำมันจะส่งผลต่อระยะเวลาที่เหมาะสมในการบำบัดเนื่องจากความต้องการปริมาณอลูมิเนียมอิออนที่ปล่อยออกจากขั้วไฟฟ้าที่แตกต่างกัน กล่าวคือ น้ำมันที่มีความเข้มข้น 0.5 1.0 และ 2.0 กรัมต่อลิตร จะต้องใช้เวลาในการบำบัด 60 90 และ 120 นาที ตามลำดับ การทดลองในถังปฏิกิริยาทั้ง 2 ชนิดจะได้ประสิทธิภาพการบำบัดเท่ากัน แต่ถังปฏิกิริยาแบบอากาศยกจะสามารถลดปริมาณตะกอนน้ำมันที่เกิดขึ้นที่ผิวน้ำได้ โดยรูปแบบของส่วนไหลเวียนภายนอกที่เหมาะสมจะเป็นท่อลักษณะยกขึ้น 135 องศาตามแนวดิ่ง ขนาดเส้นผ่านศูนย์กลาง 5.1 เซนติเมตร และความสูง 100 เซนติเมตร และเมื่อวิเคราะห์ความสัมพันธ์ระหว่างตัวแปรการเดินระบบกับประสิทธิภาพการบำบัดด้วยวิธีการ ANOVA จะได้ตัวแปรที่มีความสำคัญ ได้แก่ ความหนาแน่นของกระแสไฟฟ้า และเวลาที่ใช้ในการบำบัด นอกจากนี้ เมื่อนำสภาวะที่เหมาะสมในถังปฏิกิริยาทั้ง 2 แบบมาเดินระบบแบบต่อเนื่องโดยใช้อัตราการไหลของน้ำเสีย 10 ลิตรต่อชั่วโมง พบว่า ประสิทธิภาพการบำบัดจะลดลงเล็กน้อยเนื่องจากมีน้ำเสียไหลเข้าสู่ระบบตลอดเวลา และเมื่อทำการวิเคราะห์รูปแบบการไหลด้วยการศึกษาการกระจายตัวของเวลากัก (Residence time distribution) จะพบว่าถังปฏิกิริยาทั้ง 2 แบบจะมีการไหลในส่วนใต้ขั้วไฟฟ้าเป็นแบบการไหลในท่อ (Plug flow) และเปลี่ยนเป็นแบบกวนผสมอย่างสมบูรณ์ (Completely mixed) เมื่อผ่านขั้วไฟฟ้า และยังพบส่วนที่ไม่มีการไหล (Dead zone) ในถังปฏิกิริยาแบบอากาศยกอีกด้วย รูปแบบการไหลดังกล่าวนี้น่าจะมีผลกระทบต่อประสิทธิภาพการบำบัดที่ได้จากการเดินระบบแบบต่อเนื่อง

สาขาวิชา การจัดการสิ่งแวดล้อม ลายมือชื่อนิสิต .....

ปีการศึกษา 2557 ลายมือชื่อ อ.ที่ปรึกษาหลัก .....

5687512320 : MAJOR ENVIRONMENTAL MANAGEMENT
KEYWORDS: CUTTING OIL WASTEWATER / ELECTROCOAGULATION/FLOTATION (ECF) / EXTERNAL-LOOP AIRLIFT REACTOR (ELALR) / TURBIDITY REMOVAL EFFICIENCY / PREDICTION MODEL / REACTOR CONFIGURATION

JITTRAPA MONGKOLNAUWARAT: TREATMENT OF CUTTING OILY WASTEWATER BY ELECTROCOAGULATION/ FLOTATION (ECF):REACTOR CONFIGURATIONS AND OIL CONCENTRATION. ADVISOR: ASSOC. PROF.PISUT PAINMANAKUL, Ph.D.{, 144 pp.

This work aims to study the treatment of the stable cutting oil emulsion by the eletrocoagulation/flotation process (ECF). Effects of current density, electrode gap, oil concentration, and reactor type on the treatment performance were determined. Three oil concentrations of 0.5, 1.0, and 1.5 g/l were used. The ECF was operated in the bubble column reactor (BCR) and the external loop airlift reactor (ELALR). Moreover, the configuration of the downcomer for the ELALR was also investigated. Finally, the ECF with the optimal configuration from the batch experiment was tested in the continuous operation.

It was found that the ECF can effectively treat the cutting oil emulsion with the highest efficiency higher of 99% in the batch operation. The electrode gap of 2.5 cm and the current density of 100 A/cm^2 were obtained as the appropriate configuration. The oil concentration can affect the reaction time as the highest efficiency can be achieved at 60, 90, and 120 minutes for 0.5, 1.0, and 1.5 g/l oil concentration, respectively. In addition, similar treatment efficiency can be attained from the operation in the ELALR but with less oil sludge production. The best downcomer in this work was the 135º tilt-up with 100 cm height and 5.1 inside diameter. The ANOVA analysis was also conducted in order to specify the important parameter on the process performance. The current density and the reaction time were found to be the parameter governing the treatment efficiency. Finally, the best configuration of the ECF in both BCR and ELALR were tested with the continuous operation. The efficiencies were slightly decreased in both cases as the wastewater was constantly fed into the reactor. The flow pattern in the reactors was also analyzed by the residence time distribution (RTD). The flow in the columns can be separated into 2 zones including (1) the plug flow zone under the electrodes and (2) the CSTR zone from the electrodes onwards. Furthermore, the dead zone was also observed in the ELALR. These flow patterns can affect the process performance and could be used for improving the overall treatment efficiency.

Field of Study: Environmental Management Student's Signature .....

Academic Year: 2014 Advisor's Signature .....

ACKNOWLEDGEMENTS

Firstly, I wish to thank my thesis advisor, Assoc. Prof. Pisut Painmanakul for his insight, patience and editing skills in helping me to conduct the experiments and write this thesis. Moreover, I would also like to thank Dr. Nattawin Chawaloesphonsiya for his helpful advice, comment, and guidance to solve problems during experiments.

Secondly, this thesis would not have been possible without the assistance of these two Ph.D. students: Miss Ploypailin Romphophak and Mr.Kritchart Wongwailikit. I am grateful for their guide knowledge and support the equipment for hours of residence time distribution lab. Moreover, I am appreciate for their proofing and editing content for this thesis. Thank you for your patience and support.

Finally, I am sincerely thankful to my family, friends, and laboratory colleagues for supporting and encouraging me during my study and laboratory works periods. I could encounter all problems with this supportive will.

CONTENTS

Page

Page

Page

Page

TABLE OF FIGURE

LIST OF TABLE

CHAPTER 1
INTRODUCTION

1.1 INTRODUCTION

Oily wastewater is one of the environmental emerging issues since there are many source of oil which comes from both domestic sector and industrial sector. The oily wastewater from domestic sector, typically, is generated from cooking and cleaning activities which could be mostly separated via oil and grease trap tank as well. Industrial sector, on the other hand, produced more toxic oily wastewater due to the chemical agent contaminated into wastewater steam line such as heavy metal (i.e. cadmium, copper, chromium, lead, mercury, nickel, silver, zinc). When oily wastewater was discharged improperly, the oil particle and other toxic substance would inhibit most of the activities in aquatic organism and later, the ecological failure would be seen (Abass O.Alade, 2011).

Metalworking activities are one of the oily wastewater sources from industrial sector that contained stabilized oil such as cutting oil, metal particle and other additive agent to form hazardous wastewater. Cutting oil is water soluble oil due to the addition of surfactant and other additives. Normally, the cutting oil concentration in metalworking is between 3- 10 % by weight (Dixit et al., 2012). During usage, the ability of being coolant and lubricant of cutting fluid was damaged by thermal deformation, thus oily wastewater presented as hazardous wastewater as well.

There are several methods in oily wastewater treatment process such as hydro-cyclone, air flotation, and membrane filtration. Coagulation/flocculation is one of the wastewater treatment processes that aim to remove suspended particle and decrease toxic level by dosing the coagulant such as alum and ferric chloride into wastewater. However, the effluent needs pH adjustment process for pH neutralization before discharge since the chemical reaction in this process acidified the effluent. Recently, the alternative coagulation technology had introduced the electrocoagulation (EC) to be another environmental friendly treatment process, since the neutralized reaction which maintain the pH and also deliver the coagulant on site to reduce chemical cost

and storage space. The sacrificial anode, usually iron and aluminum plate, generates metal ion and also micro-size hydrogen bubble to enhance mixing process. Finally, the floatable floc could remove most of the suspended particle and pollutant.

According to the reactor configuration, electrocoagulation, usually, was operated in conventional tank or bubble column. The micro-size bubble was generated by the cathode electrode to enhance floc to move upward and to form packed floatable floc which was easily disposed. The development of reactor configuration in order to recirculate coagulant is a new issue to increase treatment efficiency and also treatment capacity, so the external airlift reactor was proposed to be the alternative reactor for electrocoagulation which would fulfill this requirement. The research is objective to study the reactor configuration of external airlift reactor in order to develop the capacity of cutting oily wastewater treatment system by electrocoagulation.

1.2. HYPOTHESIS

1. Cutting oily wastewater could be effectively treated by electrocoagulation/ flotation process
2. Application of external loop airlift reactor could enhance the treatment efficiency and reduce the sludge production
3. Downcomer configuration in the airlift reactor could improve the treatment efficiency

1.3. OBJECTIVE

1. To investigate the treatment efficiency of cutting oily wastewater by electrocoagulation/flotation (ECF) and to determine the optimal operating condition;
2. To compare the treatment efficiency of electrocoagulation/flotation between in bubble column and in different configurations of external loop airlift reactor;
3. To determine the best downcomer configuration (diameter, height and configuration) for cutting-oily wastewater treated by electrocoagulation/ flotation in the external loop airlift reactor; and
4. To propose a mathematical model for the efficiency prediction

1.4. SCOPE OF STUDY

This research was conducted at the Department of Environmental Engineering, Faculty of Engineering, Chulalongkorn University. The following details can be summarized as followed:

1. The research was conducted by using concentrated cutting oil (Castrol cooled BI) mixed with tap water at concentration 0.5, 1, 1.5 g/l as synthetic oily wastewater. The oil concentration was selected from the average oil concentration of domestic wastewater.
2. The 14-cm diameter with 180-cm height cylindrical acrylic column was used in this research as the bubble column. Moreover, PVC pipes (1, 1.5, and 2 inches in diameter) were used as downcomer of external loop airlift reactor with 3 levels of the vertical incline: 45º, 90º, and 135º.
3. The height of downcomer was studied in 3-levels: 50, 75, and 100 cm measured by the center of top downcomer inlet to the center of bottom downcomer outlet.
4. The batch system is used to determine the optimal operating condition of cutting oily wastewater treated by electrocoagulation in bubble column. Then electrocoagulation in external airlift reactor and the continuous system (10 LPH) would be conducted with the optimal operating condition to verify the treatment efficiency.

1.5. EXPECTED OUTCOME

1. The optimal operating condition of electrocoagulation/flotation process in the bubble column
2. The best downcomer configuration for cutting oily wastewater treatment by the electrocoagulation/flotation in the external-loop airlift reactor
3. The mathematical model for the efficiency prediction with the considerable accuracy

CHAPTER 2
THEORETICAL BACKGROUND AND LITERATURE REVIEW

2.1. THEORETICAL BACKGROUND

2.1.1. Oily wastewater

Oil and water are immiscible; however, there are some forms of oil that presence in the water with physical and chemical properties enhances. Oil in water may make up of mineral, animal and vegetable. There are four forms of oil in water classified by physical form (Althers, 1998).

1. Free oil or floating oil or thin film.

Floating oil appears in rainbow-like reflection surface via naked eye. The oil droplet rises quickly to the water surface and agglomerate to form the thin film of oil. Though this type of oil is in a very low proportion comparing with the other oil in wastewater, the rapid expansion and contamination of thin film problem of the environmental issue. This oil prevents oxygen transfer between water and atmosphere.

2. Dispersed oil or non-stabilized oil

The dispersed oil in water turns water into semi-milky wastewater. The mechanical mixing generates unstable emulsion to combine oil and water together. After stop stirring, oil and water will take time to separate. The fine oil droplet in dispersed oil is stabilized by the electrical charges without surfactants. There is a possibility of oil agglomeration due to the stability of oil droplet and the degree of dispersion.

3. Emulsion or stabilized oil

The stabilized oil differs from non-stabilized oil because of the presence of surfactant at the interface zone between oil and water. Most of municipal wastewater contains stabilized oil from washing in the kitchen. The surfactants comprise of two components: hydrophobic and hydrophilic to provide high stability of oil droplet and presented as milky wastewater. This kind of oily wastewater need sophisticated treatment system to breakdown the oil's stability.

4. Dissolved oil

The dissolved oil is in transparent form, the invisible droplet; the oil detection cannot use physical method except smelling. The properties such as solubility, volatility, polarity and molecular weight are useful to determine wastewater as dissolved oily wastewater since most of dissolved oil has high solubility, high volatility, high polarity and low molecular weight.

Table 2.1 Means oil droplet size of wastewater (Coca et al., 2011)

Oily wastewater	Means droplet diameter, D_p (μm)
Primary dispersions	>50
Secondary dispersions	3-50
Mechanical emulsions	<3
Chemical emulsions	<2
Dissolved hydrocarbon	-

In order to find the appropriate treatment technology, the type of oil and the oil concentration is the most essential data. The design of wastewater treatment system needs type of oil to scope the treatment technology, and also needs oil concentration for design calculation. The table 2.2 shows source of oily wastewater and its oil concentration that use to estimate the oil concentration of oily wastewater.

Table 2.2 Source of oily effluents (Coca et al., 2011)

Industrial process	Oil concentration (mg/l)
Petroleum refining	200-4000
Metal processing and finishing	100-20000
Aluminum rolling	5000-50000
Copper wire drawing	1000-10000
Food processing (fish and seafood)	500-14000
Edible oil refining	4000-6000
Paint manufacturing	1000-2000
Cleaning bilge water from ships	30-2000
Car washing	50-2000
Aircraft maintenance	500-1500
Leather processing (tannery effluents)	200-40000
Wood scouring	1500-12500
Wood preservation	50-1500

2.1.2. Cutting oil

Cutting oil is one of the common cutting fluids in the metal work, for example, boring, drilling and grinding. Its functions are coolant, lubricant, shear strength reducing agent and flushing liquid to move metal chips away from cutting zone. Moreover, the corrosion protection of work surface and heat exchange capacity is another function that prolongs mechanical apparatus usage life and reduces thermal deformation from high-temperature cutting work as well. There are four types of cutting oil: straight oils, soluble oils, semi-synthetic fluid and synthetic fluid(Dixit et al., 2012).

1. Straight oils or neat oils are usually used in high concentration or undiluted form. It consists of mineral oil, petroleum and fat or esters. Moreover, Chlorine, Sulfur and Phosphorus are added as additive to improve the ability of high-pressure resistance. This kind of oil has high capacity in being lubricant, but very low performance in being coolant.
2. Soluble oils are oils in emulsion form since there are some emulsifiers adding into this aqueous solution. Usually, these soluble oils are used in low concentration (3-10%)(Dixit et al., 2012)mostly in metal work of industry processes. There are high coolant capacity and also lubricant properties too.
3. Semi-synthetic fluid or micro-emulsion are mixed solutions between synthetic oils and soluble oils which present main advantages of each oil, for instant, high corrosion resistance, contamination tolerance and heat transfer performance as well.
4. Synthetic fluids are oil-free solutions since they contain only alkaline organic-inorganic compound and corrosion inhibitor agent that have no petroleum or mineral oil. These oils are applicable in low concentration by mixing with water to make 3-10% aqueous solution. Its outstanding property is the best coolant in industrial practices.

Classification of cutting oils

Furthermore, criteria for selecting cutting oil fluid depend on the type of metal operation processes: process performance, cost performance, environmental performance and health hazard performance (Dixit et al., 2012).

1. Process performance: In industrial processing, heat transfer and lubrication are two main criteria to classify cutting oil since there are high pressure and temperature while cutting process. In addition, after cutting process, the specimen is needed to be flushed, so the fluid and metal chip should be easily removed from the metal surface with flushing water. Later, corrosive inhibition and fluid stability will be concerns because these will affect to the future when doing oil disposal.
2. Cost performance: Typically, soluble oils are the most cost effective cutting oils since they are the least expensive and can be used in most metal work as well.
3. Environmental performance: Since cutting oils are biodegradable oil and non-biodegradable oil, wastewater containing cutting oil is needed to do the pretreatment to secondary treatments before discharge. For biodegradable oils, mostly are vegetable base oil(Emel Kuram, 2013)
4. Health hazard performance: From Material safety data sheet (MSDS) of cutting oil, it may cause mucous membrane irritation when inhalation and skin irritation when contact with these oils directly. The level of health problem depends on the type of fluid and concentration while contacting time. Moreover, there is a study claimed that working with metalworking fluid may increase cancer possibility such as skin, bladder, rectum and pancreas(Emel Kuram, 2013). The cancer possibility depends on the component in the cutting oil. Fortunately, the ingredient of cutting oil had been changing to be more environmental friendly by adding natural agent to replace the synthetic compound.

However, before cutting oil disposal, there are several parameters that need to investigate, for instant, the concentration of soluble oil emulsion, pH and particulate matter like metal scarp. Moreover, the physical pretreatments are skimming of tramp

oil or particle separation by using hydro cyclone(Emel Kuram, 2013) which will be mention in the next topic.

2.1.3. Oily wastewater treatment process

Particle separation, mostly, use the difference of density between the continuous phase which is water and the dispersed phase which is colloidal particle. The upflow velocity is what the outcome of the separation process. The calculation of upflow velocity follows the Stoke's law as shown in Equation 2.1.

$$W = \frac{\Delta\rho * g * d_d^2}{18\mu_c} \qquad \text{(Eq 2. 1)}$$

Where; W: Upflow velocity of the particle (m/s)

$\Delta\rho$: Different density between the dispersed phase and the continuous phase (kg/m^3)

d_d : Diameter of dispersed phase (m)

μ_c : Viscosity of the continuous phase ($kg\ s\ m^{-2}$)

g : Gravitational acceleration (m/s^2)

Oil in wastewater can observe as same as small particle. The principle of Stoke's law leads to four treatment method to increase upflow velocity

1. Increasing the oil droplet's size
2. Increasing the different density between the dispersed phase and the continuous phase
3. Increasing the gravitation acceleration
4. Decreasing the viscosity of the continuous phase

These four principles lead to many treatment applications

1. Droplet's size ↑ : Coalesces
2. Difference of density ↑ : Dissolved air flotation (DAF), Induced air flotation (IAF)
3. Gravitational acceleration ↑ : Cyclone, gravity separator
4. Viscosity ↓ : Surfactant injection

The other process of physical treatment system is in the following list;

1. Thermal treatment: Thermal treatment system can treat oily wastewater by heating water temperature to 160 degree Celsius and settle down for 8 hours to break down emulsified oil.
2. Adsorption: Activated carbon is used to treat some type oily wastewater
3. Membrane filtration: membrane can separate dissolved oil in solution form and stabilized oil in emulsion form by microfiltration, by ultrafiltration, and by Nano filtration.

Oily wastewater treatment system

To separate oil from water, there are many factors that use as application criteria such as oil concentration, the presence of an emulsifier, the specific density of each substance, and the temperature of the influent. There are three main types of treatment processes: physical treatment, chemical treatment and biological treatment processes

1. Physical treatment systems

The oily wastewater treatment system using physical properties of oil has many applications such as coalesces, bubble column, DAF, IAF, and cyclone. Moreover, there are another application of physical treatment processes such as thermal treatment and microwave irradiation.

The principles of treatment systems using Stoke's law shows at the following application;

- Coalescing treatment: The objective of coalescing process is to increase the size of oil droplet that affect to upflow velocity and consequence to higher removal efficiency. There are many application equipment that use coalescing methods such as API, CPI or TPI, DAF and IAF.
- API and CPI (TPI): the coalescing process that use the collision of oil droplet to encourage the agglomeration of larger droplet. The equipment that use in the system is plate. The plates are packed and placed in the coalesce reactor as shown in Figure 2.1.

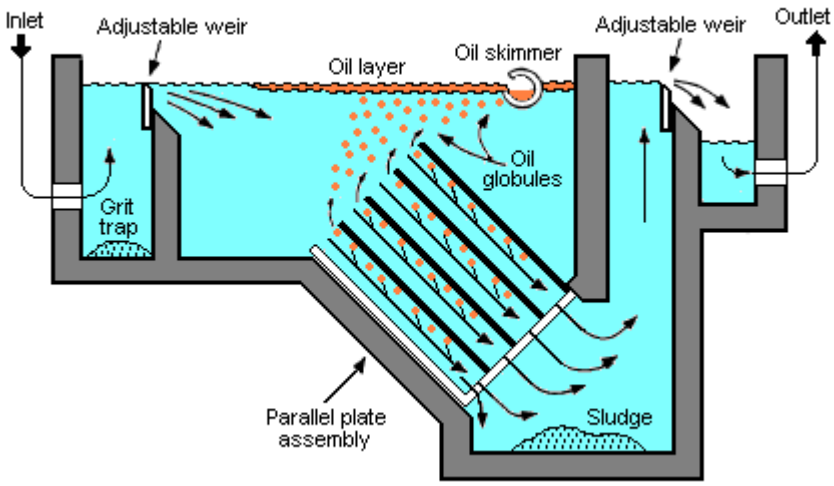

Figure 2.1 The water pathway in API unit ("oil/water separator," 2014)

- Density differentiation: The key factor of density differentiation is the buoyant force since the bubble attach the oil droplet and small suspended particle decrease the overall density of the combined particle (oil/particle with bubble). As a result of greater buoyant force to bring both bubble and particle to the water surface. Later, the floating sludge at the water surface can be removed by the skimming process. There are two interesting applications of this principle as shown below;
    - DAF: The pressurized water, water with air in supersaturated condition, mixing with wastewater at ambient atmosphere. The supersaturated water will release 30 – 120 micron bubble floating upward and collect particle to float to the water surface as scum. (R.Alther, 1997)
    - IAF: water and air are mixing by mechanical process to induce bubble formation in the liquid. Bubble are generated by high-speed rotation impellers, by diffuser, or by recycle of a slip
- Gravitational acceleration: To increase upflow velocity, increasing gravitational acceleration is one of the interesting processes. There are two effective devices that implement this principle to separate oil and water which is called hydrocyclone and centrifuge. The hydrocyclone is a small cylindrical cone device with one inlet and two outlets. The inlet is in the tangent line of hydrocyclone to produce circular motion when inject the influent to

hydrocyclone. Water and oil will separate in the hydrocyclone since the difference of weight in high gravitational acceleration condition; water is much heavier than oil. Then, the moving pathway of water will go downward to the bottom outlet. While, the oil phase flow upward to the top outlet

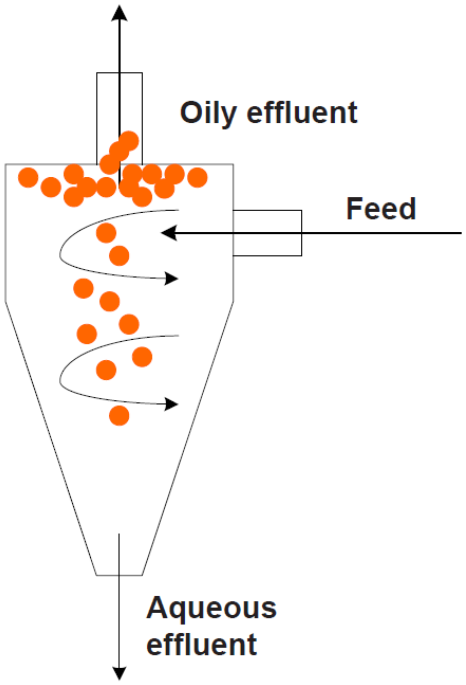

Figure 2.2 The schematic diagram of hydrocyclone (Coca et al., 2011)

Figure 2.3 The effluent at the top and bottom outlet ("Produced water treatment," 2014) (left) influent, (middle) oil from the top outlet , (right) effluent from the bottom outlet

2. Chemical treatment systems

Adding chemical substance to wastewater to remove pollutant in wastewater, especially oil droplet, aims to destabilize the oil droplet and reduce surface tension of the colloidal oil droplet. Most common chemical solutions adding to wastewater are aluminum sulfate or alum ($Al_2(SO_4)_3$), ferric chloride ($FeCl_3$), calcium chloride ($CaCl_2$) and aluminum chloride ($AlCl_3$). These chemical solutions are in coagulation and flocculation unit in the secondary wastewater treatment system section. The treatment efficiency, especially COD and turbidity removal, turn the treated water to be clear, odorless and colorless. However, the sludge generated from the unit needs to dispose of properly since the sludge is in hazardous waste category.

3. Biological treatment systems

Typically, biological treatment system is at the end of wastewater treatment system to ensure that the quality of the effluent is good enough for the environment. The limit of biological treatment system is that the high concentration of the pollutant may fail the whole system since microorganism in the system cannot live in such that high toxic condition. Oily wastewater treatment in the biological approach reveals that the soluble oil and low concentration emulsified oil are applicable to treat. While free oil and thin film are not applicable because of the enormous structure that takes very long time to degrade. Recently, experiment from China use conventional activated sludge with biofilter to treat oily wastewater from oil refinery plant. The dominant group of oil degrader microorganism are *Pseudomonas, Planococcus, Agrocuccus, and Acinetobacter* which degrade oil in water more than 64% with 18 hours detention time.(Kun Tong, 2013)

4. Electro-chemistry/ Electrostatic process

The electrostatic process is a recent alternative technology since people found that electrochemistry can do water purification and also water separation too. The reaction is as simple as the galvanic cell or electrolytic cell. There are three types of electrochemistry that use to treat oily wastewater

- Electrocoagulation (EC)

The electrocoagulation is new environmental friendly technology since there is no hazardous by-product generating in this process. Typically, the electrocoagulation

uses stainless steel, cast iron and aluminum as electrode to deliver aluminum ion and ferric ion while the other reaction generates hydrogen bubble to help particle and oil droplet to move upward. The metal ion reacts with water and turns into metal hydroxide that presented as coagulants. The metal hydroxide destabilizes the oil droplet stability to form floc and move upward due to buoyancy. The floatable sludge is dry and packed, so the sludge management is easy to operate.

- Electroflotation

The electroflotation, usually, uses graphite and titanium as electrode to produce ultrafine bubble. The gas bubble has both hydrogen bubble and oxygen bubble, because the anode produces oxygen bubble and cathode gives hydrogen bubble.

- Electro oxidation

This process uses electrostatic to generate oxidants such as hydrogen peroxide and ozone. The pollutant is rapid oxidized by those oxidants agent. The example of the electrooxidation is electro-Fenton which is the reaction between iron and hydrogen peroxide to generate hydroxyl radicle, the second strongest oxidant, to oxidize pollutant in wastewater. This process can be called mineralization process too.

Table 2.3 Oily wastewater treatment process

Process	advantage	disadvantage
Physical treatment system: Stake's law implementation (droplet size ↑) 1. API, CPI/TPI	• Treat free oil in water effectively • Simple to operate and maintenance	• Spend large area for a single unit • Cannot be expand the unit • Cannot treat dissolve oil and oil in emulsion form
Physical treatment system: Stake's law implementation (Difference of density ↑) 2. DAF	• High removal efficiency • Short detention time • Can treat high oil concentration wastewater	• Consume high energy to pressurized water • The recycled water is limited because of the increasing of TDS in the water

Process	advantage	disadvantage
3. IAF	• Less maintenance cost • Simple to operate • High recycle rate (60%)	
Physical treatment system: Stake's law implementation (Gravity↑) 4. Cyclone	• Use less space • High treatment efficiency	• Cannot treat wastewater with dissolve or oil in water in emulsion form
Physical treatment system: Thermal treatment 5. Heating	• Mineralization the pollutant	• Not cost-effective to operate • The air pollution is needed to concern
Physical treatment system: Adsorption 6. Carbon adsorption	• Can treat all oily wastewater	• Cannot treat high oil concentration wastewater • Not applicable for a large-scale operation
Physical treatment system: Membrane filtration 7. Microfiltration (MF) 8. Ultrafiltration (UF) 9. Nano filtration 10. Reverse osmosis (RO)	• Can treat all oily wastewater • High treatment efficiency	• Need high pressure • The decrease of treated water over time • Membrane fouling due to surfactant • Oil may adsorb on the pore wall • Gel layer formation on the membrane to

Process	advantage	disadvantage
		decrease filtration rate
Chemical treatment system	• Applicable for a large amount of wastewater with high suspended solid	• The sludge is need to manage properly • High cost for chemical reagent
Biological treatment system	• Environmental friendly process • Can treat biodegradable soluble oil	• Wastewater with high toxic may cause of system failure • Cannot treat high oil concentration wastewater
Electrochemistry	• Produce less sludge with no hazard • High treatment efficiency • Can treat all kind of oily wastewater	• Need to replace new electrode regularly due to electrode corrosion • In the case of high oil concentration, the treatment efficiency may decrease

2.1.4. Coagulation/flocculation

Coagulation

The coagulation starts when adding the coagulant into the water. The coagulant, usually has a positive charge, attract the colloidal particle due to the difference of charge. The significant notification of coagulation is the precipitation of insoluble hydroxide forms ($Al(OH)_3$ or $Fe(OH)_3$) Later, the flocculation start since the destabilized particle move together to form floc. Finally, the particle is removed from the water in the form of sludge.

There are five types of mechanism in the coagulation process:

1. Adsorption and charge neutralization

Charge neutralization occurs when different charge combines together and leads to net zero particles. Usually, the colloidal particle has a negative charge, and the adding coagulant is a positive charge. The charge neutralization encourages floc settle down via gravitation. This mechanism, itself, is a sophisticated method since the optimum range of charge neutralization is very short region. The coagulation is not present, unless the appropriated amount of coagulant is added; however, the excessed coagulation will turn the neutralized adsorbing particle to positive charge floc, and later the floc will expel each other. This expelled floc phenomenon is called charge reversal.

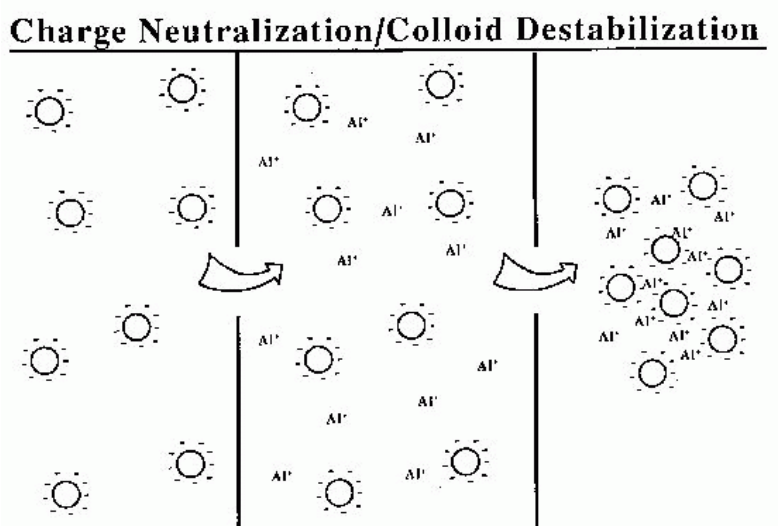

Figure 2.4 The schematic diagram of charge neutralization ("Tramfloc, inc," 2014)

2. Sweeping coagulation

In the case of very high concentration of coagulant in order to produce a saturated coagulant solution, the form of crystalline coagulant occurs. This crystal form consists of aluminum hydroxide form which takes the particle into cluster of particle and crystal. The cluster will settle down by gravity as same as the adsorption and charge neutralization process.

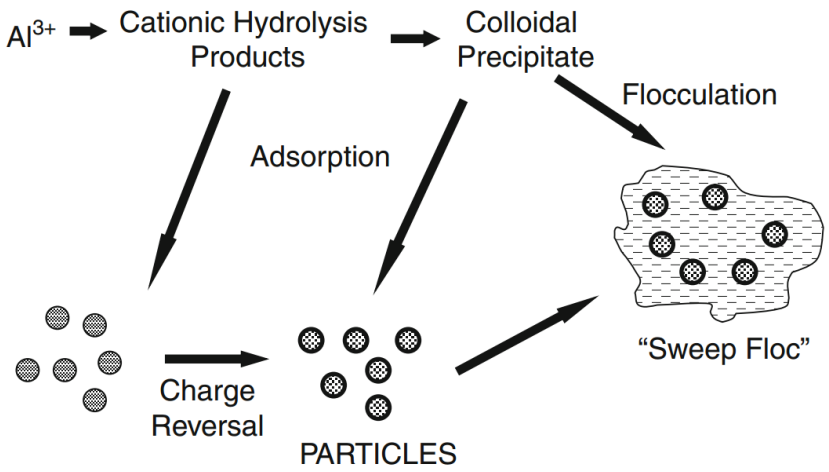

Figure 2.5 The sweeping coagulation-flocculation diagram ("Flocculation Fundamentals," 2013)

3. Combination coagulation

The combination mechanism is the condition that sweeping coagulation and charge neutralization mechanism occur at the same time. This phenomenon is the transition zone between charge neutralization and sweeping coagulation. The combination coagulation occurs when the amount of coagulant adding into the water is higher than the charge neutralization region but lower than sweeping coagulation region.

4. Diffuse layer

The zeta potential depletion of the outer side of colloidal particle occurs when continuously adding the coagulant

5. Polymer bridging

When adding polymer or coagulant aid compound, the branch of the polymer chain entrap the particle and later form floc.

Coagulation reaction

There are two common reactions of the coagulation process: the aluminum reaction and iron reaction.

Aluminum reaction: Alum

Alum: $Al_2(SO_4)_3$

$$Al_2(SO_4)_3 \rightarrow 2Al^{3+} + 3SO_4^{2-} \qquad \text{(Eq 2.2)}$$

After aluminum sulfate dissolution by hydrolysis the Al^{3+} and aluminum ligands formation process in the water, especially complex substance between aluminum and hydroxide ion as follow;

$$Al^{3+} + H_2O \rightarrow Al(OH)^{3+} + H^+ \quad \text{(Eq 2.3)}$$

$$Al^{3+} + 2H_2O \rightarrow Al(OH)_2^+ + 2H^+ \quad \text{(Eq 2.4)}$$

$$7Al^{3+} + 17H_2O \rightarrow Al_7(OH)_{17}^{4+} + 17H^+ \quad \text{(Eq 2.5)}$$

When the alum concentration is above saturation point, the hydrolysis process continues to the final product which is aluminum hydroxide crystalline. The reaction is expressed as follow;

$$Al^{3+} + 3H_2O \rightarrow Al(OH)_3 + 3H^+ \quad \text{(Eq 2.6)}$$

Iron reaction: Ferric chloride

Ferric chloride: $FeCl_3 \cdot 6H_2O$

$$FeCl_3 \rightarrow Fe^{3+} + 3Cl^- \quad \text{(Eq 2.7)}$$

After ferric chloride dissolve in the water, the ferric hydroxide is formed as the reaction as follow;

$$2FeCl_3 + 2H_2O \rightarrow 2Fe(OH)_{3\,(s)} + HCl \quad \text{(Eq 2.8)}$$

The difference between alum and ferric chloride is the treatment efficiency in water with hardness and color. Alum might not be effective when compare with ferric chloride.

Coagulants or flocculants

Coagulant is a chemical substance with charge after dissolution. The common coagulant in particle removal is alum or aluminum sulfate ($Al_2(SO_4)_3$). The classification of coagulant categorizes by the composition of the substance

1. Metal salt:
    a. Aluminum salt such as aluminum sulfate (alum) and aluminum chloride
    b. Iron salt such as ferric sulfate($Fe_2(SO_4)_3$) and ferrous sulfate ($Fe_2(SO_4)_3 \cdot 7H_2O$

The most important coagulants in this type are listed as follow(M.Armenante, 2014):

- $Al_2(SO_4)_3 \cdot 14H_2O$

- $Al_2(SO_4)_3 \cdot 18H_2O$ (Alum)
- $FeCl_3$
- $FeCl_3$ with lime
- $FeSO_4 \cdot 7H_2O$ (copperas) (with lime)

The guideline for adding metal salt coagulant is shown in the table as follow;

Table 2.4 The criterion of metal salt coagulant adding in different water properties (M.Armenante, 2014) :

Colloid concentration	Alkalinity level	Destabilization mechanism	Coagulant addition response
High	Low	Charge neutralization	Simple coagulation
High	High	Charge neutralization	High dose usage in case of no pretreatment to decrease alkalinity
Low	Low	Sweeping floc	Simple coagulation with high dose usage
Low	High	Ineffective	Need another type of coagulant

2. Polymer (Coagulant aid)

The polymer consists of the monomers bonding together to form a chain, for example, acrylamide, the synthetic polymer that use to classify the coagulant aid type. The advantage of polymer is that the small amount of dosage using in the coagulation. There are three types of polymer classified by charge

a. Cationic polymers: polydialydimethyl ammonium (PDADMA, cat-floc)
b. Anionic polymers: polyacrylamide acid (PAA), hydrolyzed polyacrylamide (HPAM) and the polystyrene sulfate (PSS)
c. Non-ionic polymers: cellulose, gelatin and starch (natural non-ionic polymer)

3. Lime

Lime is a common name refer to compound between calcium and oxygen such as $Ca(OH)_2$ or CaO (quicklime). Typically, magnesium is often found in lime. Lime reacts with bicarbonate, the water buffer, to generate calcium carbonate that precipitate and form of floc. The floc can trap the particle and settle down that is called sweeping floc as well.

Flocculation

Flocculation refers to the conglomeration of destabilized particle that removed from wastewater. The flocculation process depends on the frequency of the floc collision to form larger floc, and later settle down by the gravity. The frequency of collision is reverse proportion to shear rate. The floc can form large floc when low shear rate. On the other hand, the floc will break up when the intensity of shear rate is too high.

Jar test

Jar test is the experimental method in laboratory to investigate the appropriate amount of coagulant dosage for each water. The objective of Jar Test are finding the appropriated treatment condition to reach the optimum in treatment cost and treated quality. The main apparatus using in Jar test is Jar test stirrer, and the parameters in Jar test are listed as follow;

1. Coagulant selection
2. Dosage selection
3. Coagulant aid type and dosage selection
4. The optimum initial pH

The coagulation in Jar test takes only a few minute for rapid mixing (100-300 rpm), while flocculation takes much longer detention time, approximately 15-30 minute, for slow mixing (30-60 rpm). Later, the settlement period takes about 15-30 minute to allow large floc to settle at the bottom of beaker. Then, measure the treated water as effluent to calculate the removal efficiency. The considered parameters are COD, turbidity, pH and hardness.

Table 2.5 Advantage and disadvantage of chemical coagulation

Advantage	Disadvantage
• Conventional coagulation is simple to process • High efficiency of turbidity removal	• For some coagulant, the final pH is higher than the effluent standard, so the pH adjustment needs to consider • Cannot treat very low turbidity wastewater, another treatment process is needed

2.1.5. Electrocoagulation

The electro-coagulation is new environmental friendly technology since there is no hazardous by-product generating in this process. Typically, the electrocoagulation uses stainless steel, cast iron and aluminum as electrode to deliver aluminum ion and ferric ion while the other reaction generates hydrogen bubble to help particle and oil droplet to move upward. The metal ion reacts with water and turns into metal hydroxide that presented as coagulants. The metal hydroxide destabilizes the oil droplet stability to form floc and move upward due to buoyancy. The floatable sludge is dry and packed, so the sludge management is easy to operate (Holt et al.,2005).

The electrocoagulation process consists of two parts: anode and cathode sides. According to the difference of electrode, the reaction occurring at the electrodes differ from each other. Most of electrocoagulation process used aluminum and iron as electrode the half-reaction can be express as shown below;

Anode electrode

The anode side, also known as “sacrificial electrode”, release metal ion and electron to wastewater which cause electrode erosion. The chemical expression is shown as follow;

Aluminum as electrode:

$$Al \rightarrow Al^{3+} + 3e^{-} \qquad \text{(Eq 2.9)}$$

After the metal ion dissolving in the solution, the formation of coagulant depends on the pH of wastewater

Aluminum hydroxide formation in alkaline wastewater

$$Al^{3+} + 3OH^{3-} \rightarrow Al(OH)_3 \qquad \text{(Eq 2.10)}$$

Aluminum hydroxide formation in acidic wastewater

$$Al^{3+} + 3H_2O \rightarrow Al(OH)_3 + 3H^{+} \qquad \text{(Eq 2.11)}$$

In addition, Anode can also produce ultrafine oxygen bubble as by product. The oxygen bubble helps floc to float upward to the water surface. The reaction expresses as follow;

$$2H_2O \rightarrow O_2 + 4H^+ + 3e^- \qquad \text{(Eq 2.12)}$$

Cathode electrode

The cathode electrode generates large amount of hydrogen in micro-bubble size. The reaction is the same in every condition of wastewater. The reaction expresses as follow;

$$2H_2O + 2e^- \rightarrow H_2 + 2OH^- \qquad \text{(Eq 2.13)}$$

Or sometimes hydrogen bubble can be generated from hydrogen ion in the water. The reaction expresses as follow;

$$2H^+ + 2e^- \rightarrow H_2 \qquad \text{(Eq 2.14)}$$

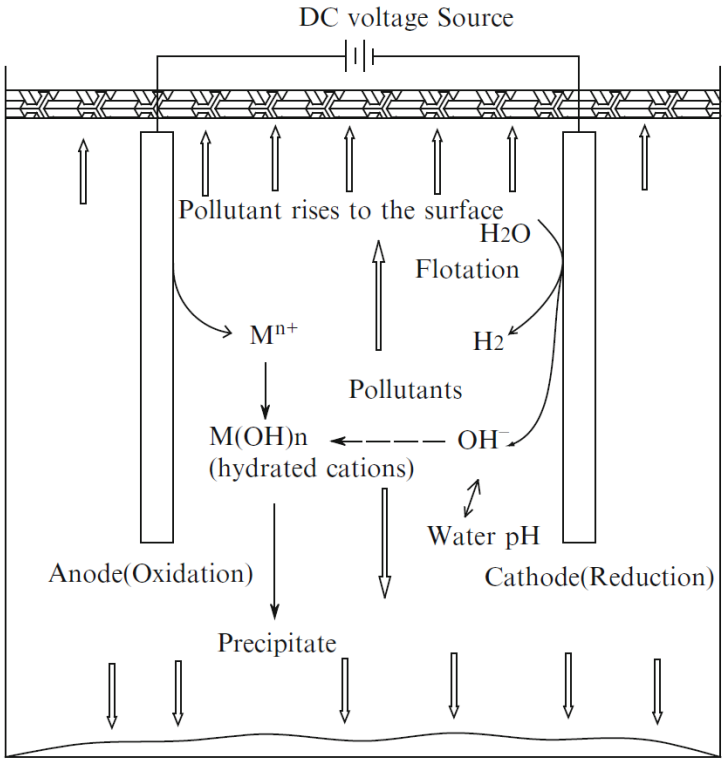

Figure 2.6 Schematic diagram of a two-electrode electrocoagulation cell (Huijuan Liu, 2010)

Factors affecting electrocoagulation

There are four main factors that provide great effect to electrocoagulation: current density, conductivity, temperature, and initial pH

1. Current density

Current density is the greatest factor that affect to coagulant dosage rate, bubble generation rate, solution mixing and mass transfer at the electrodes. The correlation between current density and the amount and dissolving metal can be explained by Faraday's law as shown below;

$$W = \frac{itM}{Nf} \quad \text{(Eq 2.15)}$$

Where W : The amount of metal dissolved in the solution (g of M cm^{-2})

i : Current density (A cm^{-2})

M : The relative molar mass of the electrode concerned (g/mol)

N : Number of electrons exchanged in the reaction (C/mol)

t : Detention time (s)

F : Faraday's constant (96,487 A*sec/C)

2. Conductivity

Conductivity is related to electrode passivation since low conductivity provides system with low treatment efficiency. Sodium chloride (NaCl) or salt is added to increase conductivity and also to inhibit Ca^{2+} and Mg^{2+} deposition and oxide layer formation due to the presence of CO_3^{2-} and SO_4^{2-}

3. Temperature

Water temperature also affects to treatment efficiency in electrocoagulation. The dissolution of aluminum electrode was founded that the current efficiency increased rapidly when water temperature is between 2– 30 degree Celsius. Increasing temperature helps treatment efficiency due to decreasing aluminum oxide layer.

However, the treatment efficiency will decrease when the temperature rise above 60 degrees Celsius.

4. pH

According to the mechanism of electrocoagulation, pH plays an important role for the floc formation in both aluminum and iron electrodes. In addition, the reaction of floc formation by hydrolysis and polymerization which form the complex polymer compound are in the chemical equations as follow;

$$Al^{3+} + H_2O \rightarrow Al(OH)^{2+} + H^+ \quad \text{(Eq 2.16)}$$

$$Al(OH)_2 + H_2O \rightarrow Al(OH)_2^+ + H^+ \quad \text{(Eq 2.17)}$$

$$Al(OH)_2^+ + H_2O \rightarrow Al(OH)_3 + H^+ \quad \text{(Eq 2.18)}$$

$$Al(OH)_3 + H_2O \rightarrow Al(OH)_4^- + H^+ \quad \text{(Eq 2.19)}$$

These chemical reactions occur in pH range 4 to 9 since pH above 9 $Al(OH)_4^-$ will be the predominant specie which drop the treatment efficiency rapidly. Moreover, in the acidic condition below, the predominant specie is Al^{3+} which has no effect to destabilize the pollutant in the water at all. The optimum treatment efficiency was $Al(OH)_3$ dominant regions which are pH range between 6 and 7, since Ca^{2+} and Mg^{2+} will be attached to the flocs $Al(OH)_3$.

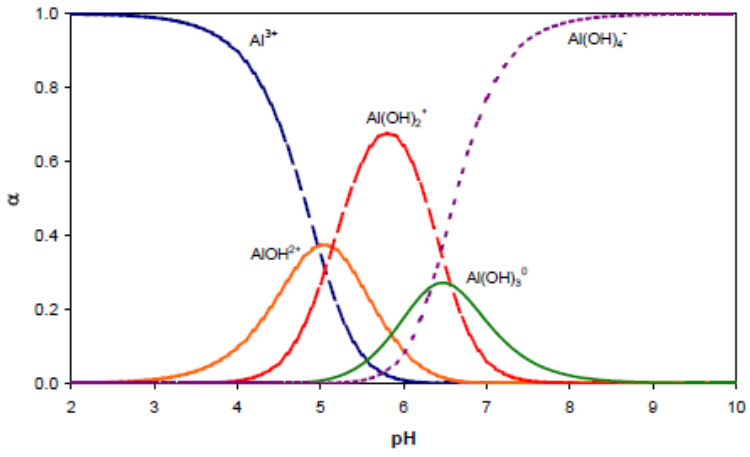

Figure 2.7 The distribution of aluminum species in Al-H_2O system (Marques, 2012)

Table 2.6 Advantage and disadvantage of electrocoagulation

Advantage	Disadvantage
• Electrocoagulation can treat even the smallest colloidal particle in wastewater because the reaction happens in the molecular level; therefore, the effluent is colorless, transparent and odorless • The electrocoagulation neutralizes the pH: no pH increase nor decrease significantly • Although, the amount of sludge produced by EC is much larger than chemical coagulation, the sludge quality is much better than the chemical coagulation since the sludge contains less water, more stable and more acid resistant • The Sludge generated by EC is settle able and easy to de-water • Electrocoagulation requires less maintenance cost than the other treatment process	• The oxide film coating at cathode provides the decreasing of treatment efficiency. • The operating cost was mainly for DC power supply • Some time, wastewater did not provide enough conductivity to support electrocoagulation, salt might be added to increase conductivity • In large scale electrocoagulation, hydrogen gas, the by- product of electrocoagulation, can be dangerous since hydrogen gas is fire hazard agent. • Water with low conductivity may need chemical addition in order to decrease power supply consumption

2.1.6. Airlift reactor(ALR)

Airlift reactor or ALR was firstly discovered by Lefrancois in 1955. This reactor consists of two main parts: riser and downcomer. Riser is the upward movement zone, while downcomer is a downward movement region to generate the recirculation system. The connecting part between riser and downcomer is called Gas-liquid separator. The circulation in airlift reactor occurred when riser had continuously received air bubble from the air sparger. The density differentiation between riser and downcomer space

induced circulation to take place. In comparison of bubble column, airlift reactors have higher mixing performance due to the effect of induced circulation as well. The advantage and disadvantage of external loop airlift are shown in the following table

Table 2.7 advantage and disadvantage of airlift reactor

Advantage	Disadvantage
• Simple in design and construction • No moving part that could minimize operating maintenance cost • High mixing performance : mass transfer, heat transfer • Low energy consumption • Can provide mild condition for bioreactor to get high yield of cell	• The circulation liquid was sudden decrease in viscous liquid • Too high circulation velocity cause dramatically decrease in mas transfer efficiency

2.1.1.1.Type of airlift reactor

Typically, there are 2 type of airlift reactor: internal-loop airlift reactor (ILALR) and external-loop airlift reactor (ELALR).Internal airlift reactor contains another cylindrical tube or plate separator in order to separate the column into two parts : riser and downcomer. While the external-loop airlift reactor exclude another column with connecting tube which is called gas-liquid separator as shown in the schematic flow diagram of airlift reactor in figure 2.8.

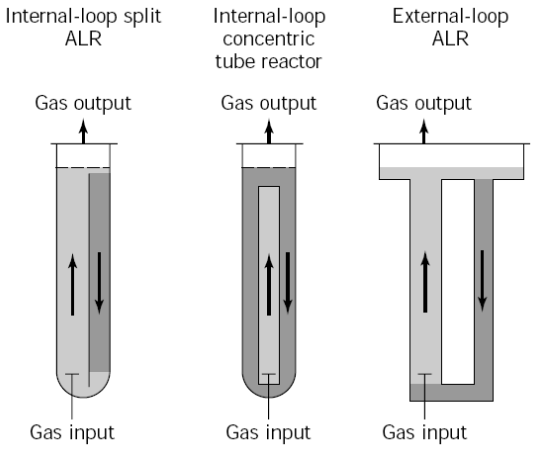

Figure 2.8 Type of airlift reactor

2.1.7. Factorial design

Factorial design was one of the experimental design which usually applied to observe the effluent of each factor in the experiment. In the other word, this method had been used for preliminary experiment that which factor would be higher weight than the others. In this thesis, three-level full factorial design was applied. The fundamental knowledge of this method would be provided as follow;

Three-level factorial design was written as 3^k factorial design. It meant that there were k factors with 3-level of each factor. Typically, three-level would be defined as low, intermediate and high which expressing as 0, 1 and 2. The objective of this experimental design was to construct the model of curvature in the response function.

The 3^2 design

This is the simplest three-level design. There were two factors which each at three levels. Therefore, 9 experiment or treatment combinations for this design were conducted. The notation of response for this design is shown in Figure 2.9 as follow;

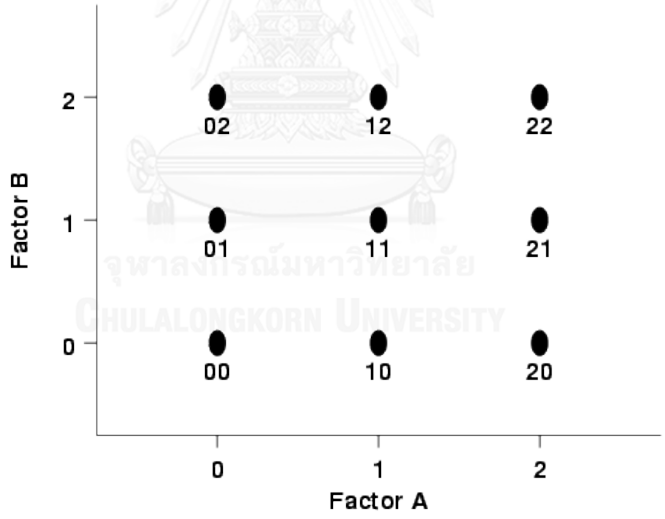

Figure 2.9 factorial design response

The 3^3 design

This is more complicated design experiment than 3^2 design since there were 3 factors with 3-level for each. The total experiments/treatments would be 3 x 3 x 3 = 27 combination experiments. The model for this type of design is shown in the following equation;

$$Y_{ijk} = \mu + A_i + B_j + AB_{ij} + C_k + AC_{ik} + BC_{jk} + ABC_{ijk} + \epsilon_{ijk} \quad \text{(Eq 2.20)}$$

2.1.8. Resident time distribution study

Typically, liquid flow in the reactor could be defined as an ideal flow which consists of two explicit forms: plug flow and completely mixed. Plug flow was a representative of well mixing which had the same concentration of substance in every sampling point. The plug flow, in contrast, showed no mixing condition in the reactor; neither diffusion nor back mixing were found in this flow pattern. In addition, the concentration of cross sectional area in plug flow system was the same. Actually, dead zone and short cut (bypassing) occurred during system operation see in Figure 2.10.

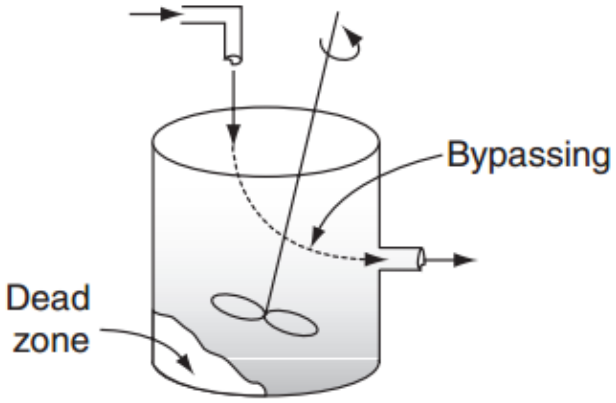

Figure 2.10 Schematic diagram of dead zone and short cut (bypassing) in the reactor

Residence time distribution curve of E-curve or E(t) was employed in Figure 2.10. The calculation of E(t) followed the Equation 2.21 ;

$$E(t) = \frac{C(t)}{\int_0^\infty C(t)dt} \qquad \text{(Eq 2.21)}$$

Where; E (t) = conductivity portion in specific duration t to t+dt

C (t) = conductivity (µS)

The function E(t) was applied to calculate the mean residence time or τ which show the average time that tracer (salt) had travelled in the reactor. Moreover the variance of the E(t) distribution are defined in Equation (2.22) as follow;

$$\sigma_t^2 = \frac{\int_0^\infty (t-\tau)^2 C(t)dt}{\int_0^\infty C(t)dt} = \frac{\int_0^\infty t^2 C(t)dt}{\int_0^\infty C(t)dt} - \tau^2 \qquad \text{(Eq 2.22)}$$

Data analysis

The flow analysis could be divided into two different model: Axial dispersion model and tank in series model

1. Axial dispersion model

Theoretically, the ideal flow states that the velocity of liquid in the single cross section appear to be the same because the elimination of friction loss in pipe. In contrast, flow velocity in practice was not constant due to driving force, back mixing and friction loss. In order to identify the flow pattern by this model, Peclect number (Pe) was employed to express the flow scheme. The E(t) function could be rearrange into Peclect term as shown in Equation 2.23;

$$E(t) = \sqrt{\frac{Pe}{4\pi\,\tau\,t}}\; e^{\frac{-(\tau-t)^2 Pe}{4\,\tau\,t}} \qquad \text{(Eq 2.23)}$$

Pe is the dimensionless parameter which express the ratio between convection flux and dispersed flux seeing in Equation 2.24. Less Peclect number means the actual flow is close to CSTR model, while high Pe number shows the plug flow effect in the actual flow.

$$Pe = \frac{uL}{D_z} = \frac{convective\ flux}{dispered\ flux} \qquad \text{(Eq 2.24)}$$

2. Tank in series model

Tank in series model is another flow pattern model that use to determine the number of equivalent CSTR tank that could provide the same flow pattern. The E(t) function was rearrange to include number of CSTR tank , N term as shown in Equation 2.25 as follow;

$$E(t) = (\frac{N}{\tau})^N \,.\frac{t^{N-1}}{(N-1)!}\,.e^{\frac{-Nt}{\tau}} \qquad \text{(Eq 2.25)}$$

2.2. LITERATURE REVIEW

2.2.1. Oily wastewater characterization

Physical properties of oily wastewater, mainly, are turbidity, oil droplet size, pH and viscosity. According to the limitation of some equipment such as turbidity meter, the indirect methods are required. The study of oil characterization was conducted by K.Bensadok in 2007 to measure turbidity and pH of two-different components cutting oily synthetic wastewater varying oil concentration from 2-10%: TASFALOUT 22B and MEDACOUPE 250. The result showed that oil concentration was a linear function to turbidity; however, each types of oil gave different turbidity function. Furthermore, the presence of surfactant affects the turbidity. The dilution curve, therefore, need to prepare. In addition, the oil droplet size was examine and was reported that the range of oil droplet in this experiment was lower than 0.1 micron as well. The initial pH of synthetic oily wastewater showed the increasing trend with higher oil concentration.

2.2.2. Oily wastewater treatment process

Oily wastewater present as environmental emerging issue. There are some types of oil that can be easily removed by skimming such as free oil which presence on the top of water surface. The stabilized oil such as cutting oil, on the other hand, required more complicated treatment process to remove oil droplet from the water system. The stabilized oily wastewater is one of the most complicated oily wastewater due to the presence of surfactant that stabilize oil droplet in the form of micelles (Yang, 2007) . The treatment by 1318 fold of gravitation force in centrifugation and electrofloatation can treat only 50% of the turbidity removal. The other treatment unit, thus, was required. K.Bensadok (2007) had studied about cutting oily wastewater treatment process by chemical coagulation combined with dissolved air flotation unit. As a result, chemical coagulation, itself, required very high coagulant dosage and 60-90 minute of operating time depend on oil concentration to achieve 99% turbidity removal. The residual turbidity, however, higher than the discharge regulation, so chemical coagulation cooperated with fine bubble from DAF was suggested to increase overall treatment efficiency with shorten detention time. This is the same idea as electrocoagulation which combines both coagulant dosage and micro-bubble

generation as well. The electrocoagulation for stabilized oily wastewater treatment was primarily studied in a bench scale to develop for the further scaling up in the future.

2.2.3. Oily wastewater treatment by electrocoagulation

There were many research papers interesting in oily wastewater treated by electrocoagulation. Many source of oily wastewater such as food manufacturing process, oil extraction process, automotive & metal working activities and domestic sewage were observed with the treatment efficiency mostly COD, turbidity ,and oil & grease level. The lab scale experiments were operated in order to study and investigate the correlation between treatment efficiency and other parameters. The influent parameters that affect to the treatment efficiency could be divided into 2 subcategories: physical factor and operating factors. Physical factors included electrode type, gap between electrode, and reactor configuration. While operating factors were oil concentration, current density, operating time, and initial pH of wastewater (Bensadok et al., 2008). The correlation between each parameter to treatment efficiency could be described as follow;

1. Oil concentration: the treatment efficiency of high oil concentration wastewater required longer operating time to achieve satisfied removal level. In order to shorten operating time, the higher current density, pH adjustment, and number of electrode were required.
2. Current density: usually the optimal operation current density is between100 - 200 A/m^2 depends upon the oil concentration and conductivity in wastewater.
3. Initial pH, usually, in neutral was preferred
4. Gap between electrode: typically, 1-2 cm is applicable without salt addition

2.2.4. Hydrodynamic study

There were many researchers studying the effect of hydrodynamic properties mainly the gas holdup parameter. In hydrodynamic behavior of the external-loop airlift system, the effect of airlift configuration to gas holdup can be described as follow;

1. Opened and closed downcomer have significant effect to the downcomer gas holdup. The downcomer gas holdup was twice when closed downcomer system

was applied comparing to the downcomer gas holdup in the opened downcomer system (Choi et al., 1996).

2. Higher of A_d/A_r reduces riser gas holdup and also the overall gas holdup
3. The length of the conduit between riser and downcomer affect the gas holdup since longer conduit did not encourage bubble to recirculate in the downcomer section. The overall gas holdup, thus, dramatically decreased.
4. The heights of external-loop airlift have direct influence on riser gas holdup. Seeing that the increasing height decrease the overall

2.2.5. Electrocoagulation in external-loop airlift reactor

There was a few research paper that applied electrocoagulation in the external-loop airlift reactor. The study that related to this topic recommended that there were some interesting aspects of the operating condition of electrocoagulation in this type of reactor such as the electrode position (Essadki et al., 2008). The position of electrode affect to the over treatment efficiency since the electrodes were the representative of the air diffuser equipment. The position, thus, effect the liquid movement in the reactor as well. According to the review, the correlation between operating parameter and the treatment efficiency were investigated as follow;

1. The liquid velocity was a function of hydrogen bubble generation rate which effected from the current applied. The liquid velocity should not be exceeding 9 cm/s since higher liquid velocity decrease flocculation mechanism. The treatment efficiency, therefore, decreased.
2. The effect of current density to treatment efficiency showed that more than 80% COD removal occurred in high current density (28.6-34.3 mA/cm^2). The optimal current, therefore, needed to be estimated.
3. The recirculation function of external-loop airlift reactor could prolong the electrode operating cycle and also reuse the coagulant

CHAPTER 3
RESEARCH METHODOLOGY

3.1 RESEARCH OVERVIEW

The purpose of this study was to investigate the treatment efficiency of Electrocoagulation/Floatation (ECF) for cutting oil wastewater. Both bubble column reactor (BCR) and External Loop Air Lift Reactor (ELALR) were studied to determine the best operating condition and configuration of ECF reactor. The oily wastewater was first characterize the properties, for instance, turbidity and subsequently examine feasibility of coagulation treatment process. After approved, ECF experiments in batch BCR were conducted to obtain the optimum operating condition (i.e. current density, electrode gap distance). The optimum condition for BCR were further used to determine the best configuration of ELALR and afterward developed from batch into continuous process.

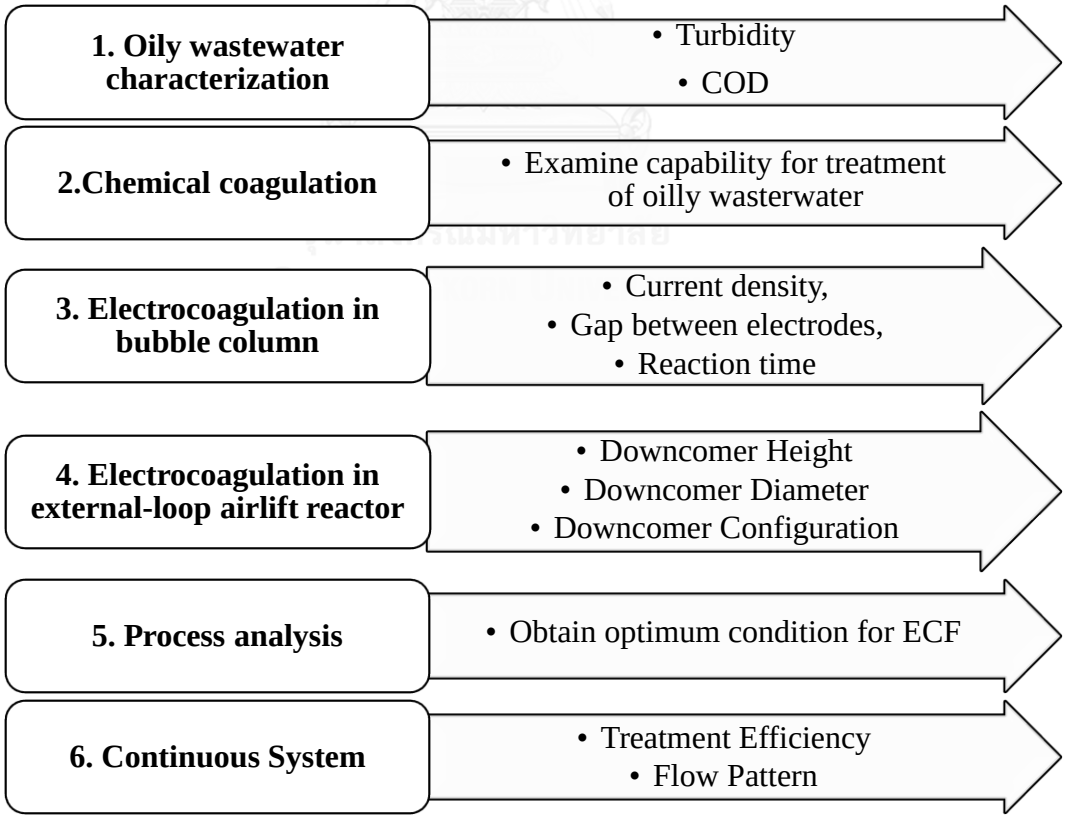

Figure 3.1 Experimental framework

3.2 EXPERIMENT SET UP

The schematic diagram of the electrocoagulation in the bubble column is shown in figure 3.2. In the figure, the 14-cm diameter column (A) was equipped with pair of aluminum electrodes (C) at 30-cm above from column bottom including with direct current power supply (D). For batch experiments, the column was filled with 25 liter of synthesis wastewater (mixture of tap water with cutting oil) by pumping from storage tank (E). The sampling point (B) was at 25-cm below the water surface which used to collect the sample to analyze the characteristics as a function of time. For continuous experiment, the reactor was remained all conditions from batch experiment expect for sampling point that converted to be reactor outlet.

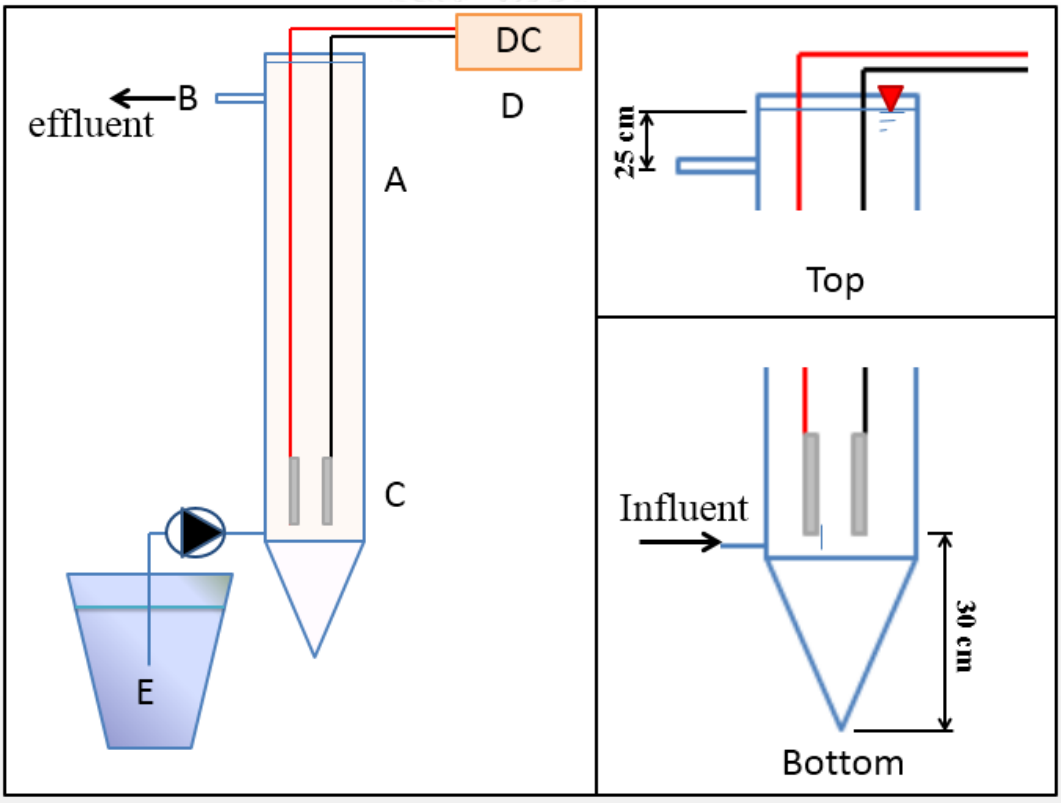

Figure 3.2 Experimental schematic diagram of electrocoagulation in bubble column

For airlift reactor experiment, variety configurations of external loop downcomer were added to bubble column. PVC pipes were applied as downcomer with variation of diameter among 1, 1.5 and 2 inch. Effect of downcomer length was studied at length of 50, 75 and 100 cm (illustrated configuration in figure 3.3). Moreover, the

connection angle between column and downcomer was also varied at 45, 90 and 135 degree as shown in figure 3.4.

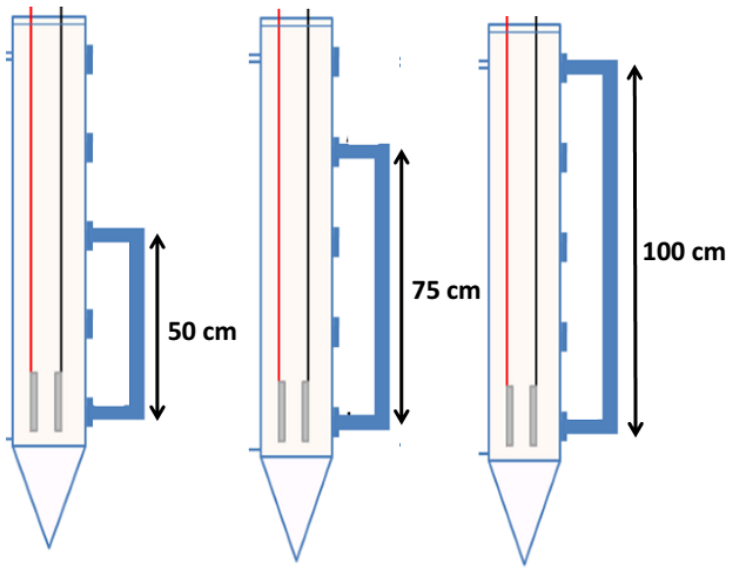

Figure 3.3 Downcomer length of external-loop reactor

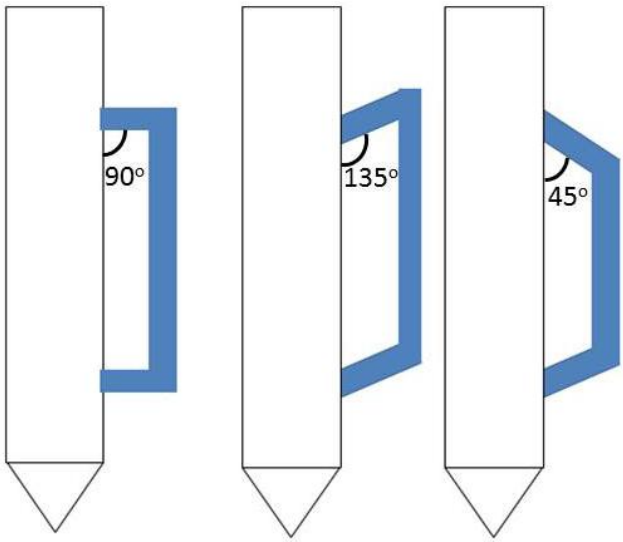

Figure 3.4 Connection angle between external loop downcomer and column

3.3 MATERIAL AND METHOD

3.3.1. Apparatus

1. Acrylic column with 14-cm inner diameter and 180-cm height. The connector hole is made up of PVC pipe fitting (1”, 1.5”) with 25-cm interval between holes.

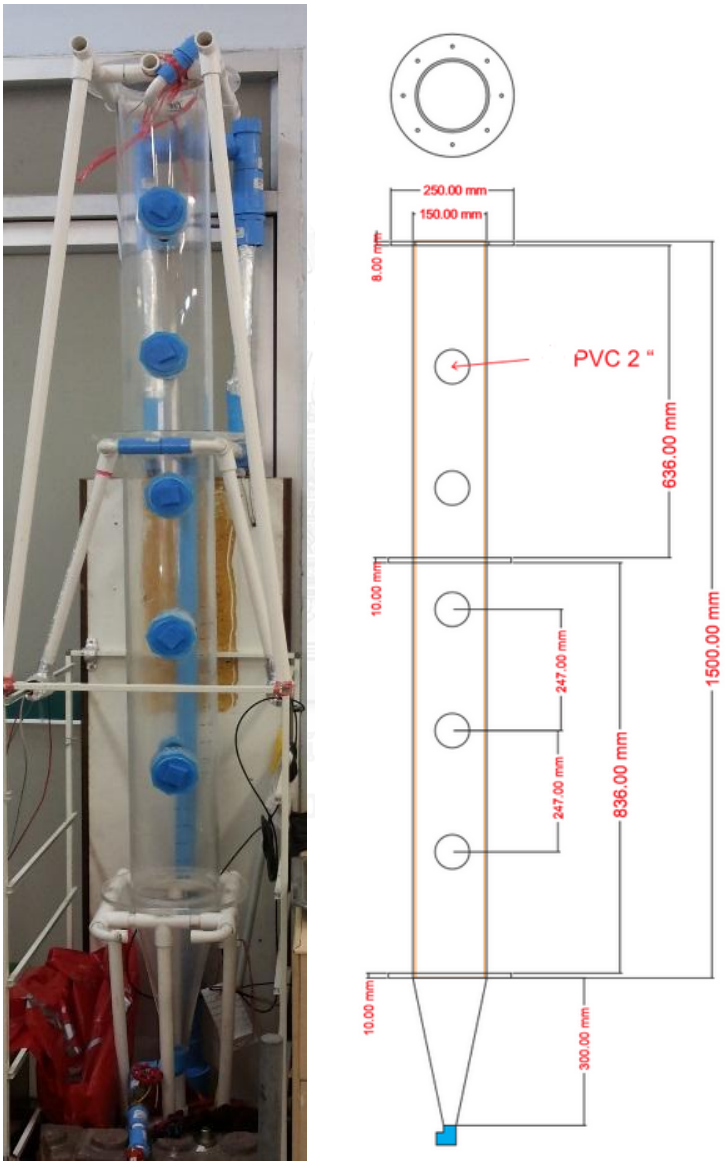

Figure 3.5 Reactor configuration of bubble column

2. External loop airlift set i.e. PVC pipe and joint for 1, 1.5 and 2 inch of diameter with 50, 75 and 100 cm of length and 45, 90 and 135 degree of joint connection.

3. Pairs of Aluminum electrode (50 x 200 x 2 mm)
4. Direct Current Power supply (60 V, 5 A)
5. Connection and electrode holding set
6. Submersed pump
7. Plastic tank 25 L

3.3.2 Analysis Equipment

1. pH meter
2. Turbidity meter (2100P Turbidimeter)
3. Microscope with camera
4. Stop watch
5. Digital Camera
6. Jar test set
7. Particle size analyzer
8. COD measurement set
   8.1. Test tube (16 x 150 mm) with Tetrafluoroethylene (TFE) cap
   8.2. Hot air oven 600 by Memment (150 ± 2 ºC)
   8.3. Volumetric flask size 100 and 1000 ml.
   8.4. Cylinder size 200, 500 and 1000 ml.
   8.5. Pipet Size 1, 5, 10 and 25 ml.

3.3.3. Reagents

1. Cutting oil; Castrol Cooledge ® BI
2. Deionized water (DI-water)
3. COD test chemical reagent :
   a. Potassium Dichromate , $K_2Cr_2O_7$
   b. Ferrous Ammonium Sulphate , $NH_4Fe(SO_4)_2 \cdot 12\ H_2O$ (FAS)
   c. Sulfuric Acid, H_2SO_4
   d. Silver sulfate, Ag_2SO_4
4. Coagulants : Alum, $Al_2(SO_4)_3.18H_2O$
5. RTD Tracer : Sodium chloride , NaCl

3.4 ANALYTICAL METHOD

3.4.1 Physical Parameters

3.4.1.1 Turbidity

Turbidity of wastewater was measured with turbidity meter. The meter used light absorbing and scattering of suspended particle to determine the turbidity in unit of NTU. In this research, the sampling was collected from reactor and measured turbidity with 2100P Turbidmeter (Hach). However, According to the model of turbidity meter, it was limited to detect the turbidity of sample only under 1000 NTU. Therefore, wastewater dilution was applied to measure the substances which turbidity was above 1000 NTU. The method of dilution and measurement was detailed in Appendix I

3.4.1.2 Oil Droplet size

As oil droplet was suspended particle in emulsion, the droplet size was observed in order to ensure the continuity size of oil droplet. Pictorial observation under microscope was conducted with color staining to separate oil and water with oil staining color.

3.4.1.3 Oil Droplet Size Distribution

Oil droplet size distribution was detected with particle size analyzer. It was more convenient comparing with measuring from microscope as it can determine the size range and average size of the particle.

3.4.1.4 pH

pH measurement was measured via pH meter that detect the electronic potential of aqueous solution comparing with reference electrode and sensing electrode. The difference electric potential between electrodes are referred to different amount of hydrogen ion (H^+) which can further calculate to pH.

3.4.1.5 Sludge Thickness

Sludge thickness was measuring with direct method. The ruler was applied to the column to determine length of the sludge generated at the liquid surface. The sludge thickness (h) could be used to analyze the volume of the sludge from equation 3.1 as following equation

$$\text{Volume of sludge} = \pi \times r^2 \times h \qquad \text{(Eq 3. 1)}$$

3.4.1.6 Conductivity

Conductivity is representative parameter dissolved ion in the liquid. In this experiment, conductivity measurement was used in residence time distribution studied in order to determine fluid flow pattern in reactor.

3.4.2 Chemical Properties

3.4.2.1 Chemical Oxygen Demand (COD)

COD is an explicit chemical parameter that can determine the treatment efficiency of each process. Potassium dichromate digestion or close reflux COD was employed to this experiment in order to evaluate the effluent property. The procedure of COD measurement was followed standard method 5520C which capable to detect COD in range of 40-400 mg O_2/l.

3.4.2.2 Aluminum Concentration

Atomic adsorption spectrophotometer (AAS) is used in total dissolved aluminum analysis. The sample was digested under acidic condition (nitric acid digestion) with heat following standard method of 3005A

3.4.3 Turbidity Removal Efficiency

The turbidity removal efficiency is used to determine the performance of reactor. It is calculated from difference between initial turbidity of wastewater in comparing with final turbidity divided by initial turbidity. The expression was shown in equation 3.2 as follow.

$$\text{Turbidity removal efficiency} = \frac{\text{initial turbidity-final turbidity}}{\text{initial turbidity}} \times 100 \quad \text{(Eq 3. 2)}$$

3.5 EXPERIMENT PROCEDURE

The experiment procedure was divided into 6 categories as outline in section 3.1 which could be detailed as follow.

3.5.1. Wastewater characterization

This part was aimed to study the physical and chemical properties of synthetic cutting-oily wastewater. The oil concentration of 0.5 – 1.5 g/L was prepared by mixing the tap water with cutting-oil and stirred with 125 rpm for 30 minute. Afterward, the synthetics were analyzed with instruments to obtain waste properties: turbidity, pH, COD and droplet diameter. These parameters, especially turbidity, were further used to calculate removal efficiency of ECF process.

3.5.2. Chemical coagulation

Jar test method was conducted to determine the optimal coagulant dosage as well as appropriate pH for chemical coagulation process. In order to compare with aluminum electrode of ECF, aluminum sulfate ($Al_2(SO_4)_3 \cdot 16H_2O$, AR Grade) was selected as a coagulant agent as it produced the same type of ion. The rapid mixing process took approximately 1 minute at 100 rpm and, then, converted to slow mixing at 30 rpm for 30 minute. After sedimentation time of 30 minute, the turbidity, COD, pH and oil droplet diameter were measured. Table 3.1 summarized all procedures mentioned above. Data and optimum condition from jar test could further used to determine the operating condition for ECF process.

Table 3.1 Parameter measurement for chemical coagulation process

Fixed variable	**Parameter**
Oil concentration	0.5 , 1.0 , 1.5 g/l
Wastewater volume	1 L
Coagulant	Aluminum sulfate
Independent variable	**Parameter**
Coagulant dose	40,80,120,160,200,240 mg/l
Dependent Variable	**Parameter**
Wastewater quality	Turbidity, COD, pH, oil droplet diameter, oil droplet size distribution,

3.5.3. Electrocoagulation system in bubble column

This experiment part was aimed to study effect of oil concentration, current density and electrode gap distance on turbidity removal efficiency as well as sludge thickness and subsequently determine optimum condition for batch bubble column reactor. Table 3.2 displays the significant variables; fixed, independent and dependent variables in the experiment.

Table 3.2 Parameter measurement for electrocoagulation in bubble column

Fixed variable	**Parameter**
Initial oil concentration	0.5 , 1.0 , 1.5 g/l
Wastewater volume	25 L
Independent variable	**Parameter**
Electrode gap	1.25 ,2.5 ,3.75 cm
Current density	75 , 100 , 125 A/m^2
Dependent Variable	**Parameter**
Wastewater quality	Turbidity, sludge thickness

Batch bubble column reactor was set up with 25 liter of oily wastewater inside. The initial oil concentration was varied between 0.5 to 1.5 g/L according to range of domestic wastewater (Giannis et al., 2007). Electric power supply was generated current density between 75-125 A/m^2 to electrode which varied the gap distance from 1.25 to 3.75 cm. After examined effect of all variables, the optimum condition was obtained and further utilized to study ECF in external loop airlift reactor (ELALR)

3.5.4. EC in the external airlift reactor: the effect of downcomer configuration

This experiment part was goaled to investigate the effect of downcomer in the external-loop airlift reactor. Eighty-one configurations of downcomer were test the treatment performance to obtain the optimum configuration for external loop airlift reactor. Diameter, length and connection angle of downcomer were studied as show parameter in table 3.3. The best configuration was determined from sludge quality and turbidity removal efficiency.

Table 3.3 Parameter measurement for downcomer configuration study

Fixed variable	**Parameter**
Oil concentration	0.5 , 1.0 , 1.5 g/l
Operating condition	Use the optimal condition from 3.1.3.
Independent variable	**Parameter**
Downcomer diameter	2.5 ,3.8, 5.1 cm
Downcomer Length	50,75,100 cm
Connector configuration	45 ^{o} ,90 ^{o} , 135^{o} degree
Dependent Variable	**Parameter**
Wastewater quality	Turbidity, sludge thickness

3.5.5. Process analysis

This session was aimed to analyze the treatment capacity of electrocoagulation/ flotation (ECF) of bubble column and external loop airlift reactor including with other issues which consisted of:

1. Treatment efficiency
2. Bubble generation from aluminum electrode
3. Power consumption
4. Sludge production at liquid surface
5. Flow behavior in reactor
6. Empirical prediction equation of ECF reactor

The outcome of this session was to identify the most appropriate configuration of ECF reactor as well as discussing the influences of each process variable on ECF process.

3.5.6. Electrocoagulation/Flotation in continuous process

This session aimed to evaluate the treatment efficiency of ECF process in continuous system. The experiments were conducted in both bubble column and the best external-loop airlift reactor. The reactor was operated at 10 liter per hour with measuring of turbidity removal against operating time. Moreover, residence time distribution (RTD) experiment was conducted in both type of reactor in order to study the flow pattern occurring in continuous reactor. The RTD was studied by feeding the tracer into operating reactor and measuring concentration of feeding tracer at inlet and outlet along the operating time, flow pattern occurring in reactor could be identified with RTD principle.

CHAPTER 4
RESULT AND DISCUSSION

This chapter presents the experimental results aiming to determine the treatment efficiency of the cutting oil wastewater by the electrocoagulation/flotation process. The list of the sections is shown below.

1. Emulsion characterization
2. Treatment of emulsion by chemical coagulation
3. Electrocoagulation/flotation in the bubble column
4. Electrocoagulation/flotation in the external loop airlift reactor
5. Process analysis
6. Electrocoagulation/flotation in continuous system

4.1 EMULSION CHARACTERIZATION

The objective of this section was to describe the physical appearance and chemical properties of the synthetic cutting-oily wastewater. 0.5,1.0 and 1.5 g of brownish cutting oil was mixed with 1 L of tap water under 125 rpm stirred for 30 minute to form 0.5,1.0 and 1.5 g/l of oil concentration respectively. Then, the milky solution appeared seeing in Figure 4.1. The main parameters of this synthetic wastewater are shown in Table 4.1.

Figure 4.1 Synthetic cutting-oily wastewater at different concentrations (left) 0.5 g/l (middle) 1.0 g/l (right) 1.5 g/l

Table 4.1 Parameters of the synthetic cutting-oily wastewater

Parameters	**Oil concentration (g/l)**		
	0.5	**1.0**	**1.5**
Turbidity (NTU)	580 ± 45	1390 ± 50	2350 ± 53
COD (mg O_2/l)	1226 ± 179	3289 ± 159	4546 ± 109
Average oil droplet size (μm)	1.033	1.830	2.504
pH	7.4	7.9	8.6

According to Table 4.1, every parameters tended to increase with oil concentration. Higher oil concentration represents the larger number of oil droplets More turbid liquid in higher oil concentration could conclude that the oil droplet was a main source of turbidity. According to the settling observation of wastewater after settling for 3 hours, it was found that there was no change on any observed parameter. This showed that this kind of oily wastewater had high emulsion stability as shown in Figure 4.2

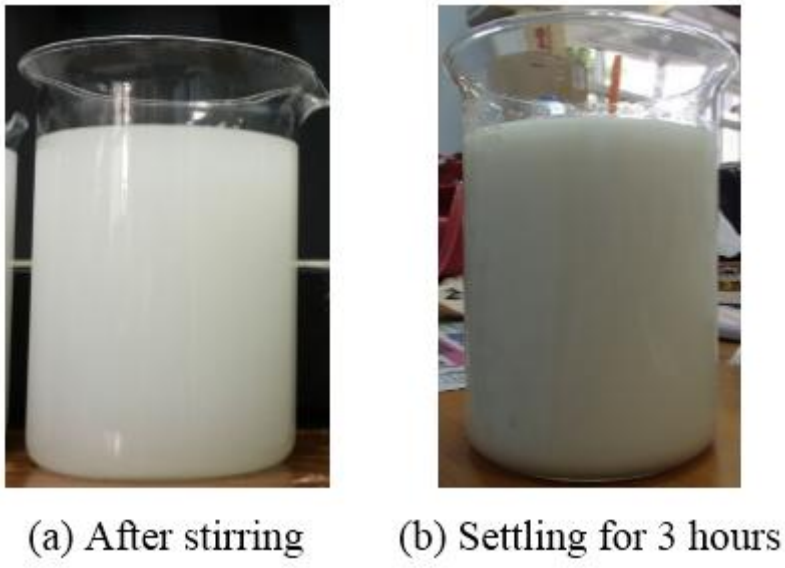

Figure 4.2 Synthetic cutting-oily wastewater

The next experiment focused on the chemical destabilization of cutting-oily wastewater using the jar test method to investigate the treatment ability of oil droplet using chemical destabilizing approach.

4.2. TREATMENT OF EMULSION BY CHEMICAL COAGULATION

As cutting-oil droplet was assumed to be a suspended particle in wastewater, this section aimed to investigate the ability of coagulation for oil particle separation. Aluminum sulfate or alum was applied as the coagulant under 100 rpm of rapid mixing for 1 minute and 30 rpm of slow mixing for 30 minute. After 30 minute of settlement, the wastewater was sampled to examine for turbidity, COD and total dissolved aluminum change.

4.2.1 Effect of alum dosage

Aluminum sulfate or alum using in the jar test experiment can provide the cationic aluminum ion on the system. This study aimed to investigate effects of alum dosage on the treatment efficiency. Moreover, the sludge generation was also visually observed.

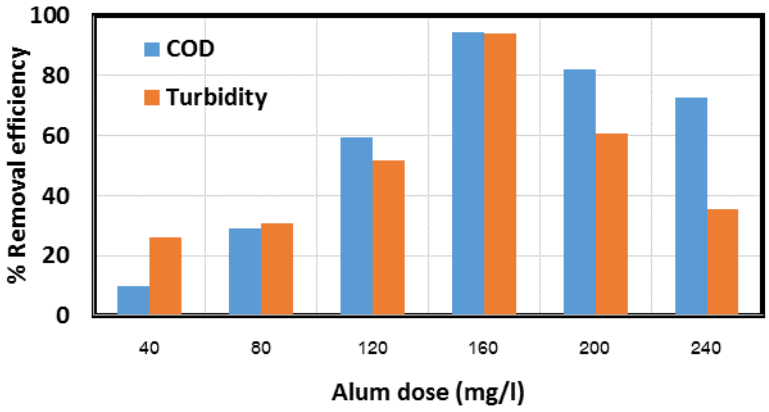

Figure 4.3 Treatment efficiency of Jar test in 1 g/l oil concentration

The result in Figure 4.3 showed that higher alum dose could remove more oil droplet until the optimal alum dose, which provide the highest efficiency, was reached. However, after that alum level, the treatment efficiency decreased dramatically due to excess alum dose. According to the coagulation reaction using alum as coagulant, the reaction would provide hydronium ion (H^+) which is the representative of decreasing pH. The pH during coagulation was a key parameter that control the speciation of aluminum hydroxide. Lower pH could cause less amount of aluminum hydroxide; therefore, decreasing of treatment efficiency of sweep flocculation would be

seen(US.EPA, 2015). According to Figure 4.3, the optimal alum dose for 1 g/l cutting oil concentration was 160 mg/l, which equivalent to 13.7 mg/l aluminum. The other oil concentration had similar optimal alum dose as shown in Table 4.2

Table 4.2 The optimal alum dosage

Oil concentration (g/l)	Optimal alum dosage (mg/l)	Equivalent aluminum dosage(mg/l)
0.5	120	10.272
1.0	160	13.696
1.5	200	17.120

Seeing that higher oil concentration required more coagulant dose. In addition, the sludge float upward due to its lighter density than wastewater. Increasing alum dose produced more sludge. However, the sludge would be broken after the system had exceeded the optimal alum dose because pH affected to less aluminum hydroxide formation under acidic condition. The physical appearances of sludge with different alum dosage are shown in Figure 4.4 as follow;

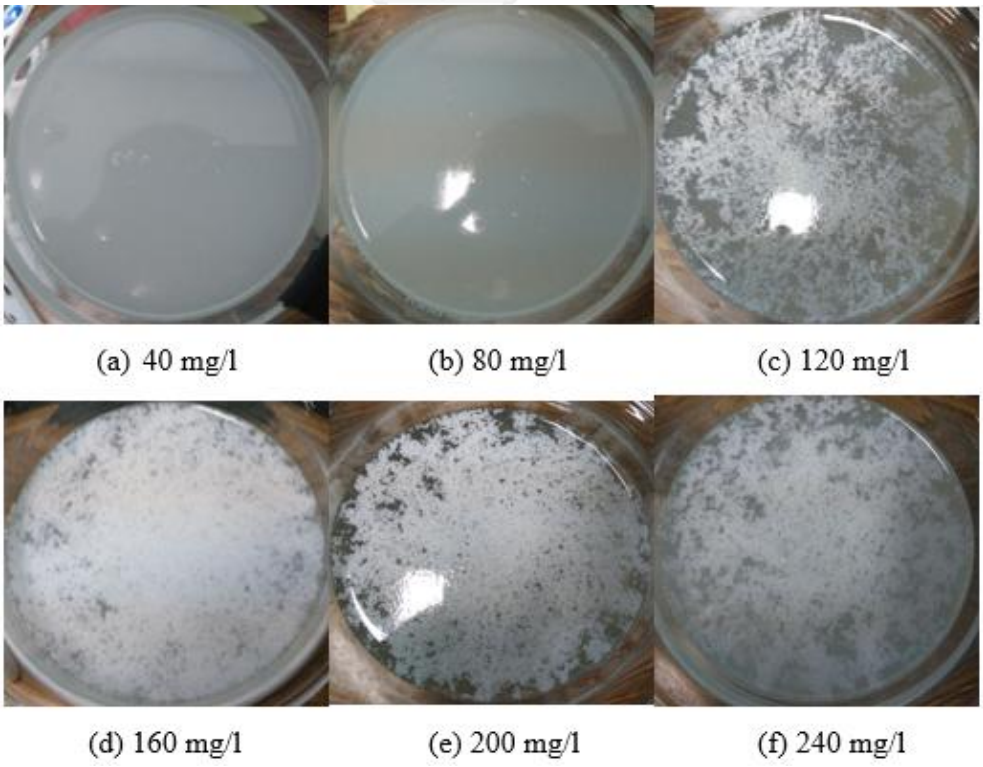

Figure 4.4 Physical appearance of sludge

In addition, the size distribution of particle in the effluent was also observed. The $d_{3,2}$ or Sauter diameter are presented in Table 4.3 . Seeing that the particle size (oil with alum) increase with higher alum dose. Until the system achieved optimal dose (160 mg/l), the diameter of particle was appeared to be the greatest size comparing among the other alum dose condition. Later, the re-stabilization due to the pH of effluent would occur since the decreasing of particle diameter as well.

Table 4.3 Size distribution of particle after jar test process

Alum dosage	$D_{3,2}$ (μm)	Multiple floc size
0	0.535	1
40	0.735	1.374
80	2.310	4.318
120	5.493	10.267
160	15.000	28.037
200	6.573	12.286
240	5.753	10.753

The results could be explained by the coagulation mechanism. At a very low concentration of alum, the aluminum ion had just attached some oil droplet's surface which affect to only some oil droplets to reduce negative charge around its surface. This phenomena was called diffuse layer process. Later, the increasing of aluminum dosage, in the other word, increasing the amount of positively charge to reach the optimal dosage was applied to the system. The aluminum ion would react with hydroxide ion to form aluminum hydroxide, a preferable coagulant, in order to proceed sweep floc coagulation process. However, exceeded alum dosage would decrease the treatment efficiency since the acidification during coagulation process. Hydronium ion (H+) was delivered to the system during coagulation. This phenomena occurred when there was high concentration of positively/negatively charge.

The effect of initial pH was studied in order to estimate the pH adjustment cost. At the same alum concentration, initial pH of oily wastewater played significant role to

treatment efficiency. Both COD and turbidity removal efficiency decrease dramatically in strong acidic condition, while the coagulation worked well in 8-9 range of pH seeing in Figure 4.5. The synthetic oily wastewater, itself, was also in this range of pH; therefore, the pH adjustment could be ignored. Moreover, the final pH of the effluent in this initial pH (8-9) was acceptable for standard discharge (5-9). The pH adjustment after treatment, thus, could also be eliminated too.

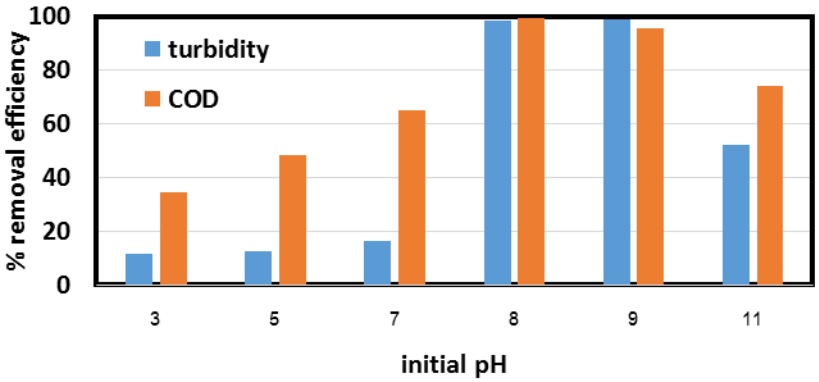

Figure 4.5 Effects of initial pH of the 1 g/l oily wastewater on the efficiency

4.2.2. Total dissolved aluminum in effluent

Total dissolved aluminum was also studied in the jar test. The result is shown in Figure 4.6. The red line represents the total dissolved aluminum calculated from the reaction stoichiometry as in Appendix II. The blue spots are the aluminum concentration in the control experiments, which measured the total dissolved aluminum of the specific alum concentration in DI water. Moreover, the dissolved aluminum from the jar test could come from 2 sources: effluent and sludge. According to Figure 4.6, aluminum was found mostly in the sludge. The total dissolved aluminum in effluent and sludge were in the ranges of 1 – 8 mg/l and 3 – 16 mg/l, respectively. Actually, there was no standard effluent for total dissolved aluminum, but the average range of total dissolved aluminum in drinking water was approximately 0.01 – 1.3 mg/l (Letterman & Driscoll, 1988; ATSDR, 1992). The post-treatment is therefore required in order to remove the residual aluminum.

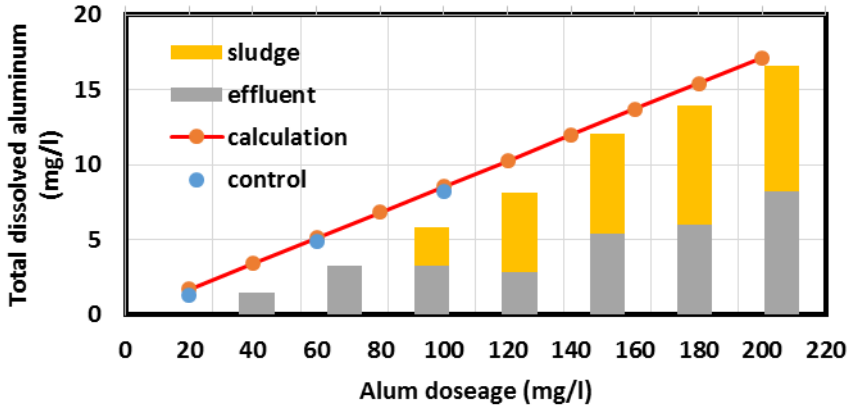

Figure 4.6 Total dissolved aluminum

4.2.3. Summary

In conclusion, the chemical coagulation by alum provided the turbidity and COD removal efficiencies of 80 – 90% at actual pH (8-9) of wastewater for the treatment of the cutting oil wastewater. Therefore, pH adjustment could be ignored since the coagulation could occur in the range of the synthetic oily wastewater. The next section present the results from the application of the electrocoagulation/flotation process for cutting-oily wastewater treatment in bubble column.

4.3 ELECTROCOAGULATION/FLOTATION IN BUBBLE COLUMN

In this section, electrocoagulation/flotation process was conducted in bubble column to identify the optimal operating condition. Several parameters such as current density, distance between electrodes, oil concentration, and reaction time were varied to investigate their effects on the turbidity removal efficiency

4.3.1. Turbidity removal efficiency

According to turbidity removal with time in Figure 4.7, the treatment phase can be divided into 3 stages including lag, reactive, and stabilizing stages (Holt et al., 2002). The detail of each stage can be given as follows.

(a)

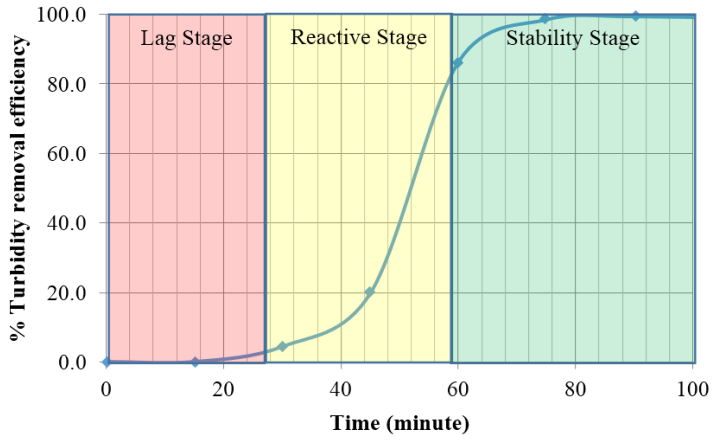

(b)

Figure 4.7 Turbidity removal by electrocoagulation of 0.5 g/l oil concentration at 100 A/m^2 current density and 2.5 cm of distance between electrodes
(a) Physical appearance of treated wastewater
(b) %Turbidity removal during reaction time

Lag stage: the turbidity was unchanged since a little amount of aluminum ions were released. These amount of aluminum ions could attach to the surface of oil droplets to reduce negative charge on oil's surface.

Reactive stage: aluminum ion diffused sufficiently through the whole column with the ultrafine hydrogen-oxygen bubble enhancement. This stage only occurred for 20 – 30 minutes as aluminum ions was sufficient to form floc and result in sweep flocculation. The floc rose upward with an assistance of hydrogen gas bubbles as well.

Stabilizing stage: the turbidity removal efficiency achieved more than 90 percent and became steady. In this stage, a clear effluent can be observed in the reactor. Longer stabilizing stage could provide as clear effluent as tap water.

Different operating conditions could give different time in each stage. Therefore, their effects was investigated by considering current density, distance between electrodes, reaction time, and oil concentration. Influence of each individual parameter and their correlation was determined as shown in the following section.

4.3.2. Effect of operating condition

4.3.2.1. Current density

Current density can play a role in the electrocoagulation/flotation since it relates to the metal ion releasing rate which consequence to faster reaction as well. It was found that higher current density provide shorter lag stage and reach stabilizing stage more quickly. According to Figure 4.8, the highest current density (125 A/m^2) achieved the stabilizing stage in shortest reaction time (60 minutes) comparing to those of 75 and 100 A/m^2 (120 and 90 minutes, respectively). While, the 75 A/m^2 doubled the lag stage period from 125 A/m^2's. However, the 125 A/m^2 was not considered as the optimal current density in this work since the 100 A/m^2 can also provide similar treatment efficiency. Moreover, both 100 and 125 A/m^2 can reach the same removal efficiency after 90 minutes of reaction time. This condition (100A/m^2) was found as high efficiency as in both lower (0.5 g/l) and higher (1.5 g/l) of oil concentration. As a result, the current density of 100 A/m^2 was chosen as the optimal operating current density for further experiments.

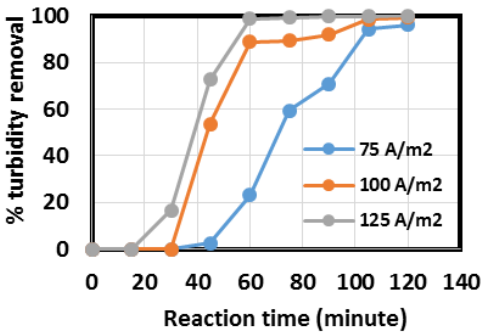

(a) 0.5 g/l 1.25 cm

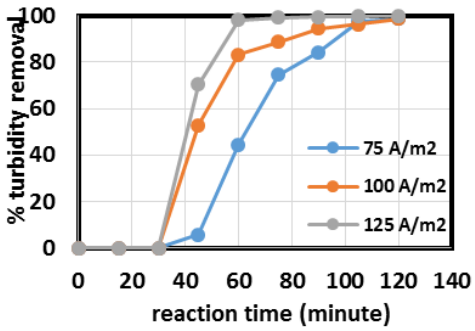

(b) 0.5 g/l 2.5 cm

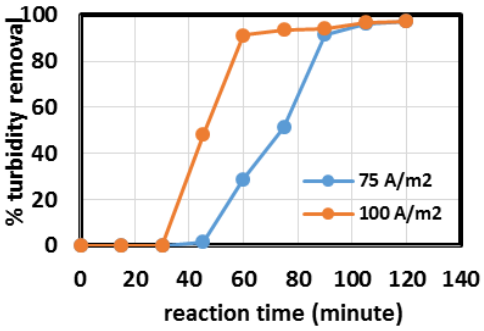

(c) 0.5 g/l 3.75 cm

Figure 4.8 Turbidity removal efficiency in various conditions

According to Figure 4.8., noted that 125 A/cm^2 could not be provided at 3.75 cm distance between electrodes due to the DC power supply limitation. Furthermore, the distance between electrodes was another interesting parameter that needed to be taken into account since longer electrode inter-spacing could affect the treatment efficiency as in Figure 4.8. Effects of the electrodes gap will be discussed in the next section.

4.3.2.2 Distance between electrodes

Distance between electrodes was identified as a liquid electrical resistance factor. To illustrate, longer distance between electrodes would increase the resistance of reactive zone, in the other words, decrease the electron transfer efficiency (Nagai et al., 2003). As a result, power consumption at longer gap was increase in order to provide the higher voltage for the same amount of current. Moreover, lengthen gap would also decrease mixing condition due to larger volume as in Figure 4.9.

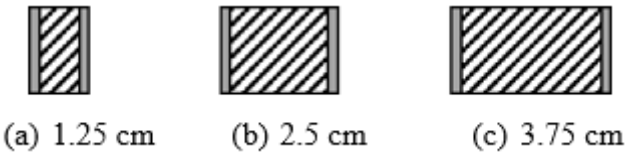

Figure 4.9 Reaction zone

The electrode gaps of 1.25 – 3.75 cm was a small range, so it showed only slight effect to treatment efficiency because the system was conducted in current control (C.C.) of direct current power supply operating mode. The 2.5 cm of electrodes' gap was selected as the best distance between electrodes since it can provided the highest efficiency as in Figure 4.10. Note that the 2.5 cm shows obvious higher efficiency than that of 3.75 cm, but similar result to the 1.25 cm distance. Noted that at

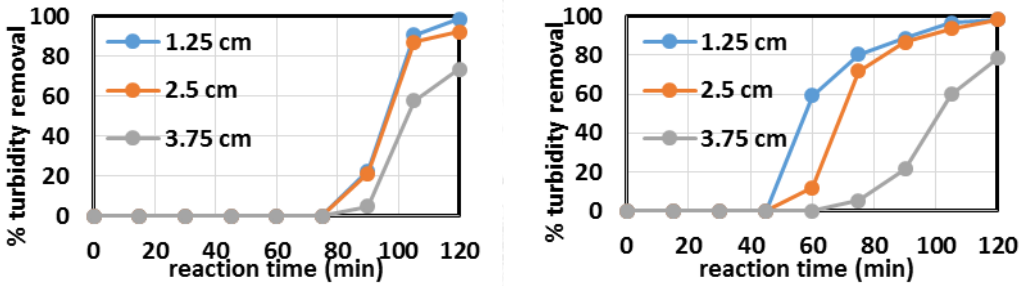

(a) 1.0 g/l 75 A/m^2 (b) 1.0 g/l 100 A/m^2

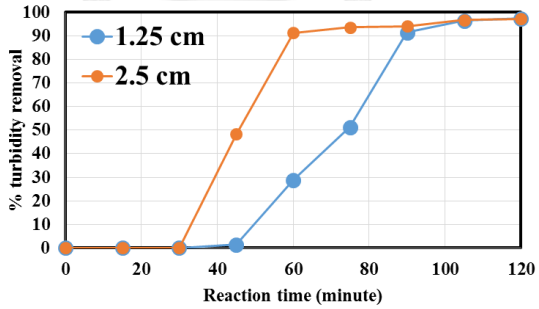

(c) 1.0 g/l 125 A/m^2

Figure 4.10 Turbidity removal efficiency in different gap between electrodes of 1 g/l oil concentration

As a conclusion, current density and distance between electrodes were related to each other. Seeing that high current density with less electrodes inter-space could provide satisfied treatment efficiency. The optimal operating condition among these parameters were stated as 100 A/m^2 with 2.5 cm of electrodes gap. The next

investigated parameter would be the reaction time since the change of the treatment efficiency was observed during operating time.

4.3.2.3. Oil concentration

The dissimilar initial oil concentrations gave different times for each removal stage. According to Figure 4.11, lower oil concentration spent less time in the lag stage and dramatically increased to achieve the stabilizing stage rapidly. Unlike higher oil concentrations, the 1.0 g/l and 1.5 g/l consumed longer reaction times to achieve lag stage and reactive stage.

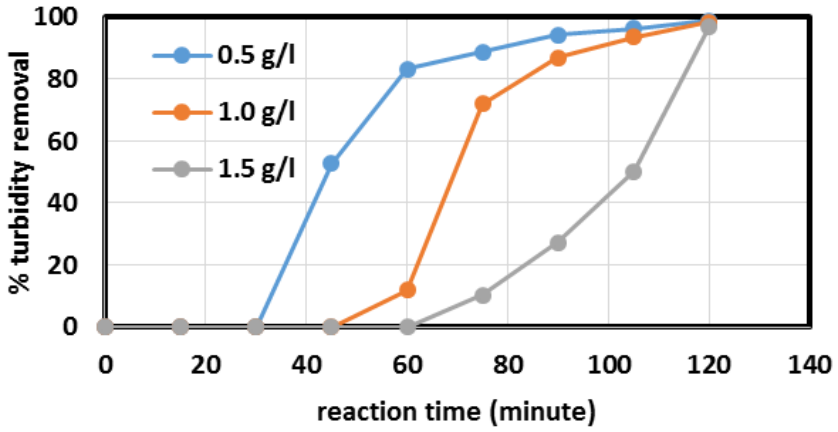

Figure 4.11 Turbidity removal efficiency in different oil concentration under operating condition of 100 A/m^2 current density and 2.5 cm electrode gap

According to Figure 4.11, oil concentration shows it effect to reaction time. Higher oil concentration required longer operating period. In addition, surprisingly, at 120 minute of reaction time every oil concentration achieved the same treatment efficiency since the sufficient aluminum concentration to treat oily wastewater. However, the appropriate operating time should be stated due to energy minimization. The optimal operating time under optimal operating condition (100 A/m^2 of current density and 2.5 cm of electrodes gap) are displayed in Table 4.4 seeing that higher oil concentration required more reaction time because of large amount of oil droplet.

Table 4.4 Optimal reaction of ECF process in different oil concentration

Oil concentration (g/l)	Optimal reaction time (minute)
0.5	60
1.0	90
1.5	120

4.3.3 Summary

As a result, 2.5 cm of gap between electrodes and 100A/cm^2 of current density were found to be an optimal operating condition. The reaction time of each oil concentration were 60, 90 and 120 minute for 0.5, 1.0 and 1.5 g/l of oil concentration, respectively. However, wastewater beneath the electrode was observed to be an untreated zone since there was no driving factor that transfer aluminum downward under the electrodes. The further experiment would aim to reduce the untreated zone and improve the overall treatment efficiency by developing the reactor configuration.

4.4 ELECTROCOAGULATION/FLOTATION IN EXTERNAL-LOOP AIRLIFT REACTOR

In this section, different downcomer configurations in 27 types were applied in order to observe effects of diameter, height, and connector (with different angles) of the downcomer to the treatment efficiency. All the downcomer set were made of PVC pipe and fitting. The union pipe fitting was applied to every configuration for reducing a permanent pipe connecting by liquid solder pipe PVC. The components of external loop airlift reactor (ELALR) is presented in Figure 4.12. The additional PVC tube as downcomer part consists of a specific term called height of downcomer. This term means the different length between top downcomer connecting tube (A) and bottom downcomer connecting tube (C) as shown in Figure 4.12.

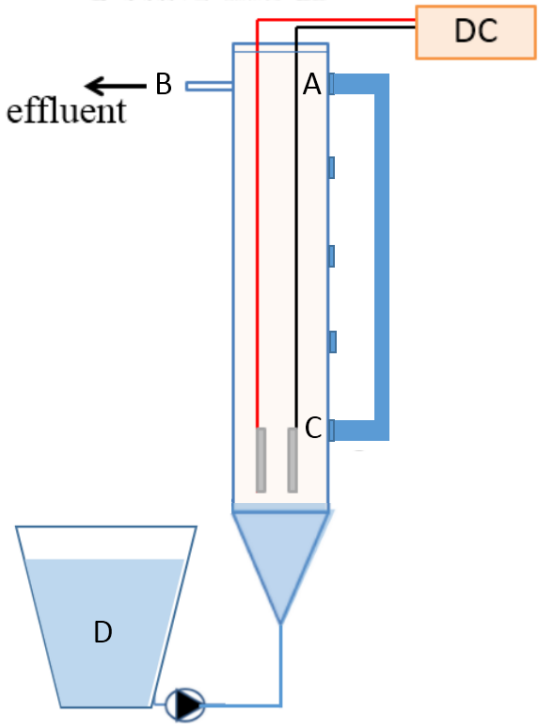

Figure 4.12 Schematic diagram of external loop air lift reactor, ELALR

Where; A = top downcomer connecting tube

B = effluent outlet

C = bottom downcomer connecting tube

D = Storage tank

The related parameters are displayed in Table 4.5 and the example of downcomer are shown in Figure 4.13.

Table 4.5 Parameters in external loop airlift reactor

Parameter	Level of the parameter		
Downcomer diameter (inches/cm)	1/2.5	1.5/3.8	2/5.1
Height of downcomer (cm)	50	75	100
Connector configuration (vertical angle)	45	90	135

Figure 4.13 Example of downcomer with 1.5 inches diameter

4.4.1 Turbidity removal efficiency

According to the turbidity removal efficiency behavior, ELALR could provide similar stage of turbidity behavior including lag stage, reactive stage and stabilizing stages with the same maximum turbidity treatment. Therefore, the best downcomer configuration determination required more parameter as treatment efficiency criteria. Finally, this experiment would include turbidity removal efficiency and sludge generation rate as treatment criteria.

4.4.2 Effect of downcomer configuration

The effect of downcomer configuration could be divided into 3 parts using connector configuration of 45, 90, and 135 vertical degrees. The effect of diameter and height of downcomer was only discussed in the case of 0.5 g/l oil concentration since

these parameters had the same treatment tendency in another oil concentration (Seeing in Appendix IV). Moreover, the possible error form turbidity dilution would be eliminated in 0.5 g/l oil concentration due to its turbidity that was not exceed the capacity of turbidity meter as well.

Increasing downcomer height would improve the turbidity removal efficiency in reactive stage, while maintained the same period of lag stage as in Figure. 4.14. The smallest downcomer size shows very small change comparing with the result in bubble column (BCR). The larger diameter, on the other hand, could obviously increase the treatment efficiency with shorter period of reaction stage. As downcomer height increase, the overall treatment efficiency remained the same which is close to 99% turbidity removal. As a result, the best height of downcomer was reported at 100 cm. This result was supported by the work of Choi (2000) that higher downcomer height /unaerated zone could provide less mixing time due to increasing of velocity in downcomer.

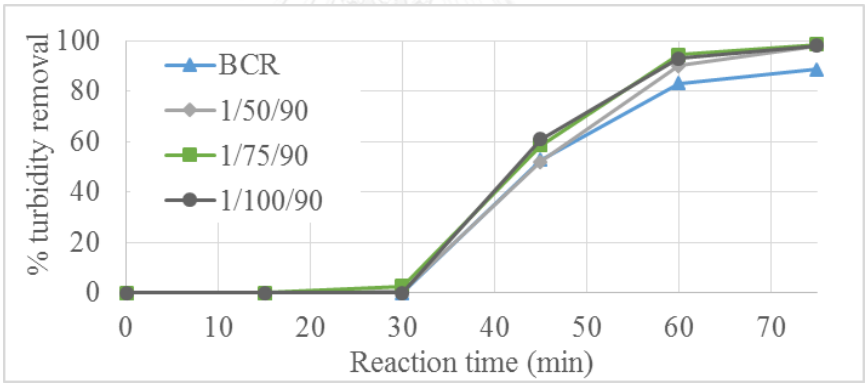

(a) Effect of downcomer height in 1” pipe

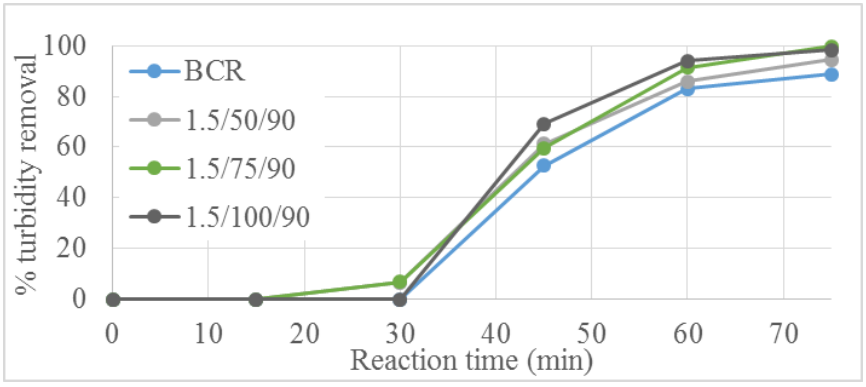

(b) Effect of downcomer height in 1.5” pipe

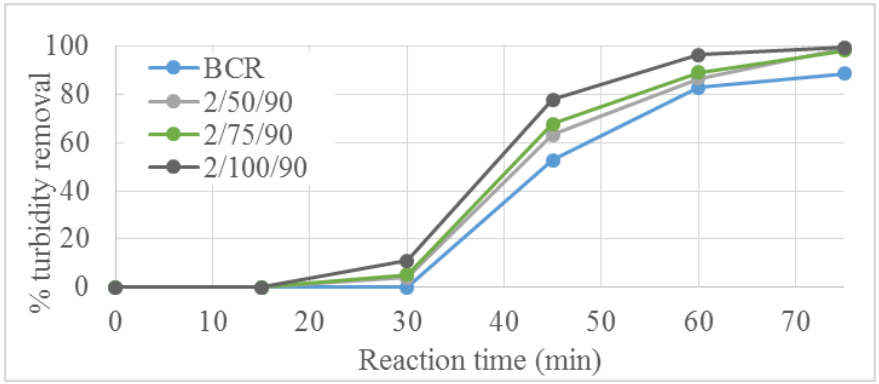

(c) Effect of downcomer height in 2” pipe

Figure 4.14 Effect of downcomer height in various diameter of 0.5 g/l oil concentration

Furthermore, effect of downcomer diameter was investigated. According to the turbidity removal efficiency in Figure 4.15, greater downcomer diameter at the same downcomer height could provide the higher treatment in reactive stage.

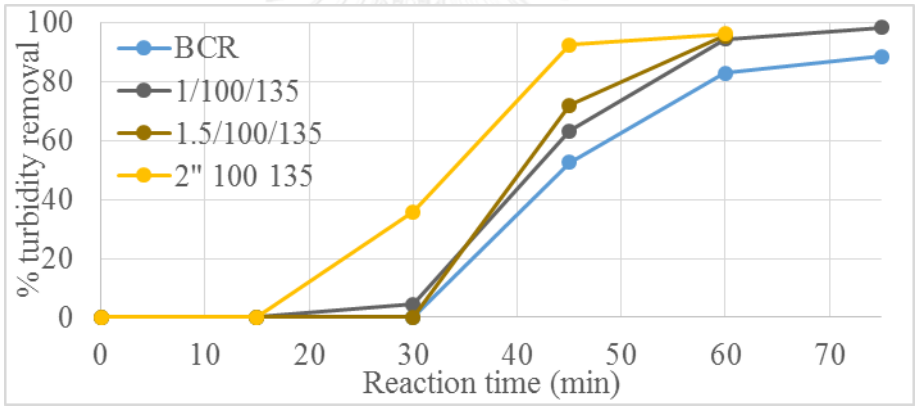

Figure 4.15 Effect of downcomer diameter

As a conclusion, 2-inches diameter pipe with 100 cm of downcomer height was reported as the highest treatment efficiency, meanwhile the 1.5 and 1 inches diameters were the second best and the third best, respectively. Later, connector configuration would be discussed with the best downcomer diameter and height as well.

Effect of connector configuration

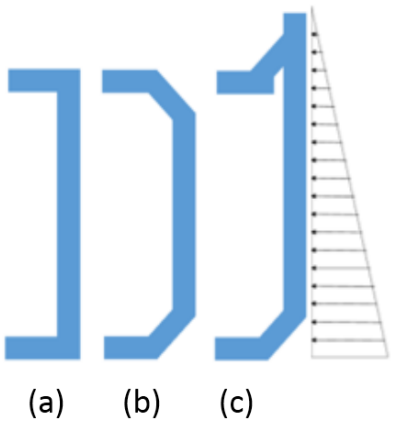

Figure 4.16 Schematic diagram of downcomer in different connector configuration (a) 90º (b) 45º (c) 135º

According to schematic diagram of connector configuration in Figure 4.16, 45° and 90° of connector configuration would be compared since it had similar vertical height of downcomer. Typically, 90° of connector configuration is a conventional downcomer in external loop airlift reactor. This pipe configuration got a little longer circulation pathway than 45°connector pipe. Treatment efficiency, therefore, slightly drop when comparing with 45 ° connector shape. This result was agreed with Yuttana (2007) which had reported the better circulation on 45 degree declined downcomer than conventional configuration one. The 45° connecting tube was defined as the shortest circulation pathway due to its geometry appearance.

Moreover, 135° connector configuration had demonstrated as the highest vertical length of downcomer among the other connector configuration. This pipe arrangement could be advantage due to the generation of the highest hydrostatic pressure in downcomer pipe as pressure diagram shown in Figure 4.16. To illustrate, first of all, the pressure diagram was conducted in 2 inches diameter which was explicit change in the vertical height as the example. At the same level of entrance and exit of downcomer, 45 º showed as the shortest vertical height while 135 º appeared to be the highest vertical downcomer height. When cathode electrode generated hydrogen bubble, water in the downcomer started to move downward to replace the void due to bubble flotation. Higher vertical length of downcomer, in the other word, greater differential pressure could induce more circulation(Rujiruttanakul et al., 2011). This result was also agreed with the experiments of Rujiruttanakul (2007) which had proofed

that the circulation improvement of downcomer was caused by vertical height of downcomer.

Comparing the treatment efficiency among different connector configuration in external loop airlift reactor to bubble column (BCR) at the best height and diameter (100 cm height and 2” diameter), lag stage was found to be shorten while the maximum treatment efficiency remain the same at 90 minute of operating period. 45° connector was found to be the second best and followed by 90° connector which was the closest performance to bubble column as shown in Figure 4.17.

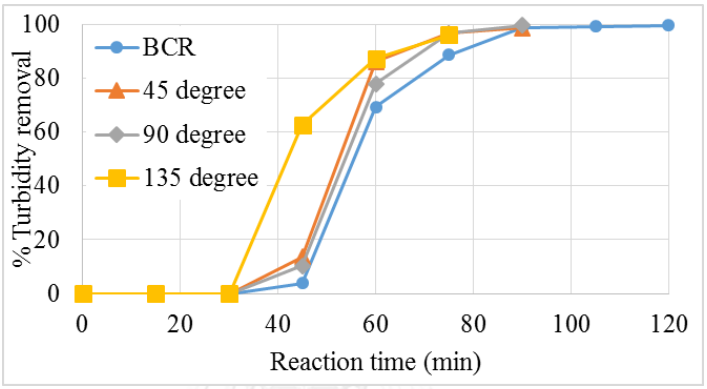

Figure 4.17 Turbidity removal efficiency in different reactor configuration of 0.5 g/l 2” in different connector configurations

Moreover, the sludge bulk density in Figure 4.18 shows the effect of circulation improvement via connector configuration on sludge appearance. Better liquid recirculation could provide less sludge with less air pocket inside the sludge cake. The oil content in the sludge increasing when lower sludge thickness which made the sludge to be moister and denser as shown in the Figure 4.18

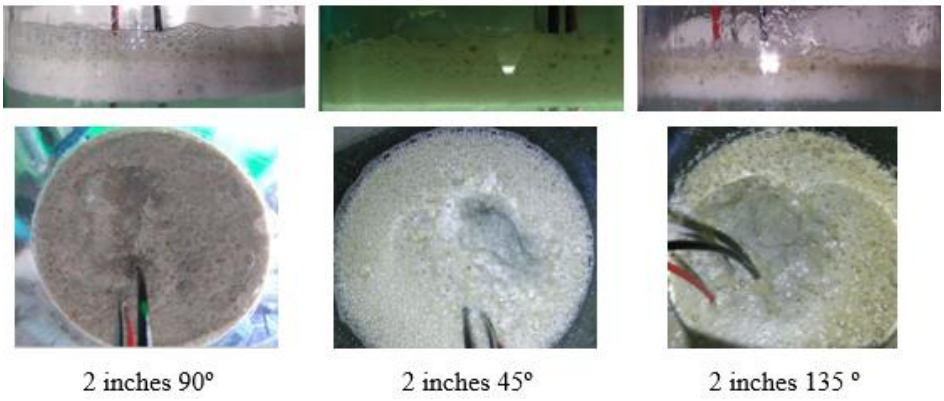

Figure 4.18 Sludge generation in different connector configuration at 100 cm 1.5 g/l

As a conclusion, the best downcomer configuration was 135 º of 2 inches diameter with 100 cm height. However, the untreated zone under electrode position was still found in every condition. Effects of other parameter on this untreated zone have to be further investigated.

4.4.3 Effect of Oil concentration

Oil concentration affected directly to reaction time and sludge quality. The physical appearance of the final sludge were observed. The sludge was divided into 2 layer:

- oily layer : the green-like layer which assumed to have other element such as cupper as electrodes impurity
- aluminum hydroxide layer : white-gray layer which had high content of aluminum hydroxide

At the same operating condition of 135° with 100-cm height and 2-inches diameter, the sludge thickness in different oil concentration are shown in Figure 4.19.

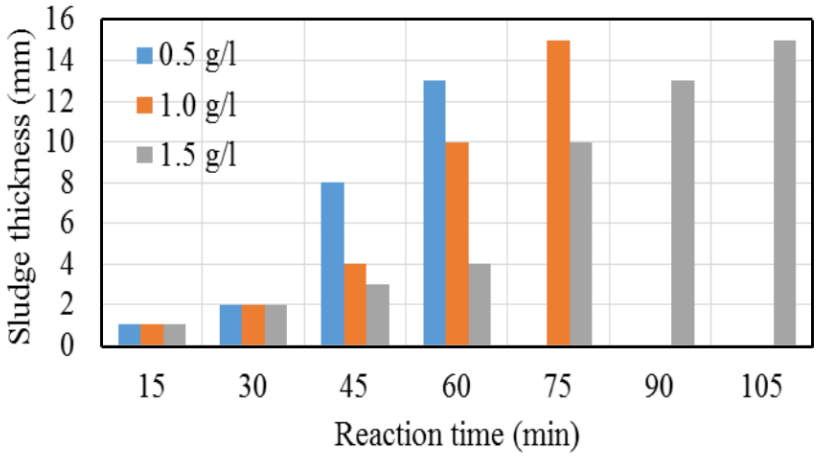

Figure 4.19 Sludge thickness in different oil concentration

4.4.4. Summary

The external loop airlift reactor could shorten lag stage and achieve reactive stage faster than in BCR. Moreover, sludge thickness was reduce and become denser, while maintained the overall turbidity removal efficiency. As a result of downcomer configuration, increasing downcomer's height and diameter could provide shorter period of reactive stage comparing to the result in BCR; therefore, 100 cm downcomer height and 2" downcomer diameter was stated as the best downcomer configuration.

Later, connecting configuration was studied. The result showed that 2” of diameter, 100 com of height and 135° of connecting configuration of downcomer was the best downcomer configuration. Additional pressure in 135 º of downcomer could be used to explain the reason of the best reactor configuration due to the increasing of the head of water in the vertical pipe of downcomer. The untreated zone, however, still appeared at the area beneath the electrodes the flow mechanism could be used to explain this phenomena of untreated zone in the next section.

4.5. PROCESS ANALYSIS

This section aimed to investigate the difference between bubble column and external-loop airlift reactor. There are many interesting issues including the treatment efficiency, bubble generation, electrode consumption, sludge production, and flow mechanism. Finally, the mathematical model for the efficiency prediction was proposed from the experimental results.

4.5.1. Treatment efficiency

Treatment efficiency was focused on turbidity removal efficiency and quality of the effluent including the total dissolved aluminum and COD which was analyzed in the best downcomer only. The final turbidity of each oil concentration form the best downcomer configuration was found similar to each other seeing in Table 4.6. Although turbidity of the effluent was appeared as a transparent clear liquid, it was assumed that there were some portion of residual oil in the effluent since the COD of the effluent was higher than the standard regulation which stated at 120 mg O_2/l. The COD was in range of 250 – 350 mg O_2/l depended on the initial oil concentration as shown in Table 4.6

Table 4.6 Effluent quality from downcomer

Oil concentration (g/l)	Turbidity (Ge et al.)	COD (mg O_2/l)
0.5	23.5	250
1.0	23.7	290
1.5	26.5	350

*Note that the turbidity of tap water is between 0.12-0.29 NTU as blank

On the other hands, at the optimal operating condition: 100 A/m^2 at 2.5-cm distance between electrodes, the dissolved aluminum was investigated in order to ensure that the total dissolved aluminum was not exceed the average dissolved aluminum for treated water which between 0.01-1.3 mg/l (Sam Keith, 2015). The result in Figure 4.20 shows that total dissolved aluminum in the effluent is lower than those calculated from Faraday's law since some portions of aluminum ion is entrapped in aluminum hydroxide form of the sludge. However, the concentration was more than 5 folds from the average dissolved aluminum for treated water. The post treatment, therefore, was required to remove the exceeded aluminum and remaining COD.

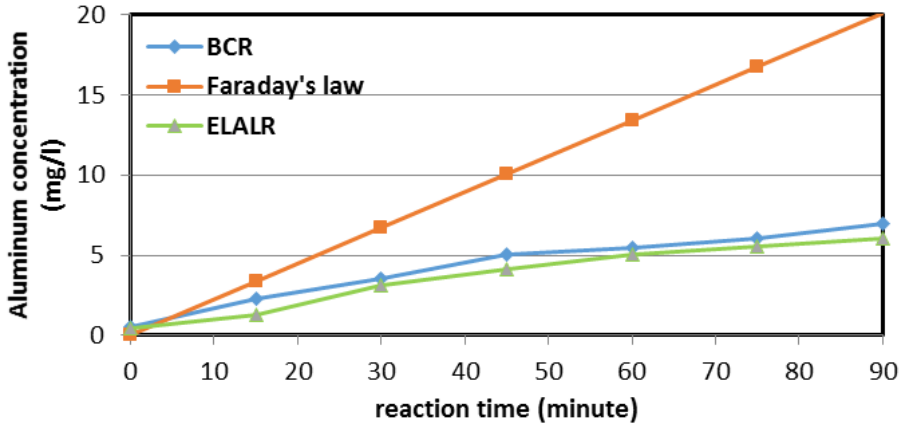

Figure 4.20 Total dissolved aluminum of 100 A/m2 2.5 cm of electrode gap

4.5.2. Bubble generation

In ECF process system, hydrogen gas was generated from cathode as in Figure 4.21(a). In this experiment, soap film meter was used to measure the gas flow rate. The assumption of this experiment was that the majority of gas was hydrogen gas. The experiment was conducted under many operating conditions using control current DC operation. The result shows that the most influent parameter was current density which shows its 0.9923-R^2 of linear relation in Figure 4.21 (b) with the correlation as in Equation 4.1. Larger amount of micro bubbles could have more chance to attach to oil particle or destabilized floc. The enhancement of higher current density, which generate more hydrogen bubbles, will increase the separation rate of oil from the wastewater.

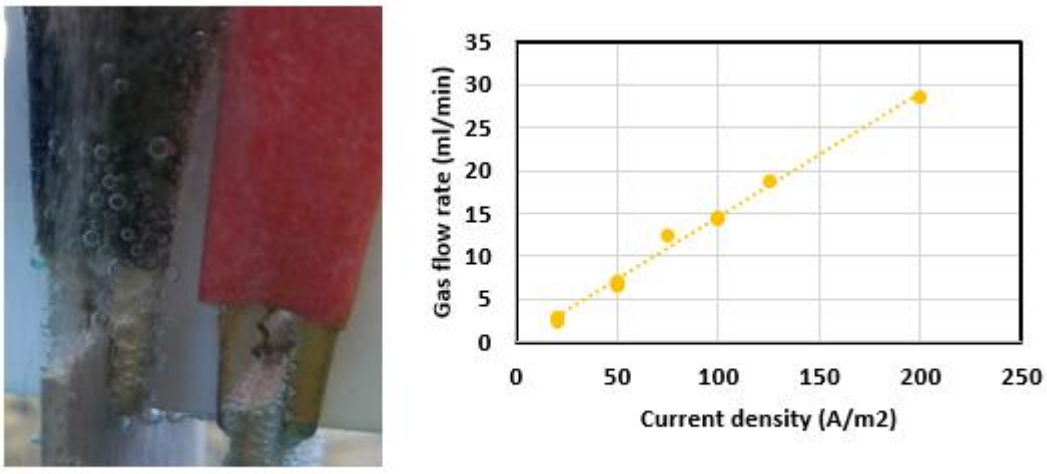

(a) physical appearance (b) Bubble generation equation

Figure 4.21 Hydrogen/oxygen bubble at cathode and bubble generation model

Gas flow rate (ml/min) = 0.1452 x Current density (A/m^2) (Eq 4.1)

According to the stoichiometry calculation in Appendix IV, it was reported that every 1 g of aluminum anode loss, the total hydrogen production would be 3.174 L. The correlation between gas production and electrode mass loss would be discussed in the next section.

4.5.3 Electrode and power consumption

During ECF operation, the sacrificial anode was continuously corroding. The average mass loss of the electrode was between 0.3 – 0.35 g (see calculation in Appendix IV) within 2 hours of operating time.

Besides, the power consumption can be calculated from energy equation as follow;

$$\text{Power consumption (Wh)} = \frac{V \times I \times t}{me\ (l)} \quad \text{(Eq 4.2)}$$

$$\text{Power consumption per wastewater volume (Wh/l)} = \frac{V \times I \times t}{wastewater\ volume\ (l)} \quad \text{(Eq 4.3)}$$

Table 4.7 Comparison of power consumption in different condition

Parameters	Chemical coagulation	ECF in BCR	ECF in ELALR
Volume of wastewater (l)	6	25	29
Voltage consumption (V)	220	40	40
Current usage (A)	0.5	1	1
Reaction time (minute)	31	60/90/120	60/90/120
Power consumption (Wh) 0.5/1.0/1.5 (g/l)	56.83	40/60/80	40/60/80
Power consumption per wastewater (Wh/l) 0.5/1.0/1.5 (g/l)	9.5	1.6/2.4/3.2	1.4/2.1/2.6

Seeing that chemical coagulation required more electricity than ECF process due to agitation. Moreover, when compare the energy consumption between BCR and ELALR, it can be seen that the ELALR can slightly reduce the energy consumption for operation due to the increasing of wastewater volume with the same operating condition

and the effect of external loop circulation too. The ELALR, in the other word, increase the loading capacity of the ECF as well.

4.5.4. Sludge production

Bubble column reactor

The oily sludge production rate was related to the phase of turbidity removal efficiency. During the lag stage, the sludge did not significantly change. Only 1 – 2 mm of sludge thickness can be seen as shown in Figure 4.22.

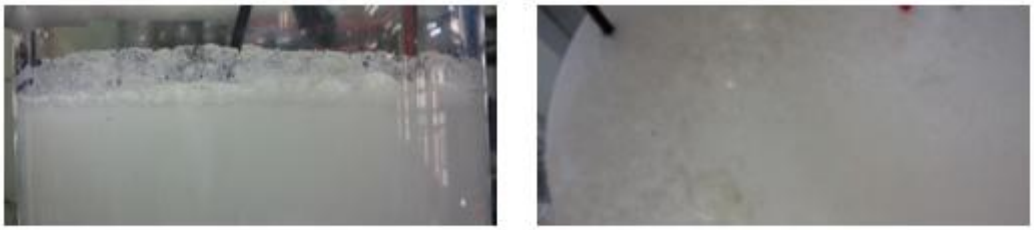

(a) Side view (b) Top view

Figure 4.22 Sludge in lag stage

During the reactive to the stabilizing stage, the sludge thickness was dramatically increased. Moreover, there were a large number of air pocket inside the sludge layer which could significantly decrease the overall density of the sludge. As a result, the sludge was appeared as foam sludge seeing in Figure 4.23.

(a) Side view (b) Top view

Figure 4.23 Sludge in reactive and stabilizing stage

Finally, when the system reached the stabilizing stage, the white layer of aluminum hydroxide ($Al(OH)_3$) was gradually appeared. The sludge itself had very low water content since the presence of large air pocket in the sludge cake as shown in Figure 4.23.

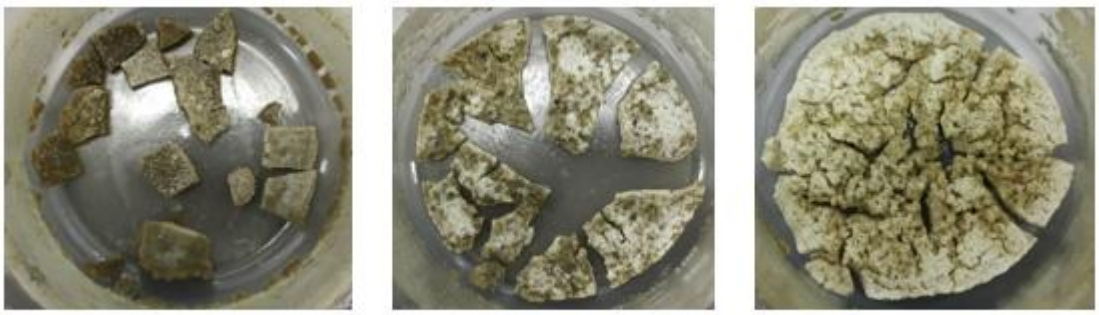

(a) 0.5 g/l (b) 1.0 g/l (c) 1.5 g/l

Figure 4.24 Dried oily sludge in various oil concentration

After drying the sludge at 103 – 105ºC for 2 hours, the dried sludge turned into dark gray color. The overall volume decrease almost half of the initial volume due to the air pocket elimination and water&oil evaporation. Moreover, oil was found in sludge when increasing the initial oil concentration as in Figure 4.24. The sludge of high oil concentration presented in oily sludge form. In addition, the sludge generation was studied with different current density. It was found that higher current density could produce more sludge since more aluminum ion was released from the anode electrode as shown in Figure 4.25.

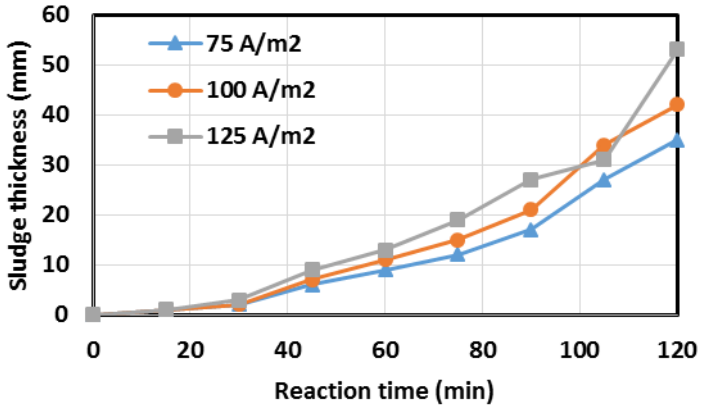

Figure 4.25 Sludge thickness during reaction time of 1 g/l oil concentration

External loop airlift reactor, ELALR

Sludge production in the ELALR was significantly decreased in different downcomer configurations. Higher vertical length could provide less sludge since the circulation in downcomer induced both particles and bubbles to flow into the downcomer. The probability of particle that would attached to the sludge layer,

therefore, decrease due to liquid circulation in downcomer. According to sludge thickness in Figure 4.26, higher vertical height of downcomer could provide less sludge thickness. As a result, the 100-cm downcomer can reduce more than 50% of the sludge volume compared to the bubble column. This is another advantage of external loop airlift reactor.

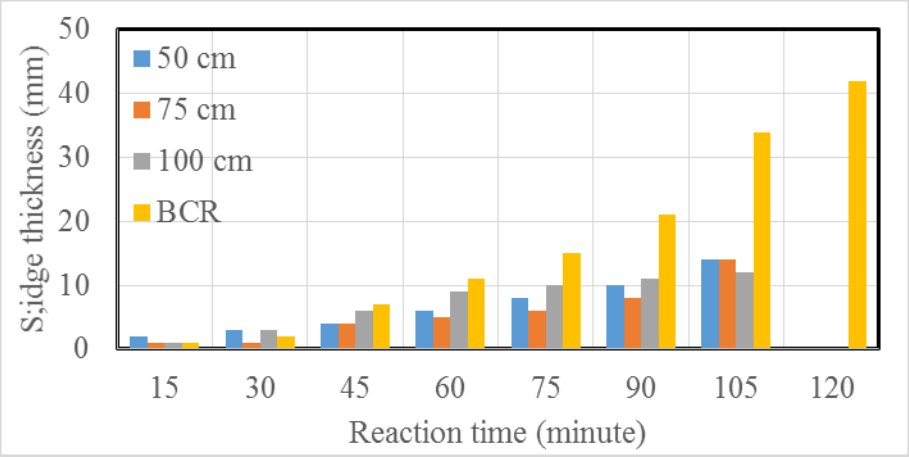

Figure 4.26 Sludge generation in various reactor Configuration (BCR, 50, 75, 100 cm of 135° connector configuration)

Moreover, the sludge appearance was found to be denser, the bubble size in sludge was smaller. Higher oil content in the sludge could be the effect of liquid circulation which was not be dried within 2-hours. The packed sludge might be another advantages of external loop airlift reactor as well seeing Figure 4.27.

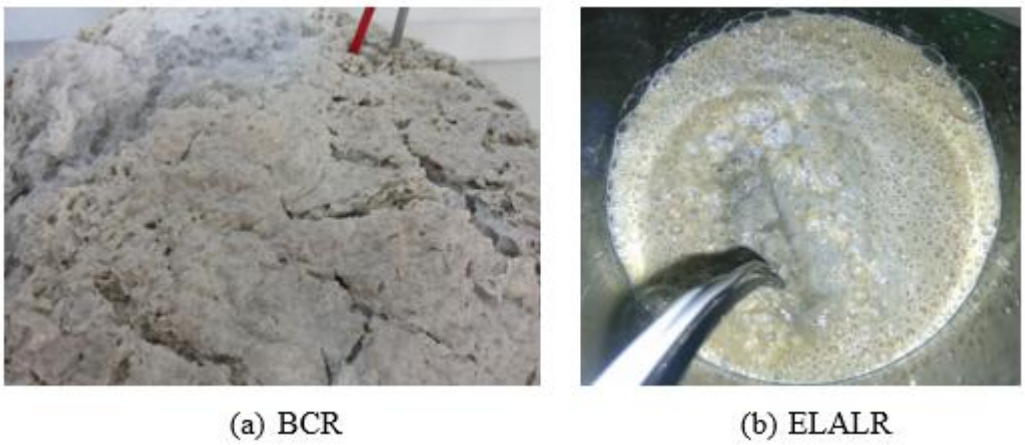

Figure 4.27 Sludge appearance in different reactor configuration

4.5.5. Flow mechanism

Bubble column reactor, BCR

Flow mechanism was used to explain the untreated zone phenomenon. First of all, 25-L of synthetic wastewater in the bubble column was prepared before operating the system. The driven flow factor was a pair of electrodes which located at the 30-cm bottom of the reactor. The hydrostatic pressure of liquid in the column is shown in Figure 4.28.

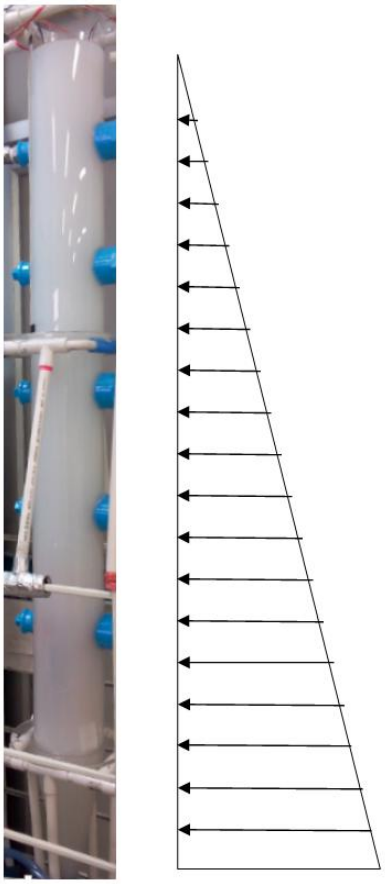

Figure 4.28 Hydrostatic pressure of liquid in bubble column

Water pressure at the electrode $= \rho g h$ (Eq.4.2.)

$$\approx 900\ \frac{kg}{m^3} \times 9.81\ \frac{m}{s^2} \times 1.5\ m$$

$$\approx 13.243\ kPa$$

After the DC power supply delivered direct current to the electrodes, the sacrificial anode release aluminum ions and the cathode produced micro-bubble of

hydrogen gas. The generated gas was gradually flow upward due to buoyancy. Adjacent wastewater beside the bubble moved to replace the space suddenly leading to the movement of the wastewater. The moving of this region was occurred at the center of the column since the electrode was placed at its center. Later, gas bubbles and moved wastewater reached the top of reactor column. Some amount of gas flow out of the system and some had been kept in the sludge. The others, while, came down since the chain reaction (the space replacement at the cathode) occurred all the time. When the downward stream reached where the electrodes were located, the mixing occurred in that region as in Figure 4.30. However, only 0.5 – 1 cm beneath the electrodes was treated since the hydrostatic pressure of liquid in the column as shown in Figure 4.29.

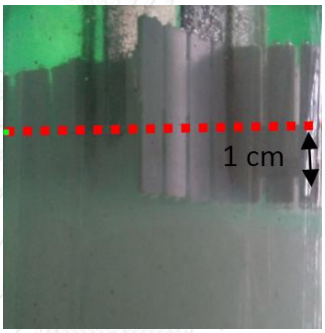

Figure 4.29 Untreated zone beneath the electrode

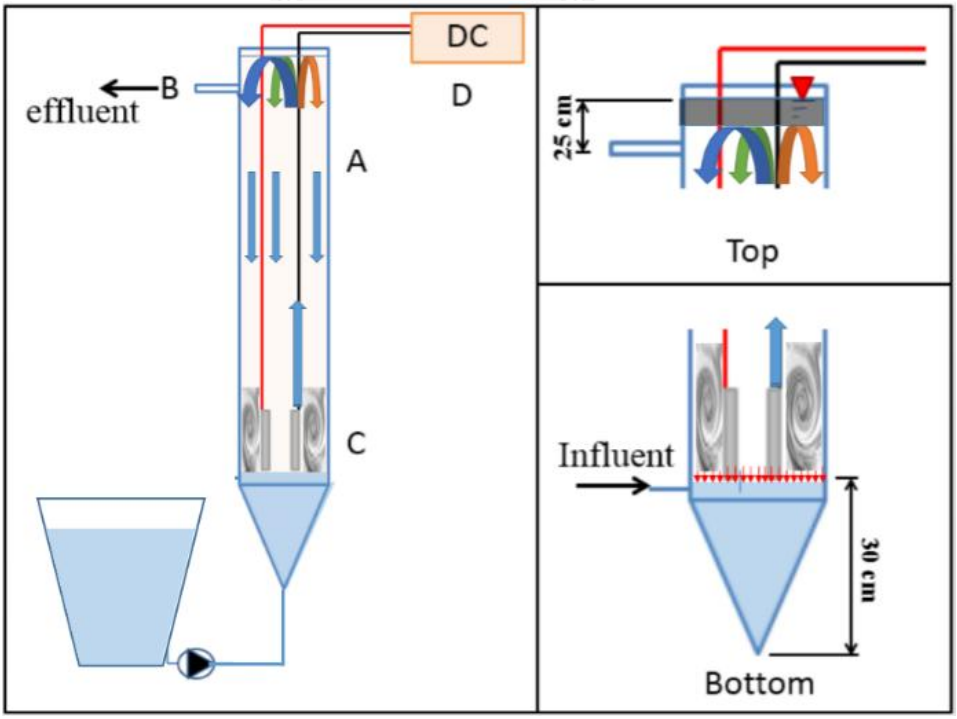

Figure 4.30 Schematic diagram of liquid circulation in bubble column

External loop airlift reactor, ELALR

Flow in the ELALR applied the same principle as in the BCR, but another phenomena of the circulation occurred due to additional downcomer. Active wastewater flew in the restricted space until it reach the top connector of the downcomer. Some portions of bubble and wastewater flew into the downcomer section. This incoming fluid then joined the movement chaining process in downcomer that happen due to mass transport phenomena. Liquid at the bottom connector of downcomer would flow by the replacement of wastewater at electrode to get mass and energy balancing in ECF process. Figure 4.31 shows the flow mechanism of ECF in different downcomer configuration.

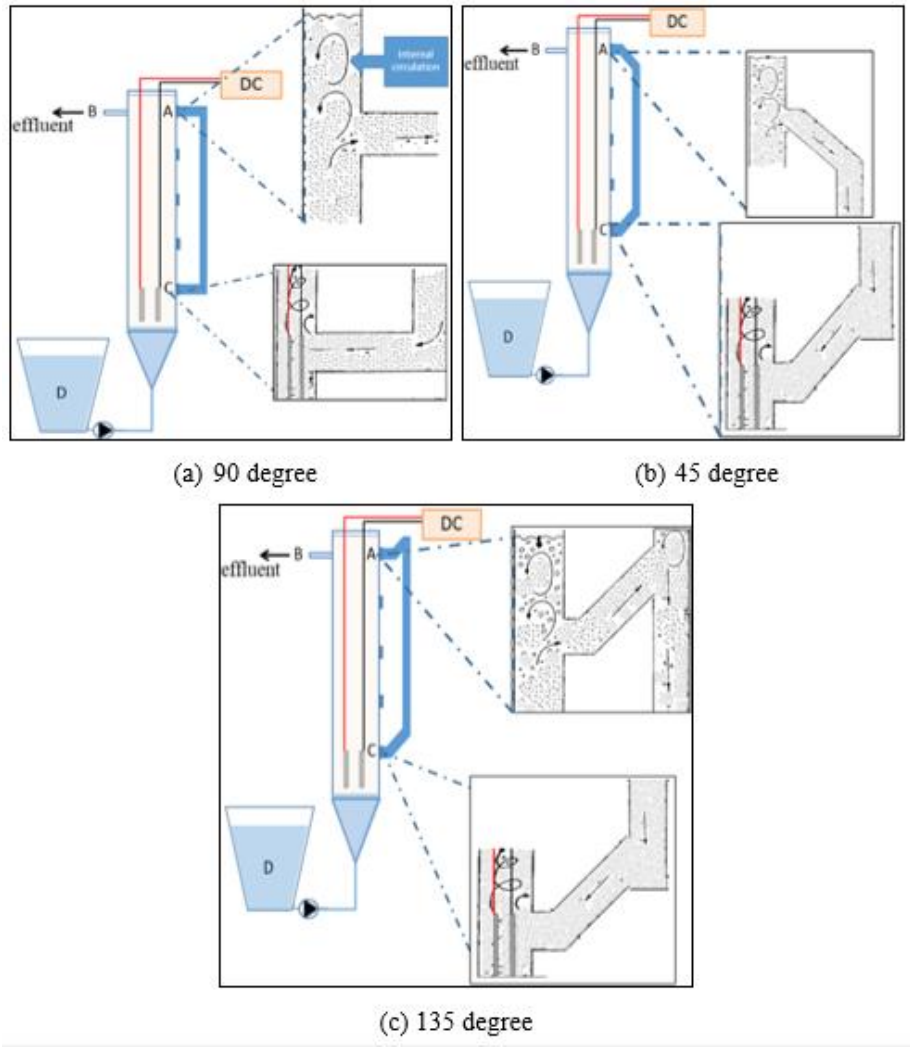

Figure 4.31 Flow mechanism in external loop airlift reactor
Adapted from Choi (2001) and Yuttana (2007)

The effect of electrode's position in ELALR

This experiments was conducted in order to investigate the untreated zone since neither BCR nor ELALR reactors can solve this problem. The position of electrodes were investigated in the best downcomer condition (2" of downcomer diameter, 100 cm of height, and 135º of connector configuration). The electrodes were lifted up 5-cm from the center of downcomer outlet as shown in Figure 4.32. When changing the position of the electrodes, the mode of recirculation was dramatically changed. It was found that there was no circulation in downcomer since no treated zone occurred beneath the electrodes. Finally, the system was turned into a bubble column reactor with large amount of untreated wastewater in downcomer. As a conclusion, the electrodes performed as a small air sparger that produced micro-size bubbles. The position of electrode and downcomer connector was related external loop circulation mechanism, since flow in downcomer would occur only from the bubble space replacement at cathode region.

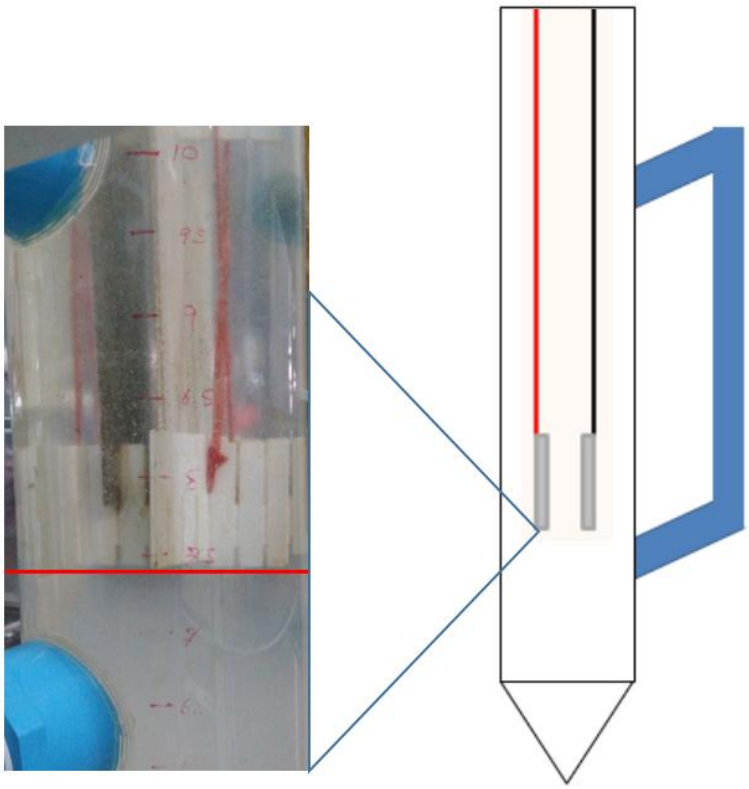

Figure 4.32 Untreated zone beneath the electrode position in external loop airlift reactor

4.5.6. Prediction model

Mathematical model had been applied to analyze the turbidity removal efficiency to describe its removal behavior. These mathematic models had been developed into three forms using three different assumptions to describe the effect of each parameter including polynomial function, logarithm relation, and s-curve. The data was analyzed by MINITAB 17 program to form the prediction model of polynomial and logarithm function, while the solver function in MS Excel was applied to create a nonlinear regression of s-curve or logistic curve. The factors used in these models are shown in Table 4.8.

Table 4.8 Factors and levels of the design of experiment

Factor	Original factors(x_i)	Coded factor		
		-1	0	1
Oil concentration [g/l]	x_1	0.5	1	1.5
Gap between electrode [cm]	x_2	1.25	2.5	3.75
Current density [A/m^2]	x_3	75	100	125
Reaction time [minute]	x_4	30	60	90

4.5.6.1. First mathematical model : polynomial function

Minitab 17 had formed 31 experimental sets of DOE for analysing 4 parameters with 3-level each. After 31 experiments, the correlation among these parameters is shown in Table 4.9. It could be seen that the current density (x_3) and the reaction time (x_4) played an important role on the turbidity removal efficiency due to the P-value < 0.005 and high range of F-value. In addition, the oil concentration in two significant parameters (x_1x_3, x_1x_4) also influenced the turbidity removal.

Table 4.9 Parameter analysis table

Linear	F-Value	P-Value	Square	F-Value	P-Value	2-way interaction	F-Value	P-Value
x_1	1.74	0.206	x_1^2	5.13	0.038	x_1x_2	6.8	0.019
x_2	0.07	0.79	x_2^2	3.18	0.094	x_1x_3	12.65	0.003
x_3	65.03	0	x_3^2	2.09	0.168	x_1x_4	28.17	0
x_4	191.51	0	x_4^2	5.17	0.037	x_2x_3	6.29	0.023
						x_2x_4	1.16	0.298
						x_3x_4	3.97	0.064

Finally, an uncoded unit of regression equation was provided by MINITAB 17 with 0.9544 of R^2 which was a representative of the goodness of fit of the prediction model (>0.90 is preferable) (Hu, 1999) as shown in Eq. 4.3.

$$\%\text{Turbidity removal} = -75.4 + 41.2x_1 + 42.1x_2 - 0.920x_3 + 0.470x_4 - 19.13x_1^2 - 2.41x_2^2 + 0.00488x_3^2 + 0.00534x_4^2 - 11.78x_1x_2 + 0.804x_1x_3 - 0.999x_1x_4 - 0.2266x_2x_3 + 0.0810x_2x_4 + 0.00750x_3x_4 \quad \text{(Eq. 4.3)}$$

Where;

x_1 = oil concentration (g/l)

x_2 = gap between electrode (cm)

x_3 = current density (A/m^2)

x_4 = Reaction time (min)

According to the prediction model, validation of the equation was required to ensure that the prediction could be applied to other experimental condition as well. The randomized experiments , therefore, was conducted. The prediction was found high accurate in the lag stage and slightly overestimate (≈ 100% removal) in stablilizing stages; however, the efficency prediction in the reactive stages was imprecise. (See in Appendix V)

4.5.6.2. Second mathematical model: Logarithm function

According to the first model, which was later found some limitation of prediction, the second experimental sets and prediction model would bring another

hypothesis to form prediction model. This model focused on the time interval as an outcome with specific removal efficiency. As turbidity treatment efficiency had been divided into 3 stages: lag, reactive and stabilizing stages. This model would give another specific terms : t_{lag} and t_{steady}. The duration of the system that used to achieve the lag stage was called t_{lag} and the time that the ECF system can reach 80% turbidity removal was given in term of t_{steady}. The conventional logarithm form in Eq. 4.4 was applied to solve this prediction model

$$\eta_{turbidity} = 100 - 100e^{-k(t-T_{lag})} \quad \text{(Eq. 4.4)}$$

Where ; $\eta_{turbidity}$ = turbidity removal efficiency

k = constant value in logarithm equation (min^{-1})

t_{lag} = lag stage period (min)

Moreover, the constant value of logarithm function could be calculated by solving the equation as shown in Eq 4.5.

$$k = \frac{-ln\,(0.2)}{(T_{steady}-T_{lag})} \quad \text{(Eq. 4.5)}$$

Finally, the Minitab 17 had formed the polunomial prediction model of t_{lag} and t_{steady}

$$t_{lag} = -26.05x_1^2 + 0.58x_2^2 - 0.00024x_3^2 + 131.4x_1 - 8.51x_2 - 0.108x_3 - 3x_1x_2 - 0.49x_1x_3 + 0.1x_2x_3 + 7.6 \quad \text{(Eq. 4.6)}$$

$$t_{steady} = -9x_1^2 - 1.32x_2^2 + 0.002724x_3^2 + 127.4x_1 + 5.9x_2 - 5.8x_3 + 9.8x_1x_2 - 0.85x_1x_3 - 0.052x_2x_3 + 343.1 \quad \text{(Eq. 4.7)}$$

Where; x_1 = oil concentration (g/l)

x_2 = gap between electrode (cm)

x_3 = current density (A/m^2)

From the calculation in Eqs. 4.5 – 4.7, the constant k was influenced by the current density more than oil concentration or gap between electrodes. The constant k in every oil concentration was between 0.011 – 0.065 min^{-1} incresing with current density. After the prediction equations were formed, the equation validation from serveral randomized experiments were conducted. This model could perform higher precision and accuracy than the first model. However, this prediction value was limited

to the operating condition of low oil concentration (0.5 - 2 g/l) and high current density (100 - 125 A/m^2). Another prediction model was proposed to provide more universal usage for turbidyt removal efficiency.

4.5.6.3. Third mathematical model: logistic function

This prediction had been applied via nonlinear regression approach. The pattern of turbidity removal efficiency of cutting-oily wastewater could be summarize as follow;

1. The turbidity could define as no change in lag stage, therefore, the horizontal line appeared.
2. After achieve lag stage. The turbidity treatment efficiency was dramatically increase within 15 – 30 minutes after the lag period.
3. When the system provide steady stage, little turbidity change was found since most of the particle had been removed during reactive stage already. The turbidity removal showed a horizontal line again.

These 3 summaries was the same description as logistic function, s-curve or sigmoid equation. The conventional sigmoid equation form is shown in Eq. 4.8.

$$Y = \frac{100}{1+ e^{-k(x-x_{50})}} \quad \text{(Eq. 4.8)}$$

Where; Y = output

k = steepness of the curve

x = input

x_{50} = input factor that provide 50% of output

Thus, the third prediction model in sigmoid curve form is presented in Eq. 4.9.

$$\%\,\eta_{\text{turbidity removal}} = \frac{100}{1+ e^{-k(t-t_{50})}} \quad \text{(Eq. 4.9)}$$

Where; k = the steepness

t_{50} = the time that the efficiency reached 50%.

The nonlinear regression of sigmoid steepness (k) and half treatment time (t_{50}) are shown in Eq. 4.10 and 4.11, respectively.

$$k = 0.273C_0^{-0.5} \quad \text{(Eq. 4.10)}$$

$$t_{50} = 3630e^{-6.07I} + 27.6C_0^{0.45}+25.97 \quad \text{(Eq. 4.11)}$$

In order to validate the predicting equation, 11 randomized experiments were conducted to evaluate the prediction model. The result of the validation reported that this model could provide less than 21% of deviation as well (See in Appendix IV)

Furthermore, the example of fitting sigmoid equation of 0.5 g/l oil concentration, 125 A/m^2 and 2.5-cm gap of electrodes is displayed in Figure 4.33. The prediction equation can be constructed as expressed in Eq. 4.12;

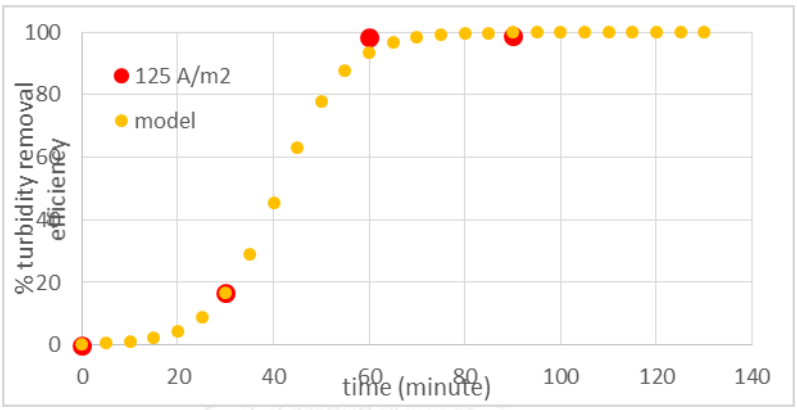

Figure 4.33 Example of Sigmoid Model Fitting

$$\%Turbidity\ removal = \frac{100}{1+e^{[-0.386(t-48)]}} \qquad \text{(Eq.4.12.)}$$

This model had continuously developed from the previous models to minimize some errors. However, the model could not be applied for universal condition since the observed parameter was in a small range. In addition, other parameters such as wastewater volume and number of electrodes should be included in the further prediction equation.

In addition, the non-linear regression of k and t_{50} of the ECF in the ELALR are displayed in Equations 4.12 and 4.13 with 10.81 % and 33.03% deviation of t_{50} and k, respectively

$$k = \frac{0.875}{C_{oil}^{0.3} D_{DC}^{0.19} V^{0.6}} + \frac{0.692}{V^{2.42}} \qquad \text{(Eq.4.12.)}$$

$$t_{50} = 77.8\, C_{Oil}^{0.45} \qquad \text{(Eq.4.13.)}$$

Where; C_{oil} = Initial Concentration of Oil (g/L)

D_{DC} = Diameter of Downcomer (m)

V = Total Volume of Reactor (Liter)

However, this prediction model was available for 100 A/m^2 of current density and 2.5 cm of distance between electrodes. Improving the prediction model required wider range of parameters; therefore, the operating condition and reactor configuration could be combined together in the future experiments.

4.5.6.4. Comprison of mathematic model

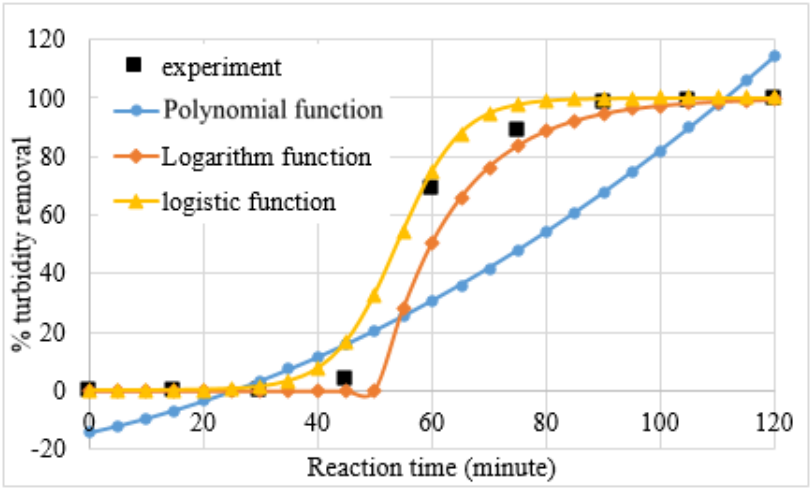

Figure 4.34 Comparison of mathematic model

To demonstrate the fittest prediction function comparing among these three models, Figure 4.34 shows that the polynomial function gave the least prediction accuracy. While, logistic function or S-curve is the most fitted function which provide very close prediction model and the logarithm function is defined as the second best prediction model as well.

4.5.7. Summary

Mathematical model were applied to predict treatment efficiency. In practice, these prediction model could help to estimate the adequate reaction time in order to design the reactor tank and operating condition. However, wider range of parameters should be considered for observing its effects and providing more universal prediction model.

4.6. ELECTROCOAGULATION/FLOTATION IN CONTINUOUS SYSTEM

The objective of this section is to investigate the capability of electrocoagulation in the continuous scheme. The studies were divided into two categories: Turbidity removal efficiency and flow pattern in reactor. The first investigation was done to verify the feasibility of ECF in continuous process. The latter was operated to examine the flow behavior of ECF in both bubble column and air lift reactor with the residence time distribution principle.

4.6.1. Treatment efficiency

In order to study the feasibility of ECF for continuous system, the turbidity removal efficiency of ECFs were observed versus time to determine the performance of the reactors. Two configurations of ECFs were selected from the best conditions of batch system to examine, which were BCR and Air lift reactor (with 2" ID with 135° and 100 cm length of external loop). The reactors were operated at flow rate of 10 liter per hour, in the other word, 2.5 and 2.9 hours for HRT in bubble column and external loop airlift reactor respectively, with the initial oil concentration at 1 g/L. The results were depicted in Figure 4.35.

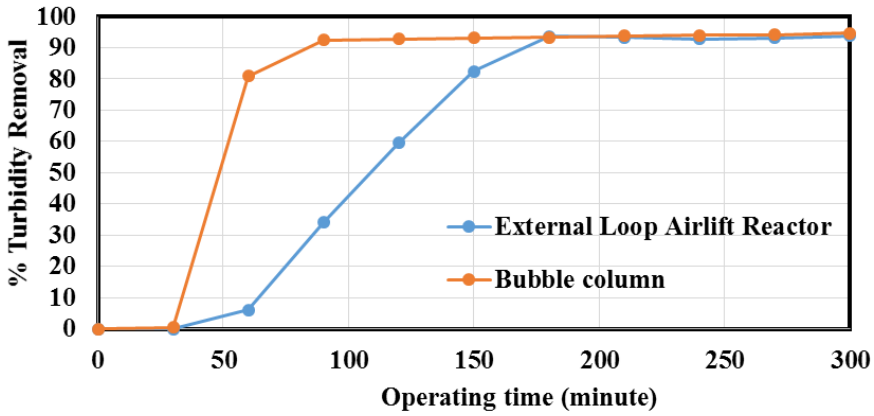

Figure 4.35 Turbidity removal efficiency of ECF in continue system (Flow Rate 10 LPH and Initial Oil Concentration 1 g/L)

The result in Figure 4.36 shows that the turbidity removals of both reactors were rose gradually from 0 to steadily 92 % after the operating time was surpassed 30 minute. Due to the stability of efficiency at steady state, it could be concluded that both types of reactors could absolutely operate in continuous process. However, these two reactors

used different amount of time to reach their maximum efficiency. As seen in the figure, BCR reactor took approximately 90 minute to get the highest value while ELALR used around 180 minute due to the different liquid volume. These significantly difference indicated the different of flow scheme occurred in both reactors which would be further studied in the next section. Moreover, the sludge generation at the surface of water was measured thickness as function of time to study the sludge quality of both reactors. The results are shown in Figure 4.36

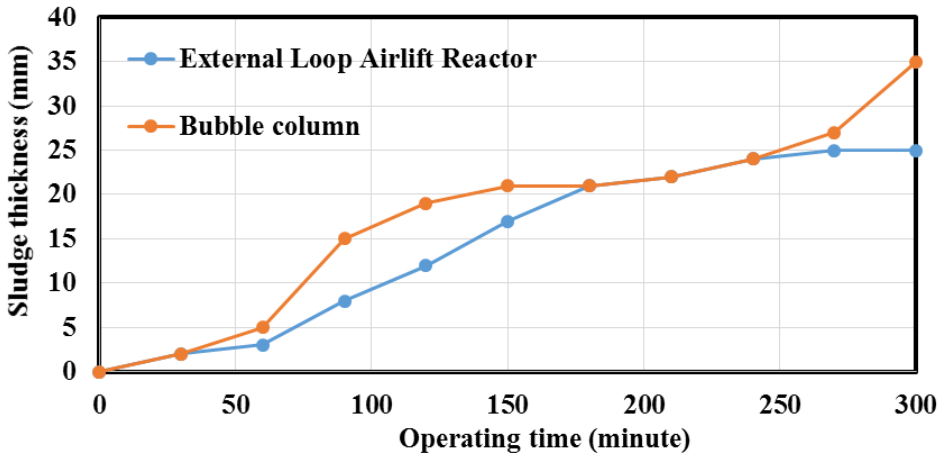

Figure 4.36 Sludge generation of continuous system

The results in figure 4.36 describes that the sludge thickness, for both reactors, were raised proportionally with operating time. It can be clearly seen that, at operating time less than 180 minute, the thickness of sludge for BCR was higher than ELALR because of its higher efficiency of removal within that operating period. Afterward, the sludge thicknesses of both equipment were approximately equal. However, after time surpassed 230 minute, sludge thickness of BCR was again raised higher than ELALR; which means that the sludge from ELALR was denser than BCR. These results were due to the different flow scheme of both reactors which tend to create different property of sludge (detail in section 4.5). Consequently, among the continuous system of ELALR and BCR, both reactors had equivalent turbidity removal efficiency, but the ELALR has advantage over BCR as it produced higher sludge density that ease to clean from the surface.

4.6.2. Flow pattern in continuous electrocoagulation/flotation

As mentioned in section 4.6.1, reactor configuration affected the flow pattern in reactors and directly influenced the sludge density. Therefore, in this section, the flow patterns were examined with Residence Time Distribution (RTD) principle to analyze the difference of flow pattern between BCR and ELALR.

4.6.2.1 Flow pattern in continuous bubble column reactor

In order to examine RTD in bubble column reactor, the change in the conductivity due to the tracer was used as the signal. The 30 g/l of sodium chloride (NaCl) solution with an artificial food color (blue) was used as the tracer. The conductivity meter was applied with the probes installed in the reactor as shown in Figure 4.37 to measure the tracer signal at the inlet and outlet of the reactor.

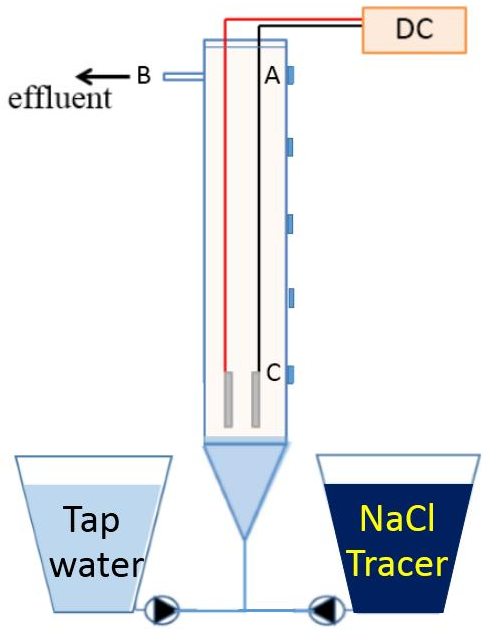

Figure 4.37 Position of conductivity sensor in bubble column reactor
(1) conductivity meter No. 1 (outlet) , (2) conductivity No.2 (Inlet)

After ECH reactor was set and operated until reached steady state, the 300 ml of tracer was injected to the column as a pulse. The conductivity represented the tracer concentration, which was transformed into the exit age distribution (E(t)) by the method shown in Appendix VI. Figures 4.48 presents the E(t) for the inlet and the outlet of the reactor.

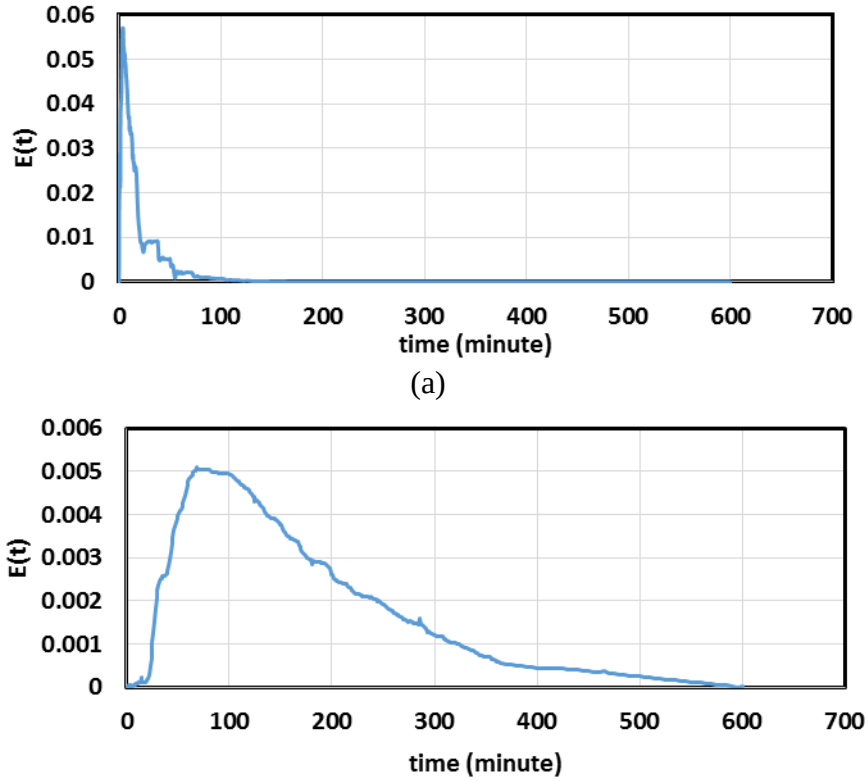

Figure 4.38 Exit age distribution of the bubble column reactor at (a) inlet and (b) outlet

Figure 4.38 (a) show the exit age distribution of the tracer at the inlet. From the graph, it was found that the tracer signal was close to the pulse signal (i.e. the ideal signal of the pulse tracer injection). At the outlet in Figure 4.38 (b), the signal was dramatically increased during 25 – 80 minutes before slowly decrease to zero at approximately 600 minutes. This curve indicated that the flow pattern in reactor was similar to the plug flow condition connected in series with the mixed flow (Levenspeil, 1999). The result was consistency with reactor configuration as shown in Figure 4.39 dividing the reactor into two parts at the electrodes. The plug flow occurred at the inlet and then converted into the mixed flow after passed through the electrodes. This change was a result of the displacement between bubble and liquid that consequently result in recirculation inside the zone.

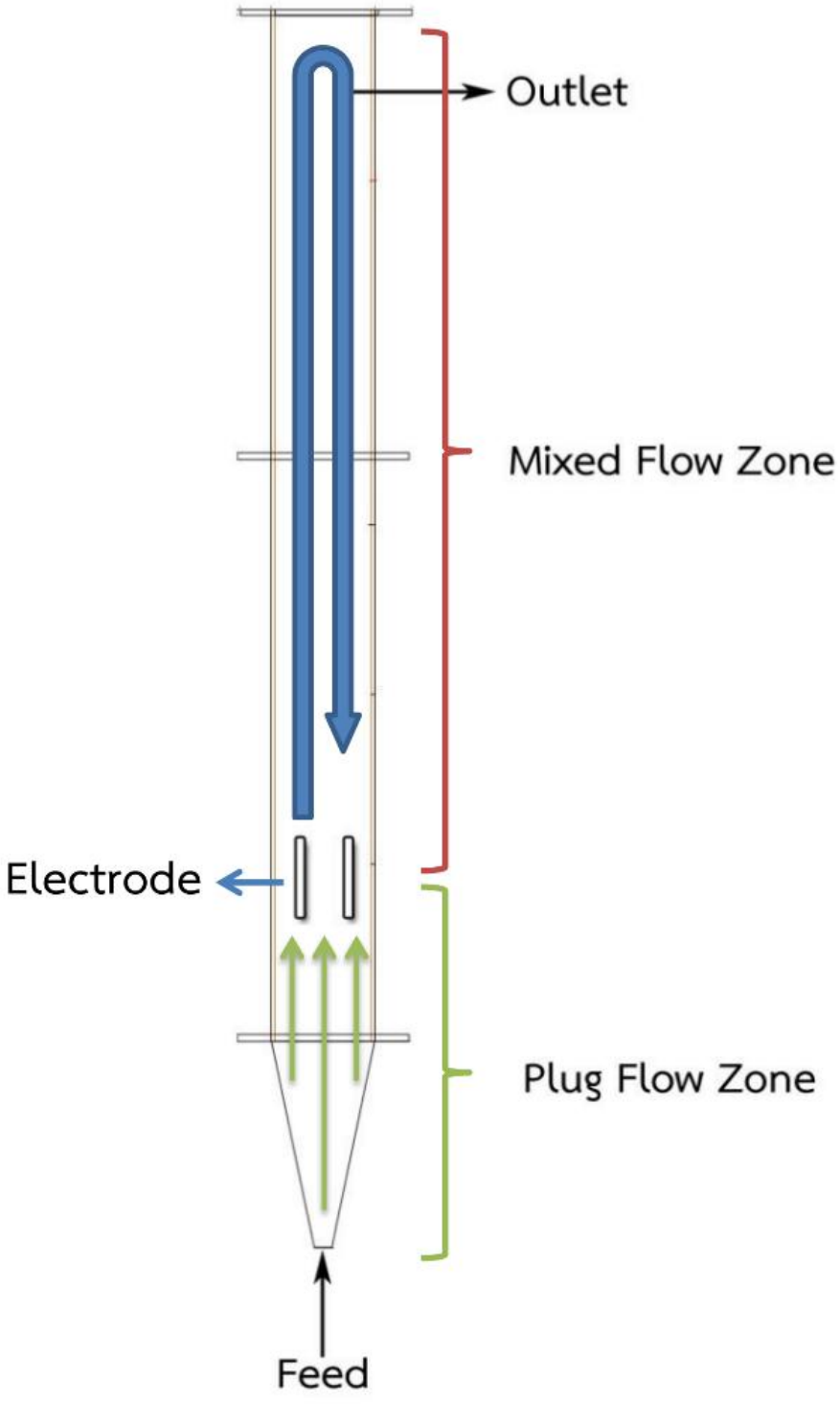

Figure 4.39 Flow pattern in bubble column ECF

4.7.2.2 Flow pattern in Continuous External Loop Airlift Reactor

The experiment in the ELALR was similarly conducted as in the BCR. However, another conductivity probe was added at the inlet of the external loop to analyze the flow into the downcomer as shown in Figure 4.40.

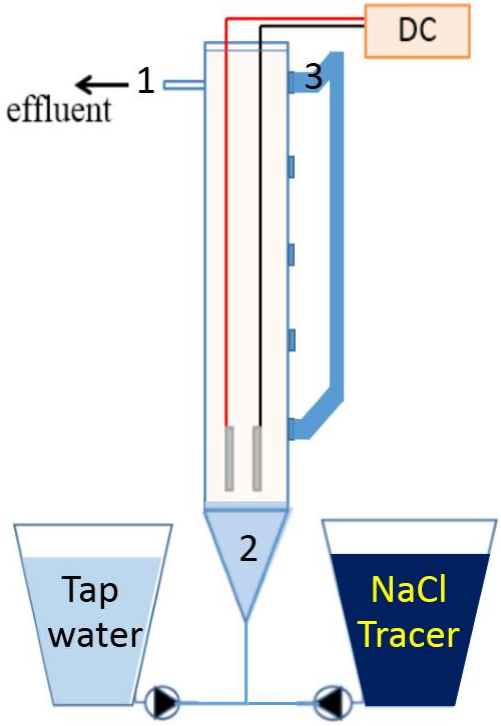

Figure 4.40 Position of conductivity sensor in external loop air lift reactor

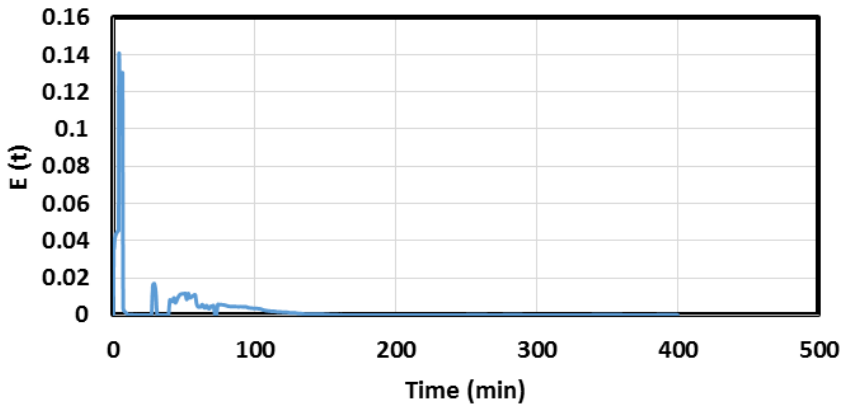

(a)

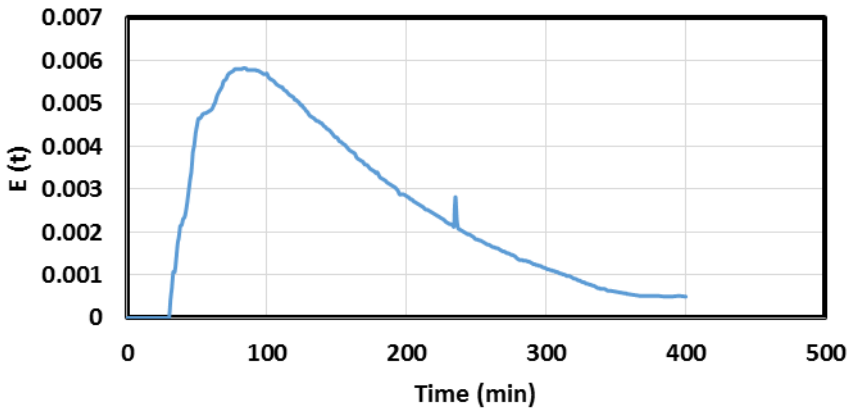

(b)

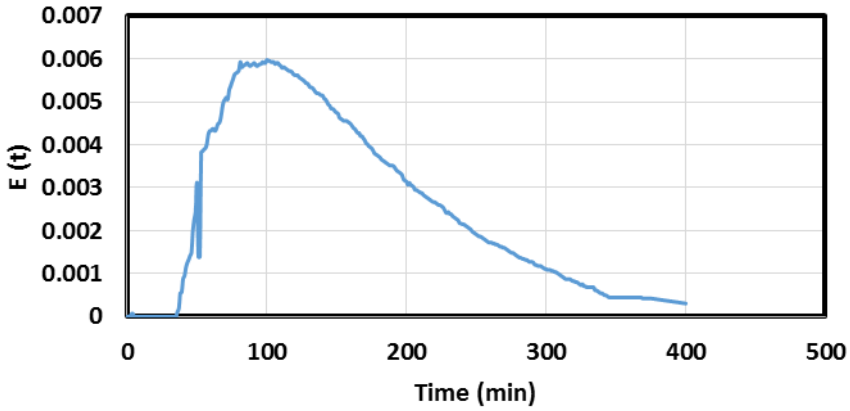

(c)

Figure 4.41 Exit age distribution of the air lift reactor
(a) at Inlet (b) at Outlet (c) at downcomer inlet

Figure 4.41 (a) indicated that the input tracer was feed appropriately as the signal was very close to the pulse signal. Meanwhile, the signal at the outlet as in Figure 4.41 (b) was similar to the outlet of the BCR meaning that the fluid flow inside the reactor was the series of plug flow to mixed flow conditions. Moreover, the signal at the inlet of the downcomer was the same as the outlet signal, which indicated that the external loop and column was performed like one completely mixed zone. The recirculation occurred rapidly between the column and the downcomer.

Although adding the external loop did not affect the overall flow inside the reactor, the recirculation occurring between the column and loop influenced the sludge property as the ELALR created denser sludge. This was due to the recirculation of the liquid in the ELALR reduce the chance of the contact between bubbles and flocs. The

sludge therefore contained less air content and was more compact. This phenomenon can be explained by the diagram in Figure 4.42.

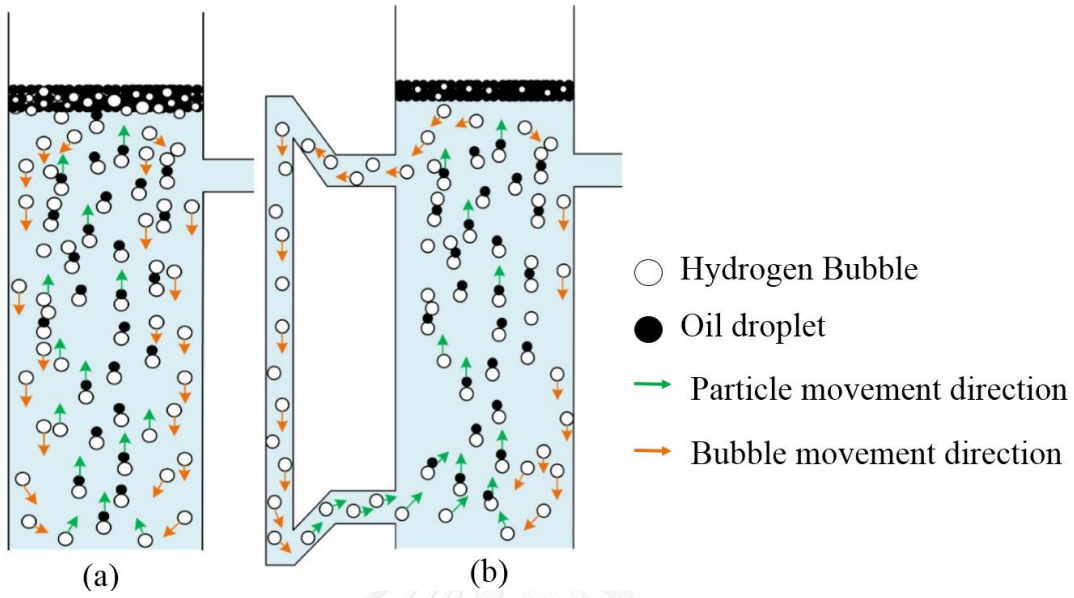

Figure 4.42 Effect of gas recirculation on sludge density
(a) Bubble Column Reactor (b) External Airlift Reactor

In addition to flow pattern, the RTD experiment data could also use to calculate the average time that substance resided inside reactor. The comparison between mean residence time and design residence time could as well imply the flow behavior in reactor. The design and experiment mean residence time of both BCR and ELALR are expressed in Table 4.10.

Table 4.10 Parameter in flow pattern model

Variable	BCR	ELALR
Design Residence Time (min)	150.0	174.0
Mean Residence Time (min)	170.2	98.9

As can be seen in Table 4.10, mean residence time of BCR was higher than the design value indicating the existence of the recirculation in the system. It conformed to previous results that the flow pattern was plug flow connected in series with mixed flow. However, for the ELALR, the mean residence time was almost half of the design residence time. According to the reactor configuration, the highest level of liquid at the top of column and external loop were equal. Therefore, the pressure head between

sections were also equal and may cause some parts in the reactor to be stagnant and became dead zone in reactor. As dead zone occurring inside reactor, the effective volume that flow in the reactor was decreased. The fluid exited from reactor faster as a result.

Moreover, the residence time distribution data was analysed with the dispersion model as well as the tank in series model. Both models were used statistic variables, for instance, mean residence time and variance to calculate the model parameters; axial dispersion number (D/uL) for dispersion model and number of tank in series (N) for tank in series model. Both parameters indicated the overall flow behaviour throughout reactor that usually in between of mixed flow and plug flow. The value nearby 0 for dispersion number referred to the plug flow behaviour, while value more than approximately 1 can be classified as the mixed flow. Meanwhile, for tank in series model, the value of N equal to 1 was referred to mixed flow behaviour and value more than approximately 10 tanks was nearly plug flow behaviour (Fogler, 2006).For this experiment, the results for both parameters were shown in Table 4.11.

Table 4.11 Axial Dispersion Number and Number of tank in series for BCR and ELALR

Variable	BCR	ELALR
Axial dispersion Number (D/uL)	0.133	0.110
Number of Tank in Series (N)	3	4

The values of the models parameters, as in Table 4.11, were about 0.1-0.15 and 3-4 for dispersion model and tank in series model, respectively. As the value was close to 0 for D/uL and 1 for N, it could be determine that the overall flow pattern of both reactor were close to the mixed flow behavior more than the plug flow. These results were consistent with the previous analysis, which was summarized that the flow inside the reactor was similar to plug flow in series with mixed flow.

4.6.3. Summary

In conclusion, both BCR and ELALR flow pattern were in the transition regime between the plug flow and the mixed flow. The plug flow behavior was occurred in the reactor the electrode while the mixed flow was above. In addition, the sludge density was raised as external air loop was equipped. The external loop helped reducing the chance of contact between floated sludge and recirculating gas by adding another way of gas to flow downward.

CHAPTER 5
CONCLUSION AND RECOMMENDATIONS

5.1. CONCLUSION

The objective of this work is to study the treatment of the cutting oil wastewater by the electrocoagulation/flotation process (ECF) with aluminium electrodes. Effects of several parameters were evaluated. The obtained results can be concluded as follow.

- The ECF can effectively treat the stable cutting oil wastewater with the highest efficiency of 99%. The variation of the turbidity removal with time consists of 3 stages i.e. lag, reactive, and stability stages, which can be explained by the amount of dissolution of aluminium in the liquid phase.
- The optimal condition of the ECF operated in the bubble column reactor (BCR) with different oil concentrations can be concluded as in Table 5.1. Effects of oil concentration can be clearly seen on the reaction time to reach the maximum efficiency.

Table 5. 1 Optimal operating condition of the ECF in BCR

Operating condition	Oil concentration (g/l)		
	0.5	1.0	1.5
Current density (A/m^2)	100		
Distance between electrodes (cm)	2.5		
Reaction time (minute)	60	90	120

- The same efficiency can be obtained from the operation in the external airlift reactor (ELALR) with the same configuration. However, less oil sludge was produced in this reactor type. The 135º tilt-up with 100 cm height and 5.1 cm inner diameter was found to be the best downcomer in this work.

Three models were applied to predict the treatment efficiency of the ECF in this study, including polynomial model, logarithm model, and sigmoid model. The best fit for turbidity removal was the sigmoid curve. The current density and the reaction time were the important parameters on the treatment efficiency indicated by the ANOVA analysis. The details of each model and their prediction errors comparing to the experimental results are demonstrated in Table 5.2

Table 5. 2 The summary of Prediction model

Prediction approach	Equation	Error of prediction
Polynomial Equation	%Turbidity removal = -75.4 +41.2x_1+42.1x_2 – 0.920x_3 + 0.470x_4 – 19.13x_1^2 – 2.41x_2^2 +0.00488x_3^2 +0.00534x_4^2 -11.78x_1x_2 + 0.804x_1x_3 – 0.999x_1x_4 – 0.2266x_2x_3 + 0.0810x_2x_4 +0.00750x_3x_4	40-50%
Logarithm Equation	$\%\ turbidity\ removal = 100 - 100e^{-(t_{steady}-t_{lag})}$ t_{lag} = -26.05x_1^2 + 0.58x_2^2 – 0.00024x_3^2+131.4x_1 – 8.51x_2 – 0.108x_3 - 3x_1x_2 – 0.49x_1x_3 +0.1x_2x_3 + 7.6 t_{steady} = -9x_1^2 – 1.32x_2^2 + 0.002724x_3^2+127.4x_1 + 5.9x_2 – 5.8x_3 + 9.8x_1x_2 – 0.85x_1x_3 - 0.052x_2x_3 + 343.1	30%
Sigmoid Equation (BCR)	% turbidity removal = $\frac{100}{1+e^{-k(t-t_{50})}}$ k=0.273$C_0^{-0.5}$, $t_{50} = 3630e^{-6.07I} + 27.6C_0^{0.45}$+25.97	21%
Sigmoid Equation (ELALR)	% turbidity removal = $\frac{100}{1+e^{-k(t-t_{50})}}$ $k = \frac{0.875}{C_{oil}^{0.3} D_{DC}^{0.19} V^{0.6} \Delta H^{0.02}} + \frac{0.692}{V^{2.42}}$, $t_{50} = 77.8\ C_{Oil}^{0.45}$	30%

Where; x_1 = oil concentration (g/l) x_2 = gap between electrode (cm)
x_3 = current density (A/m2) x_4 = Reaction time (min)
k = the steepness t_{50} = half time treatment
C_{oil} = oil concentration (g/L) D_{DC} = Diameter of downcomer (m)
V = Total volume of reactor (l)
ΔH = Difference head between column and Inlet of downcomer (m)

- The continuous operation with the optimal configuration from the batch experiment provided the slightly lower efficiency in both BCR and ELALR. This was due to the constant feeding of 10 l/hr of the cutting oil wastewater into the reactor without sufficient reaction time.
- The flow pattern obtained from the RTD study in both BCR and ELALR consisted of the plug flow below the electrodes and the CSTR from the electrodes onwards. Besides, a dead zone can be found in the case of the

ELALR. These flow patterns can affect the process efficiency under the continuous operation, which could be used for improving the overall process performance.

5.2. RECOMMENDATIONS

According to the experimental results in this work, some recommendations for a further study can be proposed as follow;

1. ECF processes in both BCR and ELALR should be applied to treat real metalworking wastewater, which composes of metal scatters and small solid particles in order to study effects of other parameters on the treatment efficiency.
2. The flow pattern in the reactor should be further analyzed in order to enhance the process efficiency. For example, larger bubbles, apart from micro-bubbles of H_2 gas produced from the electrodes, should be applied to decrease or eliminate the plug flow zone under the electrodes at which the wastewater was rarely treated.
3. The hydrodynamics of the generated hydrogen gas should be investigated.
4. Further analysis on the flow patter, especially for the liquid recirculation in an airlift reactor, should be conducted in order to improve the treatment efficiency.

REFERENCES

Abass O.Alade, A. T. J., Suleyman A. Muyubi, Mohamed I. Abdul Karim and Md. Zahangir Alam. (2011). Removal of oil and grease as emerging pollutants of concern (EPC) in wastewater stream. *IIUM Engineering Journal, 12*(4), 161-169.

Althers, G. (1998). Put the Breaks on Wastewater Emulsions. *Chemical Engineering, 102*(2), 82-88.

Bensadok, K., Benammar, S., Lapicque, F., & Nezzal, G. (2008). Electrocoagulation of cutting oil emulsions using aluminium plate electrodes. *Journal of Hazardous Materials, 152*(1), 423-430. doi: http://dx.doi.org/10.1016/j.jhazmat.2007.06.121

Choi, K. H., Chisti, Y., & Moo-Young, M. (1996). Comparative evaluation of hydrodynamic and gas—liquid mass transfer characteristics in bubble column and airlift slurry reactors. *The Chemical Engineering Journal and the Biochemical Engineering Journal, 62*(3), 223-229. doi: http://dx.doi.org/10.1016/0923-0467(96)03085-0

Coca, J., GutiÉRrez, G., & Benito, J. (2011). TREATMENT OF OILY WASTEWATER. In J. Coca-Prados & G. Gutiérrez-Cervelló (Eds.), *Water Purification and Management* (pp. 1-55): Springer Netherlands.

Dixit, U. S., Sarma, D. K., & Davim, J. P. (2012). Machining with Minimal Cutting Fluid. 9-17. doi: 10.1007/978-1-4614-2308-9_2

Emel Kuram, B. O. a. E. D. (2013). Environmentally Friendly Machining: Vegetable Based Cutting Fluids. *Springer-Verlag Berlin Heidelberg*.

Essadki, A. H., Bennajah, M., Gourich, B., Vial, C., Azzi, M., & Delmas, H. (2008). Electrocoagulation/electroflotation in an external-loop airlift reactor—Application to the decolorization of textile dye wastewater: A case study. *Chemical Engineering and Processing: Process Intensification, 47*(8), 1211-1223. doi: http://dx.doi.org/10.1016/j.cep.2007.03.013

. Flocculation Fundamentals. (2013) *Encyclopedia of Colloid and Interface Science* (pp. 478): Springer Berlin Heidelberg.

Fogler, H. S. (2006). Distributions of Residence Times for Chemical Reactors *Elements of Chemical Reaction Engineering* (4th ed.): Pearson Education, Inc.

Ge, J., Qu, J., Lei, P., & Liu, H. (2004). New bipolar electrocoagulation–electroflotation process for the treatment of laundry wastewater. *Separation and Purification Technology, 36*(1), 33-39. doi: http://dx.doi.org/10.1016/S1383-5866(03)00150-3

Giannis, A., Kalaitzakis, M., & Diamadopoulos, E. (2007). Electrochemical treatment of olive mill wastewater. *Journal of Chemical Technology & Biotechnology, 82*(7), 663-671. doi: 10.1002/jctb.1725

Holt, P. K., Barton, G. W., Wark, M., & Mitchell, C. A. (2002). A quantitative comparison between chemical dosing and electrocoagulation. *Colloids and Surfaces A: Physicochemical and Engineering Aspects, 211*(2–3), 233-248. doi: http://dx.doi.org/10.1016/S0927-7757(02)00285-6

Huijuan Liu, X. Z., and Jiuhui Qu. (2010). Electrocoagulation in water treatment *Electrochemistry for the environment* (pp. 246): Springer.

Kun Tong, Y. Z., Guohua Liu, Zhangfang Ye, Paul K. Chu. (2013). Treatment of heavy oil wastewater by a conventional activated sludge process coupled with an immobilized biological filter. *International Biodeterioration & Biodegradation*, 65-71.

M.Armenante, P. (2014). Coagulation and flocculation.

Marques, A. A. C. a. M. R. d. C. (2012). Electrolytic Treatment of Wastewater in the Oil Industry. *New Technologies in the Oil and Gas Industry*.

Nagai, N., Takeuchi, M., Kimura, T., & Oka, T. (2003). Existence of optimum space between electrodes on hydrogen production by water electrolysis. *International Journal of Hydrogen Energy, 28*(1), 35-41. doi: http://dx.doi.org/10.1016/S0360-3199(02)00027-7

oil/water separator. (2014, 11 5). *Wikipedia*. Retrieved from http://en.wikipedia.org/wiki/API_oil-water_separator

Produced water treatment. (2014, 11 5). *e-process*. Retrieved from http://www.eprocess-int.com/products/oil-water-separation/

R.Alther, G. (1997). Oils found in wastewater

Rujiruttanakul, Y., & Pavasant, P. (2011). Influence of configuration on the performance of external loop airlift contactors. *Chemical Engineering Research and Design, 89*(11), 2254-2261. doi: http://dx.doi.org/10.1016/j.cherd.2011.02.017

Sam Keith, L. I. (2015). *PRIORITY DATA NEEDS FOR ALUMINUM* Vol. 2015. D. Jones (Ed.) Retrieved from http://www.who.int/water_sanitation_health/dwq/wsh0304_53/en/index4.html

Tramfloc, inc. (2014, 11 4). *Polymer precipitation and dewatering*. Retrieved from http://tramfloc.com/flocculants-precipitation-and-dewatering/

US.EPA. (2015). Drinking Water Treatability Database : Conventional Treatment. Retrieved 15 July 2015, 2015, from http://iaspub.epa.gov/tdb/pages/treatment/treatmentOverview.do?treatmentProcessId=1934681921

Yang, C.-L. (2007). Electrochemical coagulation for oily water demulsification. *Separation and Purification Technology, 54*(3), 388-395. doi: http://dx.doi.org/10.1016/j.seppur.2006.10.019

APPENDIX

APPENDIX I

EMULSION CHARACTERIZATION

1. WASTEWATER CHARACTERIZATION

1.1. Turbidity measurement

According to turbidity measurement, 2100P Turbidimeter (Hach) was employed in the experiment. This turbidity meter was capable to detect the turbid sample under 1000 NTU; therefore, wastewater dilution was required. The standard curve of dilution is shown in figure 3.2, with 0.9989-R^2 of the linear relationship between oil concentration and turbidity. The linear function is shown in Equation I.1.

$$Turbidity = (1414.6 \times Oil\ concentration) + 0.18 \quad \text{(Eq. I.1)}$$

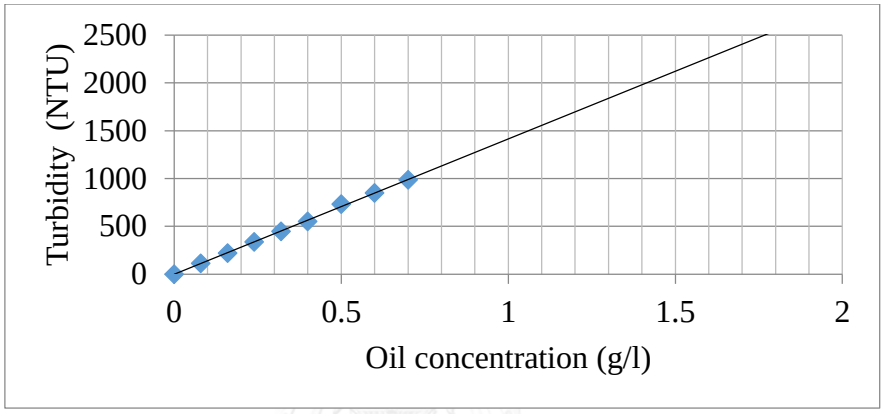

Figure I. 1 Turbidity in different cutting oil concentration

In addition, the pictorial observation was still need in order to validate the range of particle size. Before observe the oil droplet size via microscope, 0.5% O Red Oil in isopropanol or Sudan red was dropped into the synthetic wastewater in order to stain the oil droplet for 5 minutes. The result shows that the stained oil presenting in reddish small droplet (1-2 µm). While, water droplet where presenting in transparent were found in macro size (8-10 µm).

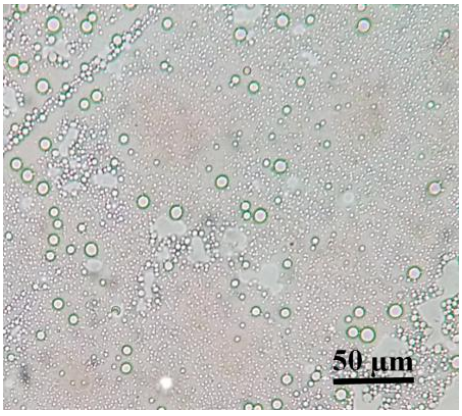

Figure I.2 oil droplet size under microscope

1.2. Particle size distribution

The droplet size distribution was analyzed by the laser particle size analyzer. The result would show the intensity of each size of oil droplet in percent by volume. This measurement process uses laser light scattering technique to estimate the average droplet size. The selected parameter from the analyzing program was $d_{3,2}$ which was the representative of the average diameter of sphere that had sphere volume equivalent to its surface area. This parameter was known as Sauter mean diameter (SMD). As a result, the droplet size was increase with higher oil concentration due to the agglomeration of oil droplet to from a larger droplet.

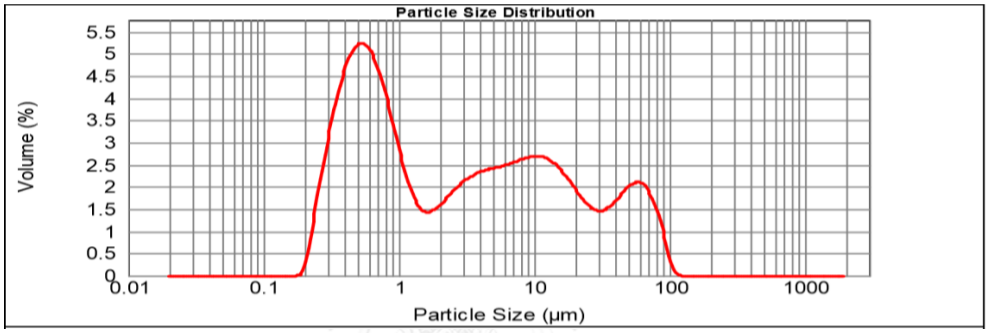

(a) 0.5 g/l SMD =1.033µm

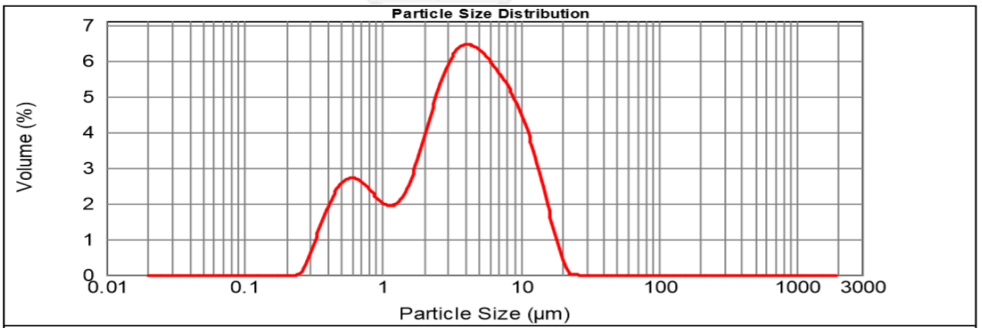

(b) 1.0 g/l SMD = 1.830 µm

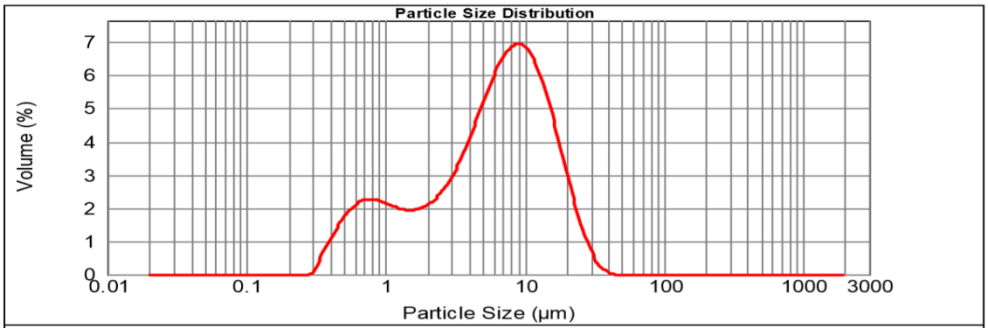

(c) 1.5 g/l SMD = 2.504 µm

Figure I.3 oil droplet size distribution

APPENDIX II

TREATMENT OF EMULSION BY CHEMICAL COAGULATION

Chemical coagulation of cutting oily wastewater: the optimal alum dose

Table II. 1 Chemical coagulation of 0.5 g/l oil concentration

Alum (mg/l)	COD (mgO_2/l)	% removal	Turbidity (NTU)	% removal
0	1220.184	0.000	628	0.000
40	1141.325	6.463	620	1.274
80	665.157	45.487	348	44.586
120	167.254	86.293	44.4	92.994
160	342.879	71.899	186	70.382
200	659.278	45.969	258	58.917
240	784.201	35.731	301	52.070

Table II.2 Chemical coagulation of 1.0 g/l oil concentration

Alum (mg/l)	COD (mgO_2/l)	% removal	Turbidity (NTU)	% removal
0	3489.765	0.000	1390	0.000
40	3148.148	9.789	1030	25.899
80	2469.136	29.246	963	30.719
120	1419.753	59.317	672	51.655
160	185.185	94.693	85.1	93.885
200	617.284	82.312	548	60.576
240	957.347	72.567	896	35.540

Table II.3 Chemical coagulation of 1.5 g/l oil concentration

Alum (mg/l)	COD (mgO_2/l)	% removal	Turbidity (NTU)	% removal
0	4562.142	0.000	2410	0.000
40	4248.659	6.871	2357	2.199
80	3015.239	33.907	1754	27.220
120	2053.452	54.989	1168	51.535
160	934.214	79.522	854	64.564
200	290.436	93.634	87.8	96.357
240	538.213	88.203	361	85.021

Chemical coagulation of cutting oily wastewater: the effect of initial pH

Table II.4 Chemical coagulation of 0.5 g/l oil concentration in different initial pH

Initial pH	% turbidity removal	% COD removal	final pH
3	12.45	32.34	2.1
5	23.86	51.02	2.3
7	37.95	79.24	4.7
8	95.31	86.98	6.3
9	96.27	93.45	6.4
11	78.25	72.01	9.2

Table II.5 Chemical coagulation of 1.0 g/l oil concentration in different initial pH

Initial pH	% turbidity removal	% COD removal	final pH
3	11.64	34.26	2.6
5	12.4	48.53	3.1
7	16.5	65.25	5
8	98.47	99.59	6.4
9	98.9	95.5	7.3
11	52.36	74.3	9.4

Table II.6 Chemical coagulation of 1.5 g/l oil concentration in different initial pH

Initial pH	% turbidity removal	% COD removal	final pH
3	25.14	36.42	2.8
5	39.65	53.48	3.5
7	56.24	75.24	5.6
8	97.25	88.14	6.1
9	98.75	91.24	7.6
11	53.37	21.23	9.4

Chemical coagulation of cutting oily wastewater: Total dissolved aluminum

Table II.7 Molecular weight of alum

Substance/element	MW	No.	
$Al_2(SO_4)_3$			
Al	26.981538	2	53.96308
S	32.065	3	96.195
O	15.9994	12	191.9928
		total	342.1509
H_2O			
H	1.00794	2	2.01588
O	15.9994	1	15.9994
		total	18.01528

Aluminum sulfate: $Al_2(SO_4)_3$ 16 H_2O (assumed that the purity of alum was 100%)

1 g of alum = $\frac{1\ g}{342.1509+(16\times 18.01528)g/mol}$ = 0.001586306 mol

Table II.8 The content of each elements in 1 g of Alum

Elements	mol molecule	Mass (g)	% by mass
Aluminum (Al)	0.003173	0.085602	8.5602
Sulfur (S)	0.004759	0.152595	15.2595
Oxygen (O)	0.044417	0.710638	71.0638
Hydrogen (H)	0.050762	0.051165	5.1165

Table II.9 The alum dose in Chemical coagulation of 1.0 g/l

Alum dose (mg/l)	Calculated Al (mg/l)	Effluent (mg/l)	Sludge (mg/l)
0	0	0.422	ND
20	1.712039	1.9308	ND
40	3.424078	3.6625	ND
60	5.136117	3.669	ND
80	6.848157	3.226	2.583
120	10.27223	5.7904	5.3
160	13.69631	6.461778	6.674
200	17.12039	8.6272	7.879

- ND = No data since no sludge/floc was formed

APPENDIX III

ELECTROCOAGULATION/FLOTATION IN BUBBLE COLUM

Table III. 1 The turbidity removal efficiency from ECF process of 0.5 g/l of oil concentration in different operating condition

Current density	75 A/m^2			100 A/m^2			125 A/m^2		
Gap	1.25	2.5	3.75	1.25	2.5	3.75	1.25	2.5	3.75
0	0.00	0.00	0.00	0.00	0.00	0.00	0.00	0.00	DC limitation
15	0.00	0.00	0.00	0.00	0.00	0.00	0.00	0.00	
30	0.00	0.00	0.00	0.00	0.00	0.00	16.55	0.00	
45	2.45	5.75	1.47	53.49	52.74	48.25	72.60	70.30	
60	23.15	44.33	28.83	88.72	83.10	91.31	98.51	98.07	
75	59.24	74.57	51.30	89.24	88.76	93.67	99.21	99.24	
90	70.85	84.21	91.46	91.83	94.32	94.12	99.69	99.36	
105	94.14	97.66	96.39	98.42	96.22	96.80	99.80	99.65	
120	95.96	98.72	97.41	99.24	98.72	97.25	99.99	99.98	

Table III. 2 The turbidity removal efficiency from ECF process of 1.0g/l of oil concentration in different operating condition

Current density	75 A/m^2			100 A/m^2			125 A/m^2		
Gap	1.25	2.5	3.75	1.25	2.5	3.75	1.25	2.5	3.75
0	0.00	0.00	0.00	0.00	0.00	0.00	0.00	0.00	DC limitation
15	0.00	0.00	0.00	0.00	0.00	0.00	0.00	0.00	
30	0.00	0.00	0.00	0.00	0.00	0.00	4.38	0.00	
45	0.00	0.00	0.00	0.00	0.00	0.00	19.85	11.59	
60	0.00	0.00	0.00	59.3	11.94	0	86.40	61.95	
75	0.00	0.00	0.00	80.4	71.95	5.241	98.51	96.93	
90	22.44	21.26	4.76	88.7	86.78	21.42	98.53	98.51	
105	90.81	87.25	57.68	96.9	93.59	59.81	99.39	99.40	
120	98.74	92.29	73.73	98.5	98.24	78.47	99.59	99.51	

Table III. 3 The turbidity removal efficiency from ECF process of 1.5 g/l of oil concentration in different operating condition

Current density	75 A/m^2			100 A/m^2			125 A/m^2		
Gap	1.25	2.5	3.75	1.25	2.5	3.75	1.25	2.5	3.75
0	0.00	0.00	0.00	0.00	0.00	0.00	0.00	0.00	DC limitation
15	0.00	0.00	0.00	0.00	0.00	0.00	0.00	0.00	
30	0.00	0.00	0.00	0.00	0.00	0.00	0.00	0.00	
45	0.00	0.00	0.00	0.00	0.00	0.00	0.00	0.00	
60	0.00	0.00	0.00	0.00	0.00	0.00	12.41	10.95	
75	0.00	0.00	0.00	15.28	10.29	0.00	58.23	48.26	
90	2.46	1.20	0.00	37.29	27.30	25.21	89.65	80.24	
105	28.58	24.20	9.75	56.81	50.20	38.25	92.86	89.22	
120	65.98	57.62	28.37	96.24	97.01	69.25	99.26	98.47	

Stoichiometry of electrocoagulation

Anode's reaction: Oxidation $Al(s) \rightarrow Al3+ + 3e-$ (1)

$2H_2O \rightarrow O_2 + 4H+ + 4e-$ (2)

Total reaction: $Al(s) + 2H_2O \rightarrow Al3+ + O_2 + 4H+ + 7e-$ (3)

Cathode's reaction: Reduction $2H_2O + 2e- \rightarrow H_2 + 2OH-$ (4)

Redox Equation: Redox + Oxidation

$2Al(s) + 4H2O \rightarrow 2Al3+ + 2O2 + 8H+ + 14e-$ ((3) x 2) = (5)

$14H2O + 14e- \rightarrow 7H2 + 14OH-$ ((4) x 7) = (6)

$2Al(s) + 18H2O \rightarrow 2Al3+ + 2O2 + 8H+ + 7H2 + 14OH-$ ((5) + (6)) = (7)

Water's Equation: $H_2O \rightarrow H^+ + OH-$ (8)

Total Reaction: $2Al(s) + 18H2O \rightarrow 2Al3+ + 2O2 + 8H2O + 7H2 + 6OH-$ (9)

$2Al(s) + 10H2O \rightarrow 2Al3+ + 2O2 + 7H2 + 6OH-$ (10)

Solution reaction: $2Al3+ + 6OH- \rightarrow 2Al(OH)3(s)$ (11)

According to chemical equations (1-11), electrocoagulation is presented as neutralization process since there is neither pH consumption nor pH generation. The equation analysis shows that every 2 aluminum atoms released into the system, 7 hydrogen gas molecules were generated. As physical amount aspect, in the other word, every 1-g of aluminum that delivered to the water system from sacrificial anode will generate 3.17-L of hydrogen gas approximately.

The correlation between aluminum mass loss and hydrogen bubble generation

Molecular weight of Al = 26.98153860 g/mol

$1g-Al = 1\ g26.98153860gmol$

= 0.03706238 mol

mol Ratio: Al : H2 (from Eq.10.) = 2 : 7

0.03706238 mol : X

X=0.03706238 × 72

X = 0.12971833 mol

Volume of H2

PV = nRT

Where; P = atmosphere pressure = 1 atm

V = gas volume

n = mol

R = Gas constant = 0.08205746 $L{-}atmK{-}mol$

T = Temperature = 25 C (room temperature) = 298.15 K

$V{=}\ nRTP$

V=0.12971833 mol × 0.08205746 $L{-}atmK{-}mol$ × 298.15 K1 atm

V = 3.174 L

Therefore, every 1 g of sacrificial anode had released, the hydrogen gas would occurred about 3.174 L.

Sludge generation and electrode consumption

Table III. 4 Sludge generation and electrode consumption of 0.5 g/l oil concentration for 120 minute

Operating condition	75 A/m^2		100 A/m^2		125 A/m^2	
	sludge	electrode	sludge	electrode	sludge	electrode
1.25 cm	43	0.4479	46	0.5145	68	0.6033
2.5 cm	45	0.4768	47	0.5158	74	0.5981
3.75 cm	45	0.4735	50	0.548	ND	ND

The average dried sludge = 0.6 g/l

Table III. 5 Sludge generation and electrode consumption of 1.0 g/l oil concentration for 120 minute

Operating condition	75 A/m^2		100 A/m^2		125 A/m^2	
	sludge	electrode	sludge	electrode	sludge	electrode
1.25 cm	44	0.5473	49	0.6479	71	0.7154
2.5 cm	45	0.5613	51	0.6498	75	0.7191
3.75 cm	44	0.5702	52	0.6510	ND	ND

The average dried sludge = 1.4 g/l

Table III. 6 Sludge generation and electrode consumption of 1.5 g/l oil concentration for 120 minute

Operating condition	75 A/m^2		100 A/m^2		125 A/m^2	
	sludge	electrode	sludge	electrode	sludge	electrode
1.25 cm	44	0.5652	49	0.6526	72	0.6943
2.5 cm	45	0.5736	52	0.6632	77	0.6831
3.75 cm	48	0.6033	52	0.6687	ND	ND

The average dried sludge = 2.3 g/l

APPENDIX IV

ELECTROCOAGULATION/FLOTATION IN EXTERNAL LOOP AIRLIFT REACTOR

Table IV. 1 Downcomer configuration 1

Diameter 2.5 cm Height 50 cm
Connector 45 º Total volume 25.3 L

Time	0.5 g/l		1.0 g/l		1.5 g/l	
	% removal	Sludge (mm)	% removal	Sludge (mm)	% removal	Sludge (mm)
0	0	0	0	0	0	0
15	0	1	0	1	0	1
30	0	2	0	2	0	2
45	51.988	7	31.322	5	0	3
60	91.464	11	46.374	6	23.602	5
75	97.780	12	93.508	10	55.427	9
90	99.226	14	99.703	12	89.968	13
105					97.666	15

Table IV. 2 Downcomer configuration 2

Diameter 2.5 cm Height 75 cm
Connector 45 º Total volume 25.5 L

Time	0.5 g/l		1.0 g/l		1.5 g/l	
	% removal	Sludge (mm)	% removal	Sludge (mm)	% removal	Sludge (mm)
0	0	0	0	0	0	0
15	0	1	0	1	0	1
30	0	2	0	2	0	2
45	54.427	6	35.609	5	0	4
60	91.898	9	59.097	8	21.599	8
75	97.893	12	93.913	12	53.045	12
90			99.722	15	89.432	16
105					97.542	20

Table IV. 3 Downcomer configuration 3

Diameter 2.5 cm Height 100 cm
Connector 45 º Total volume 25.7 L

Time	0.5 g/l		1.0 g/l		1.5 g/l	
	% removal	Sludge (mm)	% removal	Sludge (mm)	% removal	Sludge (mm)
0	0	0	0	0	0	0
15	0	1	0	1	0	1
30	13.974	4	0	3	0	2
45	65.117	7	26.291	6	0	5
60	93.798	15	53.178	11	29.939	9
75	98.387	18	93.033	17	51.435	12
90			99.681	20	89.070	15
105					99.747	18

Table IV. 4 Downcomer configuration 4

Diameter 2.5 cm Height 50 cm
Connector 90 º Total volume 25.4 L

Time	0.5 g/l		1.0 g/l		1.5 g/l	
	% removal	Sludge (mm)	% removal	Sludge (mm)	% removal	Sludge (mm)
0	0	0	0	0	0	0
15	0	1	0	1	0	1
30	6.322	3	0	2	0	1
45	62.014	6	30.787	5	0	2
60	96.164	8	74.306	8	50.676	6
75	98.244	12	99.122	11	61.501	9
90	98.816	15	99.694	14	94.587	12
105					98.263	14
120					99.448	15

Table IV. 5 Downcomer configuration 5

Diameter 2.5 cm Height 75 cm
Connector 90 º Total volume 25.6 L

Time	0.5 g/l		1.0 g/l		1.5 g/l	
	% removal	Sludge (mm)	% removal	Sludge (mm)	% removal	Sludge (mm)
0	0	0	0	0	0	0
15	0	1	0	1	0	1
30	22.668	2	0	2	0	2
45	68.642	5	32.787	4	0	3
60	94.425	7	75.049	8	24.360	6
75	98.550	9	99.147	10	64.858	8
90	99.495	10	99.703	11	94.443	11
105					98.217	13
120					99.571	15

Table IV. 6 Downcomer configuration 6

Diameter 2.5 cm Height 100 cm
Connector 90 º Total volume 25.8 L

Time	0.5 g/l		1.0 g/l		1.5 g/l	
	% removal	Sludge (mm)	% removal	Sludge (mm)	% removal	Sludge (mm)
0	0	0	0	0	0	0
15	0	1	0	1	0	1
30	0	2	0	2	0	2
45	60.987	6	26.281	5	0	5
60	93.064	10	58.725	8	25.390	7
75	98.196	12	99.086	12	60.792	9
90	99.371	15	99.681	15	91.175	11
105					97.947	15

Table IV. 7 Downcomer configuration 7

Diameter 2.5 cm Height 50 cm
Connector 135 º Total volume 25.5 L

Time	0.5 g/l		1.0 g/l		1.5 g/l	
	% removal	Sludge (mm)	% removal	Sludge (mm)	% removal	Sludge (mm)
0	0	0	0	0	0	0
15	0	1	0	1	0	2
30	11.199	4	0	3	0	2
45	24.105	8	39.289	7	0	5
60	51.301	15	53.600	12	0	7
75	98.335	17	93.095	15	51.435	14
90			99.684	18	89.070	16
105					99.747	18

Table IV. 8 Downcomer configuration 8

Diameter 2.5 cm Height 75 cm
Connector 135 º Total volume 25.7 L

Time	0.5 g/l		1.0 g/l		1.5 g/l	
	% removal	Sludge (mm)	% removal	Sludge (mm)	% removal	Sludge (mm)
0	0	0	0	0	0	0
15	0	1	0	1	0	1
30	13.038	3	0	2	0	2
45	53.054	5	31.602	7	0	4
60	93.731	12	53.878	11	0	5
75	98.370	16	93.265	17	61.103	13
90			99.240	20	99.070	15
105					99.747	19

Table IV. 9 Downcomer configuration 9

Downcomer configuration: Diameter 2.5 cm Height 100 cm
Connector 135 º Total volume 26 L

Time	0.5 g/l		1.0 g/l		1.5 g/l	
	% removal	Sludge (mm)	% removal	Sludge (mm)	% removal	Sludge (mm)
0	0	0	0	0	0	0
15	0	1	0	1	0	2
30	24.574	5	0	6	0	4
45	69.415	8	39.862	9	0	5
60	94.562	12	55.793	12	26.424	9
75	98.586	18	93.545	19	64.824	15
90			99.272	22	87.153	17
105					99.749	18

Table IV. 10 Downcomer configuration 10

Diameter 3.8 cm Height 50 cm
Connector 45 º Total volume 25.7 L

Time	0.5 g/l		1.0 g/l		1.5 g/l	
	% removal	Sludge (mm)	% removal	Sludge (mm)	% removal	Sludge (mm)
0	0	0	0	0	0	0
15	0	1	0	1	0	1
30	0	2	0	3	0	3
45	5.753	3	0	6	0	7
60	80.537	10	25.765	10	0	19
75	98.107	13	56.619	12	42.885	20
90			94.514	20	93.737	25
105			98.804	25	98.649	27
120			98.916	30		

Table IV. 11 Downcomer configuration 11

Diameter 3.8 cm Height 75 cm
Connector 45 º Total volume 26.1 L

Time	0.5 g/l		1.0 g/l		1.5 g/l	
	% removal	Sludge (mm)	% removal	Sludge (mm)	% removal	Sludge (mm)
0	0	0	0	0	0	0
15	0	3	0	3	0	2
30	0	5	0	5	0	5
45	70.524	8	3.237	7	3.339	7
60	96.318	10	49.143	11	45.246	12
75	99.015	15	93.226	20	84.285	20
90			98.585	25	97.681	25
105			99.197	28	98.808	30
120					99.184	35

Table IV. 12 Downcomer configuration 12

Downcomer configuration: Diameter 3.8 cm Height 100 cm
Connector 45 º Total volume 26.5 L

Time	0.5 g/l		1.0 g/l		1.5 g/l	
	% removal	Sludge (mm)	% removal	Sludge (mm)	% removal	Sludge (mm)
0	0	0	0	0	0	0
15	0	1	0	1	0	3
30	0	2	0	3	0	5
45	48.396	7	0	4	0	7
60	93.425	13	0	8	0	9
75	98.291	17	63.076	15	57.995	11
90			96.348	20	92.304	14
105			98.572	22	97.905	18

Table IV. 13 Downcomer configuration 13

Diameter 3.8 cm Height 50 cm
Connector 90 º Total volume 25.9 L

Time	0.5 g/l		1.0 g/l		1.5 g/l	
	% removal	Sludge (mm)	% removal	Sludge (mm)	% removal	Sludge (mm)
0	0	0	0	0	0	0
15	0	3	0	4	0	2
30	6.579	4	0	4	0	3
45	61.356	12	8.730	5	0	5
60	96.015	22	60.355	9	23.935	10
75	98.493	27	88.566	15	66.468	13
90			98.208	24	94.613	20
105			98.915	28	94.613	25
120			99.253	34	98.512	25

Table IV. 14 Downcomer configuration 14

Diameter 3.8 cm Height 75 cm
Connector 90 º Total volume 26.4 L

Time	0.5 g/l		1.0 g/l		1.5 g/l	
	% removal	Sludge (mm)	% removal	Sludge (mm)	% removal	Sludge (mm)
0	0	0	0	0	0	0
15	0	1	0	1	0	1
30	6.835	2	0	2	0	5
45	59.639	10	0	3	0	5
60	91.432	18	30.184	5	0	7
75	99.708	25	73.946	13	26.654	10
90			90.650	17	67.874	18
105			98.414	20	92.468	23
120			99.148	25	98.231	25

Table IV. 15 Downcomer configuration 15

Diameter 3.8 cm Height 100 cm
Connector 90 º Total volume 26.8L

Time	0.5 g/l		1.0 g/l		1.5 g/l	
	% removal	Sludge (mm)	% removal	Sludge (mm)	% removal	Sludge (mm)
0	0	0	0	0	0	0
15	0	1	0	1	0	1
30	0	2	0	2	0	2
45	49.092	8	27.238	3	0	3
60	94.089	15	54.991	7	21.503	9
75	98.363	20	81.864	11	62.644	16
90			95.430	16	93.260	17
105			98.543	20		

Table IV. 16 Downcomer configuration 16

Diameter 3.8 cm Height 50 cm
Connector 135 º Total volume 26.1 L

Time	0.5 g/l		1.0 g/l		1.5 g/l	
	% removal	Sludge (mm)	% removal	Sludge (mm)	% removal	Sludge (mm)
0	0	0	0	0	0	0
15	0	1	0	2	0	2
30	0	3	0	9	0	3
45	2.156	6	61.665	15	0	4
60	77.758	15	95.561	21	0	6
75	96.065	17	98.465	23	35.455	8
90	97.438	20	98.953	25	88.748	10
105					97.322	12
120					98.815	14

Table IV. 17 Downcomer configuration 17

Diameter 3.8 cm Height 75 cm
Connector 135 º Total volume 26.7 L

Time	0.5 g/l		1.0 g/l		1.5 g/l	
	% removal	Sludge (mm)	% removal	Sludge (mm)	% removal	Sludge (mm)
0	0	0	0	0	0	0
15	0	1	0	1	0	1
30	0	2	0	2	0	1
45	65.569	9	0.316	5	0	4
60	95.389	11	78.319	8	0	5
75	98.176	16	94.823	16	25.536	6
90			98.110	17	85.707	8
105					94.497	12

Table IV. 18 Downcomer configuration 18

Diameter 3.8 cm Height 100 cm
Connector 135 º Total volume 27.3 L

Time	0.5 g/l		1.0 g/l		1.5 g/l	
	% removal	Sludge (mm)	% removal	Sludge (mm)	% removal	Sludge (mm)
0	0	0	0	0	0	0
15	0	1	0	1	0	1
30	0	2	0	3	0	3
45	68.158	12	67.723	8	0	6
60	95.683	16	94.438	16	0	9
75			97.838	22	0	14
90					20.556	16
105					90.477	18
120					97.167	25

Table IV. 19 Downcomer configuration 19

Diameter 5.1 cm Height 50 cm
Connector 45 º Total volume 26.3 L

Time	0.5 g/l		1.0 g/l		1.5 g/l	
	% removal	Sludge (mm)	% removal	Sludge (mm)	% removal	Sludge (mm)
0	0	0	0	0	0	0
15	0.126	1	0	2	0	1
30	65.908	2	0	3	0	1
45	88.517	10	70.883	4	0	2
60	98.715	17	90.278	13	0	2
75			98.648	14	91.262	3
90			99.117	15	96.494	8
105					98.680	13

Table IV. 20 Downcomer configuration 20

Downcomer configuration: Diameter 5.1 cm Height 75 cm
Connector 45 º Total volume 27 L

Time	0.5 g/l		1.0 g/l		1.5 g/l	
	% removal	Sludge (mm)	% removal	Sludge (mm)	% removal	Sludge (mm)
0	0	0	0	0	0	0
15	0	2	0	2	0	1
30	0	6	0	3	0	2
45	89.372	10	0	4	0	4
60	97.432	15	80.270	5	0	5
75	98.730	17	90.205	9	38.612	9
90			98.270	13	97.103	14
105					97.103	15
120					98.933	18

Table IV. 21 Downcomer configuration 21

Diameter 5.1 cm Height 100 cm
Connector 45 º Total volume 27.6 L

Time	0.5 g/l		1.0 g/l		1.5 g/l	
	% removal	Sludge (mm)	% removal	Sludge (mm)	% removal	Sludge (mm)
0	0	0	0	0	0	0
15	0	1	0	1	0	1
30	78.825	2	0	2	0	2
45	82.619	8	62.738	4	0	3
60	96.340	13	87.398	10	9.971	4
75			96.067	15	85.642	10
90					92.751	13
105					97.272	15

Table IV. 22 Downcomer configuration 22

Downcomer configuration: Diameter 5.1 cm Height 50 cm
Connector 90 º Total volume 26.6 L

Time	0.5 g/l		1.0 g/l		1.5 g/l	
	% removal	Sludge (mm)	% removal	Sludge (mm)	% removal	Sludge (mm)
0	0	0	0	0	0	0
15	0	2	0	2	0	2
30	0	4	0	4	0	5
45	73.285	10	0	8	0	7
60	96.735	15	92.633	15	0	11
75			95.882	18	65.051	12
90					95.486	14
105					95.268	17

Table IV. 23 Downcomer configuration 23

Diameter 5.1 cm Height 75 cm
Connector 90 º Total volume 27.4 L

Time	0.5 g/l		1.0 g/l		1.5 g/l	
	% removal	Sludge (mm)	% removal	Sludge (mm)	% removal	Sludge (mm)
0	0	0	0	0	0	0
15	0	1	0	2	0	1
30	0	3	0	3	0	3
45	77.841	5	0	5	0	5
60	93.359	10	81.593	10	0	6
75	95.395	15	96.100	12	36.175	9
90					90.392	10
105					97.109	15
120					98.650	20

Table IV. 24 Downcomer configuration 24

Diameter 5.1 cm Height 100 cm
Connector 90 º Total volume 28.2 L

Time	0.5 g/l		1.0 g/l		1.5 g/l	
	% removal	Sludge (mm)	% removal	Sludge (mm)	% removal	Sludge (mm)
0	0	0	0	0	0	0
15	0	1	0	1	0	1
30	0	3	0	2	0	2
45	67.977	8	0	5	0	3
60	96.675	12	56.393	7	0	4
75			87.961	9	0	5
90			98.335	10	87.064	8
105			98.912	12	95.131	15
120			98.936	20		

Table IV. 25 Downcomer configuration 25

Diameter 5.1 cm Height 50 cm
Connector 135 º Total volume 27 L

Time	0.5 g/l		1.0 g/l		1.5 g/l	
	% removal	Sludge (mm)	% removal	Sludge (mm)	% removal	Sludge (mm)
0	0	0	0	0	0	0
15	0	1	0	1	0	2
30	78.248	3	0	3	0	3
45	92.649	10	81.328	4	56.862	6
60	95.272	17	72.117	10	82.236	8
75			95.544	12	91.826	10
90						
105						

Table IV. 26 Downcomer configuration 26

Diameter 5.1 cm Height 75 cm
Connector 135 º Total volume 28 L

Time	0.5 g/l		1.0 g/l		1.5 g/l	
	% removal	Sludge (mm)	% removal	Sludge (mm)	% removal	Sludge (mm)
0	0	0	0	0	0	0
15	0	2	0	1	0	1
30	63.752	12	0	3	0	3
45	88.752	17	43.330	5	0	5
60	98.016	20	82.268	10	37.342	8
75			95.329	13	89.553	10
90			97.515	20	94.009	13
105					98.615	16

Table IV. 27 Downcomer configuration 27

Diameter 5.1 cm Height 100 cm
Connector 135 º Total volume 29 L

Time	0.5 g/l		1.0 g/l		1.5 g/l	
	% removal	Sludge (mm)	% removal	Sludge (mm)	% removal	Sludge (mm)
0	0	0	0	0	0	0
15	0	1	0	1	0	1
30	78.825	2	0	2	0	2
45	82.619	8	62.738	4	0	3
60	96.340	13	87.398	10	9.971	4
75			96.067	15	85.642	10
90					92.751	13
105					97.272	15

Operation cost estimation

Operation cost was also another important factor that could help to determine the possibility of actual operation for any treatment technology. Operation cost including chemical agent cost and electricity consumption cost. The calculation of operation cost estimation can be shown as follow;

1. Chemical agent cost

Chemical agent cost was also included in the operating cost too. The calculation are shown as follow;

Alum cost = 14.4 Baht per kilogram
1 L of 1.0 g/l oil concentration required 160 mg Alum
Therefore, Alum cost per 1 L wastewater = $\frac{14.4\ baht}{1\ kg} \times \frac{1\ kg}{1{,}000{,}000\ mg} \times 160\ mg$

= $0.0023\ Baht\ per$ L

2. Electricity consumption cost

Within a small amount of wastewater (1L/sample, 6 sample per 1 experimental set) the power consumption could be estimated from the following equation;

Power consumption = $\frac{V \times I \times t}{1000}$ (Eq.4.2)

= $\frac{220\ V\ \times 0.5\ A \times 31\ min}{1000 \times 60\ min/hr}$

= 0.0568 kWh

Noted that *V* and *I* were stated on the Jar test specification document from vender: www. scilution.com

Power consumption per 1 L of wastewater = $\frac{0.0568\ \text{kWh}}{6\ L\ wastewater}$

= 0.00947 kWh = 0.00947 Unit

The electricity consumption cost (per 1 L) = Unit of electric consumption x cost per unit x tax

= 0.00947 Unite x 3.4230 $\frac{Baht}{Unit}$ x 1.07

= 0.0346 Baht per L

The total operating cost per 1 L = Chemical cost + electricity cost

= 0.0346 + 0.0023

= 0.037 Baht per L

BCR

Power consumption = $\frac{V \times I \times t}{1000}$ (Eq.4.2)

= $\frac{40\ V\ \times 1\ A \times 2\ hr}{1000}$

= 0.08 kWh

Power consumption per 1 L of wastewater = $\frac{0.08\ \text{kWh}}{25\ L\ wastewater}$

= 0.0032 kWh = 0.0032 Unit

The electricity consumption cost (per 1 L) = Unit of electric consumption x cost per unit x tax

= 0.0032Unite x 3.4230 $\frac{Baht}{Unit}$ x 1.07

= 0.012 Baht per L

ALR

Power consumption = $\frac{V \times I \times t}{1000}$ (Eq.4.2)

= $\frac{40\ V\ \times 1\ A \times 2\ hr}{1000}$

= 0.08 kWh

Power consumption per 1 L of wastewater = $\frac{0.08\ \text{kWh}}{29\ L\ wastewater}$

= 0.0027 kWh = 0.0027 Unit

The electricity consumption cost (per 1 L) = Unit of electric consumption x cost per unit x tax

= 0.0027Unite x 3.4230 $\frac{Baht}{Unit}$ x 1.07

= 0.010 Baht per L

APPENDIX V
PREDICTION MODEL

First model prediction: Polynomial function

The first set of experiment was conducted by Minitab 17. The operating condition in each experiments is displayed in Table

Table V. 1 operating code and result for modeling by Minitab 17

Run	oil concentration	gap between electrode	current density	detention time	Response (% turbidity removal)
1	0.5	1.25	75	30	-1.77
2	0.5	1.25	75	90	91.91
3	0.5	1.25	125	30	17.99
4	0.5	1.25	125	90	98.88
5	0.5	3.75	75	30	-15.34
6	0.5	3.75	75	90	89.89
7	0.5	3.75	125	30	-10.02
8	0.5	3.75	125	90	99.01
9	1.5	1.25	75	30	-11.97
10	1.5	1.25	75	90	16.41
11	1.5	1.25	125	30	-0.54
12	1.5	1.25	125	90	97.55
13	1.5	3.75	75	30	-11.30
14	1.5	3.75	75	90	17.24
15	1.5	3.75	125	30	-6.57
16	1.5	3.75	125	90	66.99
17	0.0	2.50	100	60	19.44
18	2.0	2.50	100	60	9.00
19	1.0	0.00	100	60	0.00
20	1.0	5.00	100	60	46.85
21	1.0	2.50	50	60	-2.85
22	1.0	2.50	150	60	88.24
23	1.0	2.50	100	0	0.00
24	1.0	2.50	100	120	99.41
25	1.0	2.50	100	60	35.28
26	1.0	2.50	100	60	26.00

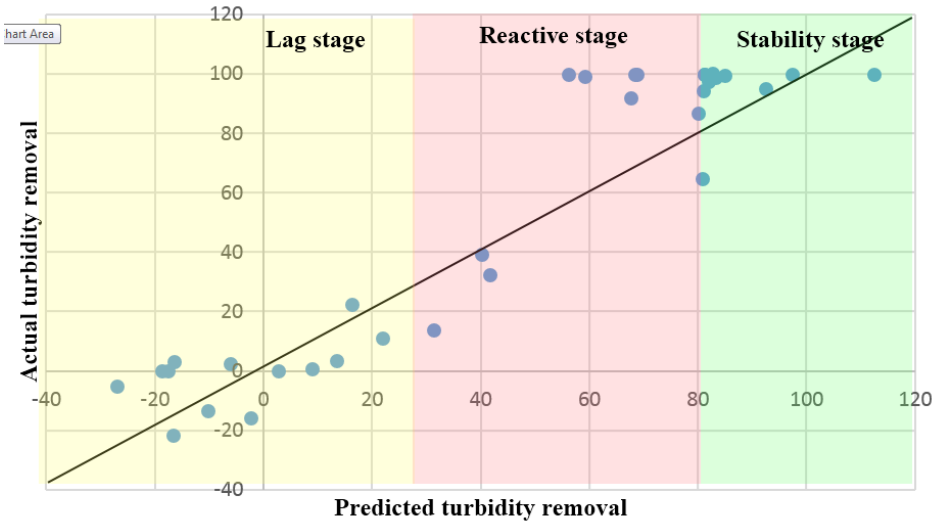

Figure V. 1 Model validation

Second model prediction: Logarithm function

This model used the previous result with another 20 additional operating code as shown in Table 23;

Table V. 2 Operating code and result for modeling by Minitab 17

Run	Oil (g/l)	Gap (cm)	current density (A/m^2)	response		
				time of lag stage	time of reactive stage	k
1	0.5	1.25	75	35	85	0.087641
2	1	2.5	100	59	91	0.136938
3	1	0.4	100	53	84	0.141356
4	1.5	3.75	125	43	97	0.081149
5	1	4.6	100	56	85	0.151104
6	1	2.5	100	45	85	0.109551
7	0.5	3.75	125	35	60	0.175281
8	1.5	3.75	75	64	179	0.038105
9	1.5	1.25	125	30	79	0.089429
10	0.5	3.75	75	43	85	0.104334
11	0.5	1.25	125	26	52	0.168539
12	1.84	2.5	100	58	120	0.070678
13	1	2.5	100	59	91	0.136938
14	1.5	1.25	75	75	140	0.067416
15	1	2.5	100	45	85	0.109551
16	1	2.5	100	47	85	0.115316
17	1	2.5	100	48	83	0.125201
18	0.16	2.5	100	9	48	0.11236
19	1	2.5	142	36	63	0.162297
20	1	2.5	58	67	214	0.02981

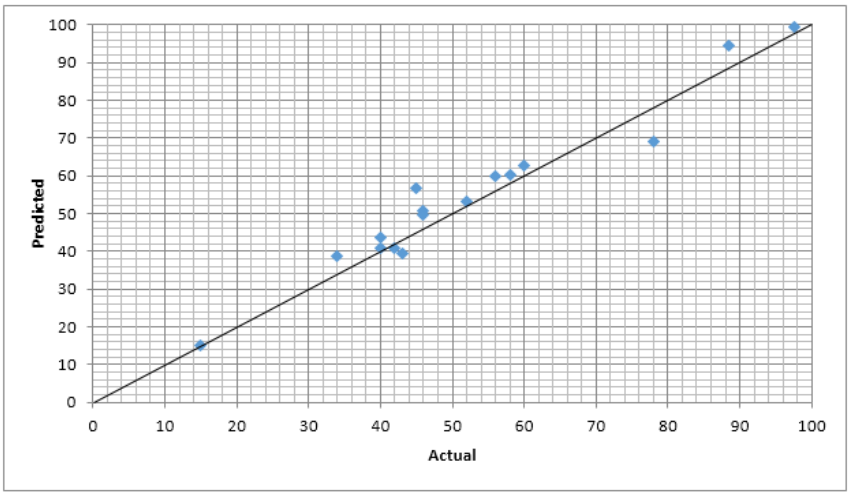

Figure V. 2 Lag time model validation

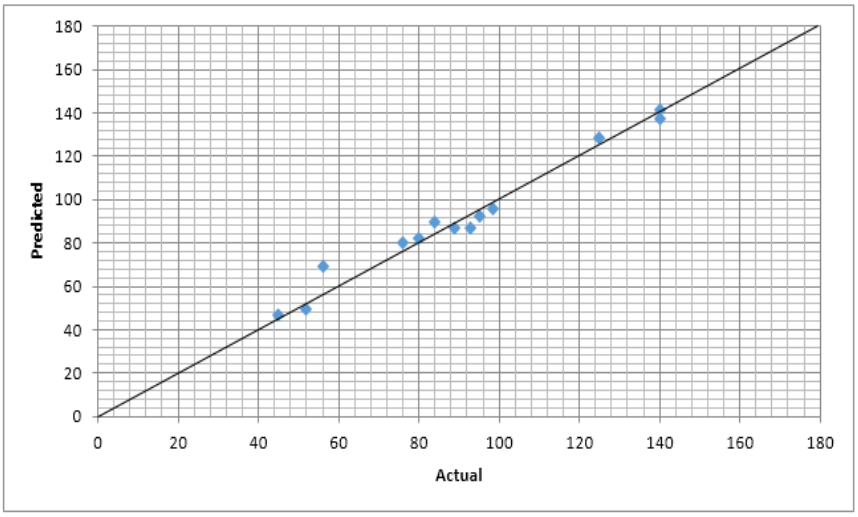

Figure V. 3 Steady stage time model validation

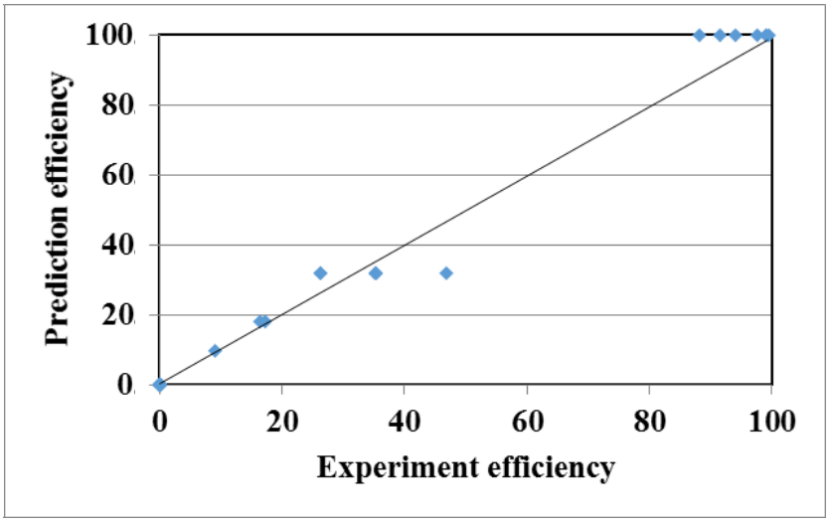

Figure V. 4 Overall treatment validation

Third model prediction: Logistic function/S-curve function/ Sigmoid function

The result of the previous two model was applied to form the logistic curve function

This prediction had applied nonlinear regression approach. The pattern of turbidity removal efficiency of cutting-oily wastewater could be summarize as follow;

1. The turbidity could define as no change in lag stage, therefore, the horizontal line appeared.
2. After achieve lag stage. The turbidity treatment efficiency was dramatically increase within 15-30 minute after lag period.
3. When the system provide steady stage, little turbidity change was found since most of the particle had been removed during reactive stage already. The turbidity removal showed a horizontal line again.

These 3 summaries was the same description as logistic function, s-curve or sigmoid equation. The conventional sigmoid equation form is shown in Eq.6;

$$Y = \frac{100}{1+ e^{-k(x-x_{50})}} \quad (6)$$

Where; Y = output

k = steepness of the curve

x = input

x_{50} = input factor that provide 50% of output

Thus, the third prediction model in sigmoid curve form is presented in Eq. 7 below;

$$\%\ \eta_{\text{turbidity removal}} = \frac{100}{1+ e^{-k(t-t_{50})}} \quad (7)$$

Where; k = the steepness

t_{50} = the time that the efficiency reached 50%.

According to nonlinear regression formation, the effect of each parameters would be analyzed in order to minimize the least affected parameters from the equation. The related parameters including oil concentration, current density and gap between electrodes as follow;

Effect of oil concentration

Oil concentration was related to the amount of oil droplet which showed in turbidity form. Higher oil concentration caused more opaque emulsion solution due to the increasing of oil droplet intensity. Figure 63 shows the turbidity removal efficiency under operating condition of 2.5-cm gap between electrodes and 100 A/m^2 current density. As a result, higher oil content in wastewater provides less steepness of the sigmoid graph. The reactive period was prolonged because higher oil concentration required larger amount of aluminum ions for the coagulation process.

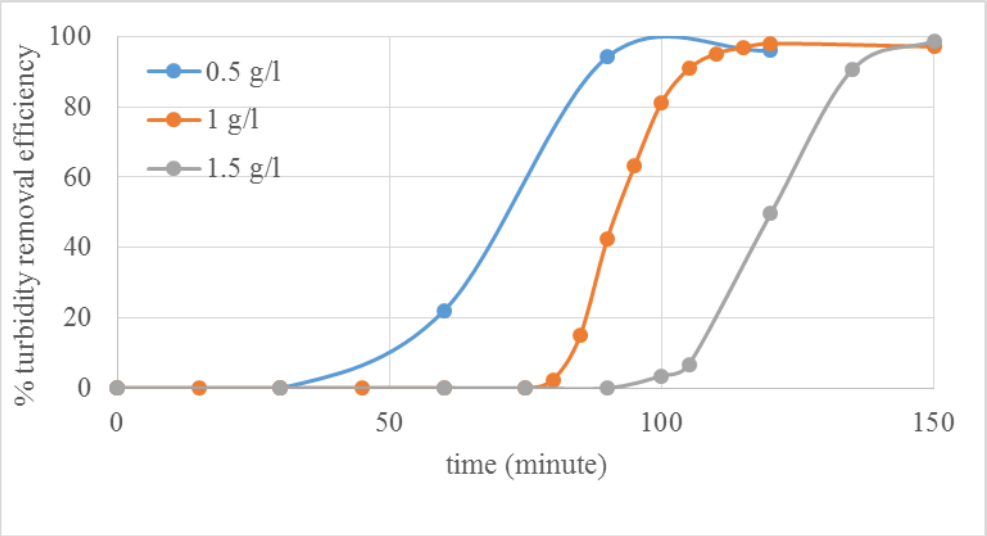

Figure V. 5 Effect of Oil Concentration to ECF Process

4.5.2.1.Effect of current density

Current density played an important role in term of key driving parameter. According to Faraday's law, the amount of aluminum increased with time and current applied. Thus, higher current density could shorten lag stage. For the turbidity removal efficiency of 0.5-g/l oil concentration and 2.5 cm distance between electrodes in Figure 7, the time in the lag stage was shifted when altering the current density. The steepness (k), on the other hand, remained the same. Therefore, the prediction model of steepness (k) would neglect the current density (i) or current applied (I) term.

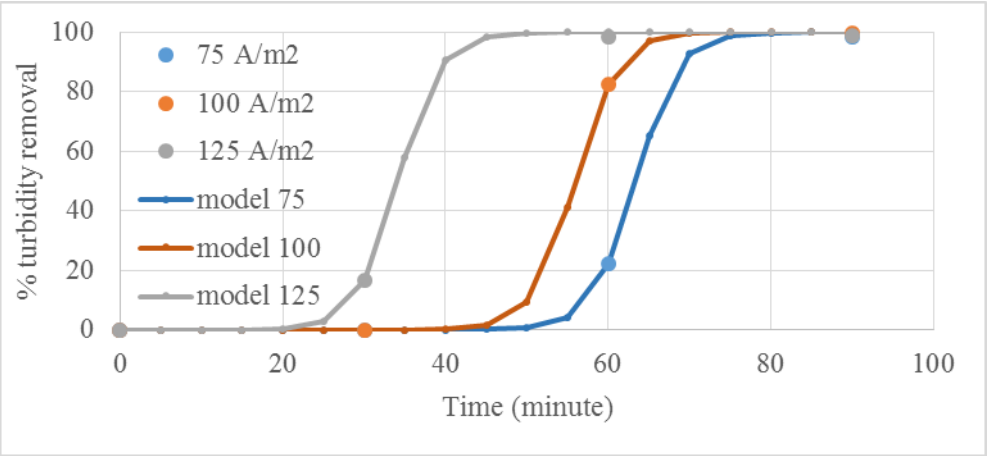

Figure V. 6 Effect of Current Density to ECF Process

4.5.2.2.Effect of distance between electrodes

During the experiment, distance between electrodes shows very small effect to the treatment efficiency since the ECF process was proceeded in current control system as shown in Figure 8 for the case of 0.5 g/l oil concentration 100 A/m^2. Moreover, 1.25-3.75 cm was a small range gap that the distance between electrodes would not show its influence. The prediction model of neither steepness (k) nor half treatment time (t_{50}), hence, eliminated the distance between electrode terms.

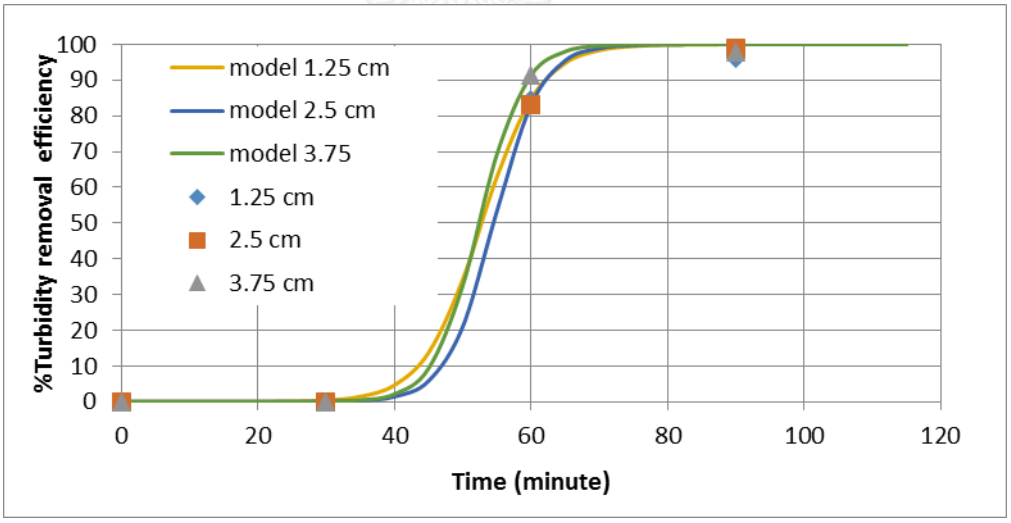

Figure V. 7 Effect of Distance between Electrodes to ECF Process

According to one-way parameter analysis, only oil concentration was found to be a key parameter that affect the steepness (k). The nonlinear regression of sigmoid steepness (k) shows in the Equation 8 as follow;

$$k = 0.273C_0^{-0.5} \quad (8)$$

In addition, the effects of electrode gap to steepness (k) and t_{50} were neglected since this factors have only slightly effects on these range of operating condition. The parameters in nonlinear regression of half treatment time (t_{50}) would include the initial oil concentration (C_0) and current applied (I) for 100-cm^2 reactive surface of the electrodes as shown in Equation 9;

$$t_{50} = 3630e^{-6.07I} + 27.6C_0^{0.45} + 25.97 \quad (9)$$

In order to validate the predicting equation, 11 randomized experiments were conducted to evaluate the prediction model. The result of the validation is shown in Figure 9 with less than 21% of deviation.

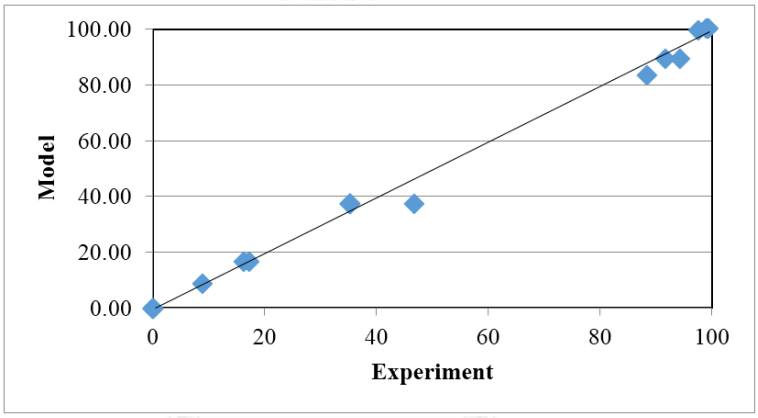

Figure V. 8 Model Validation

Furthermore, the example of fitting sigmoid equation of 0.5 g/l oil concentration, 1.25 A and 2.5-cm gap of electrodes is displayed in Figure 5. The prediction equation can be constructed as expressed in Equation 8;

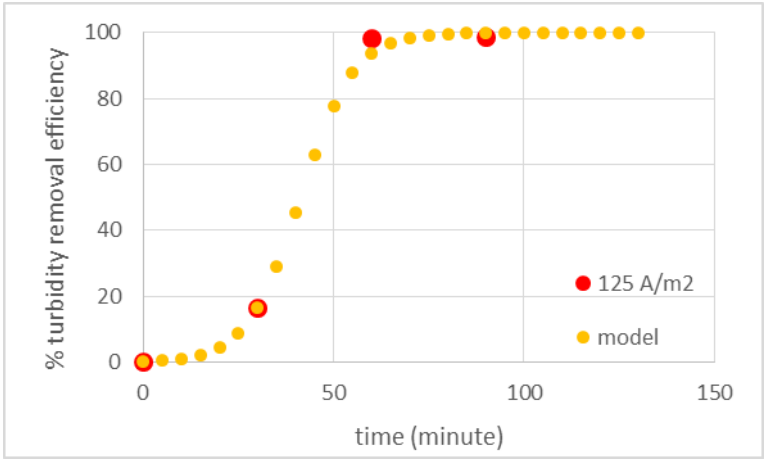

Figure V. 9 Example of Sigmoid Model Fitting

$$\%Turbidity\ removal = \frac{100}{1+ e^{[-0.386(t-48)]}} \quad (8)$$

External loop airlift reactor, ELALR

The result from the electrocoagulation/flotation in external loop airlift reactor was reported in table 25 that k and t50 was calculated from nonlinear regression using solver function in Microsoft excel. The prediction model of k and t50 is display below;

$$k = \frac{0.875}{C_{oil}^{0.3} D_{DC}^{0.19} V^{0.6} \Delta H^{0.02}} + \frac{0.692}{V^{2.42}}$$

$$t_{50} = 77.8\ C_{Oil}^{0.45}$$

Where; C_{oil} = Initial Concentration of Oil (g/L)

D_{DC} = Diameter of Downcomer (m)

V = Total Volume of Reactor (Liter)

ΔH = Difference Head between Column and Inlet of Downcomer (m)

However, this prediction model was available for 100 A/m^2 of current density and 2.5 cm of distance between electrodes. Improving the prediction model required wider range of parameters; therefore, the operating condition and reactor configuration could be combined together in the future experiments.

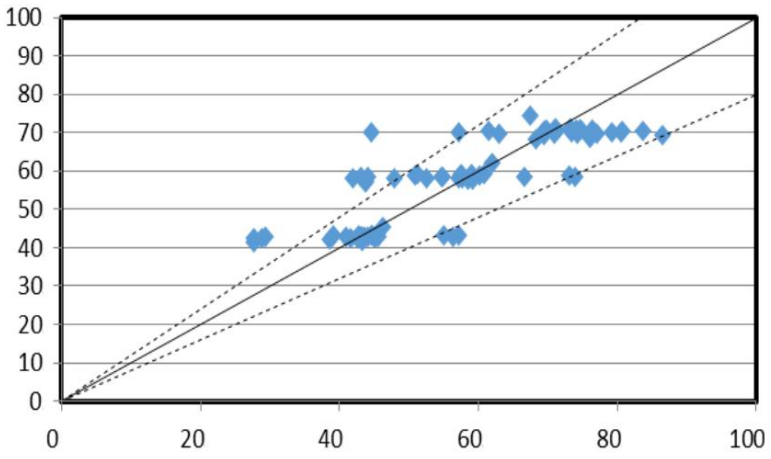

Figure V. 10 Prediction model validation

Table 25 k and t50 prediction model in ELALR

Runs	Oil (g/l)	Diameter (cm)	Height (cm)	degree	Volume of DC	Total Volume	Head in Top DC	Diff Head	K Model	K Exp	t50 Model	t50 Exp
1	0.5	0.01	0.01	0.1	0.000	25.000	0	0.01	0.34	0.38	45.31	46.2
2	1	0.01	0.01	0.1	0.000	25.000	0	0.01	0.27	0.27	61.96	62.0
3	1.5	0.01	0.01	0.1	0.000	25.000	0	0.01	0.24	0.22	74.40	67.5
4	0.5	2.54	50	45	0.329	25.329	92.5	0.75	0.16	0.35	43.32	44.8
5	0.5	2.54	50	90	0.456	25.456	105	0.625	0.16	0.21	43.26	42.7
6	0.5	2.54	50	135	0.583	25.583	117.5	0.5	0.16	0.09	43.20	57.1
7	1	2.54	50	45	0.329	25.329	92.5	0.75	0.13	0.19	59.24	60.8
8	1	2.54	50	90	0.456	25.456	105	0.625	0.13	0.13	59.16	51.3
9	1	2.54	50	135	0.583	25.583	117.5	0.5	0.13	0.16	59.06	58.9
10	1.5	2.54	50	45	0.329	25.329	92.5	0.75	0.12	0.12	71.14	73.2
11	1.5	2.54	50	90	0.456	25.456	105	0.625	0.12	0.12	71.04	71.1
12	1.5	2.54	50	135	0.583	25.583	117.5	0.5	0.12	0.31	70.93	74.8
13	0.5	2.54	75	45	0.456	25.456	117.5	0.5	0.16	0.43	43.21	44.6
14	0.5	2.54	75	90	0.583	25.583	130	0.375	0.16	0.13	43.13	39.2
15	0.5	2.54	75	135	0.709	25.709	142.5	0.25	0.16	0.14	43.01	44.0
16	1	2.54	75	45	0.456	25.456	117.5	0.5	0.13	0.14	59.08	57.4
17	1	2.54	75	90	0.583	25.583	130	0.375	0.13	0.12	58.97	50.9
18	1	2.54	75	135	0.709	25.709	142.5	0.25	0.13	0.16	58.82	59.0
19	1.5	2.54	75	45	0.456	25.456	117.5	0.5	0.12	0.13	70.95	74.0
20	1.5	2.54	75	90	0.583	25.583	130	0.375	0.12	0.12	70.81	69.7
21	1.5	2.54	75	135	0.709	25.709	142.5	0.25	0.12	0.49	70.63	74.1
22	0.5	2.54	100	45	0.583	25.583	142.5	0.25	0.16	0.16	43.03	41.0
23	0.5	2.54	100	90	0.709	25.709	155	0.125	0.15	0.25	42.85	43.2
24	0.5	2.54	100	135	0.836	25.836	167.5	0.01	0.15	0.13	42.24	38.7
25	1	2.54	100	45	0.583	25.583	142.5	0.25	0.13	0.16	58.84	59.2

Table 25 k and t50 prediction model in ELALR (continue)

Runs	Oil (g/l)	Diameter (cm)	Height (cm)	degree	Volume of DC	Total Volume	Head in Top DC	Diff Head	K Model	K Exp	t50 Model	t50 Exp
26	1	2.54	100	90	0.709	25.709	155	0.125	0.13	0.11	58.59	54.6
27	1	2.54	100	135	0.836	25.836	167.5	0.01	0.12	0.16	57.75	58.5
28	1.5	2.54	100	45	0.583	25.583	142.5	0.25	0.12	0.14	70.65	74.6
29	1.5	2.54	100	90	0.709	25.709	155	0.125	0.11	0.12	70.36	71.2
30	1.5	2.54	100	135	0.836	25.836	167.5	0.01	0.11	0.11	69.35	69.4
31	0.5	3.81	50	45	0.741	25.741	92.5	0.75	0.21	0.28	43.06	54.9
32	0.5	3.81	50	90	1.026	26.026	105	0.625	0.21	0.21	42.98	42.8
33	0.5	3.81	50	135	1.311	26.311	117.5	0.5	0.21	0.34	42.89	56.3
34	1	3.81	50	45	0.741	25.741	92.5	0.75	0.19	0.14	58.88	73.1
35	1	3.81	50	90	1.026	26.026	105	0.625	0.19	0.18	58.77	57.7
36	1	3.81	50	135	1.311	26.311	117.5	0.5	0.19	0.48	58.65	44.0
37	1.5	3.81	50	45	0.741	25.741	92.5	0.75	0.18	0.20	70.70	76.4
38	1.5	3.81	50	90	1.026	26.026	105	0.625	0.18	0.12	70.57	69.4
39	1.5	3.81	50	135	1.311	26.311	117.5	0.5	0.17	0.14	70.43	80.6
40	0.5	3.81	75	45	1.026	26.026	117.5	0.5	0.21	0.51	42.93	43.3
41	0.5	3.81	75	90	1.311	26.311	130	0.375	0.21	0.20	42.83	43.1
42	0.5	3.81	75	135	1.596	26.596	142.5	0.25	0.21	0.46	42.70	43.6
43	1	3.81	75	45	1.026	26.026	117.5	0.5	0.19	0.18	58.70	60.2
44	1	3.81	75	90	1.311	26.311	130	0.375	0.18	0.13	58.56	66.7
45	1	3.81	75	135	1.596	26.596	142.5	0.25	0.18	0.47	58.38	57.3
46	1.5	3.81	75	45	1.026	26.026	117.5	0.5	0.17	0.10	70.49	61.5
47	1.5	3.81	75	90	1.311	26.311	130	0.375	0.17	0.12	70.32	83.6
48	1.5	3.81	75	135	1.596	26.596	142.5	0.25	0.17	0.19	70.11	80.6
49	0.5	3.81	100	45	1.311	26.311	142.5	0.25	0.21	0.23	42.73	45.3

Table 25 k and t50 prediction model in ELALR (continue)

Runs	Oil (g/l)	Diameter (cm)	Height (cm)	degree	Volume of DC	Total Volume	Head in Top DC	Diff Head	K Model	K Exp	t50 Model	t50 Exp
50	0.5	3.81	100	90	1.596	26.596	155	0.125	0.21	0.19	42.53	45.2
51	0.5	3.81	100	135	1.881	26.881	167.5	0.01	0.20	0.43	41.91	43.2
52	1	3.81	100	45	1.311	26.311	142.5	0.25	0.18	0.49	58.43	73.9
53	1	3.81	100	90	1.596	26.596	155	0.125	0.18	0.09	58.16	57.8
54	1	3.81	100	135	1.881	26.881	167.5	0.01	0.18	0.62	57.30	43.8
55	1.5	3.81	100	45	1.311	26.311	142.5	0.25	0.17	0.19	70.16	73.3
56	1.5	3.81	100	90	1.596	26.596	155	0.125	0.17	0.13	69.84	70.9
57	1.5	3.81	100	135	1.881	26.881	167.5	0.01	0.17	1.19	68.81	76.1
58	0.5	5.08	50	45	1.317	26.317	92.5	0.75	0.33	1.03	42.84	29.4
59	0.5	5.08	50	90	1.824	26.824	105	0.625	0.33	0.42	42.74	45.6
60	0.5	5.08	50	135	2.331	27.331	117.5	0.5	0.33	0.54	42.63	27.6
61	1	5.08	50	45	1.317	26.317	92.5	0.75	0.31	0.48	58.58	43.1
62	1	5.08	50	90	1.824	26.824	105	0.625	0.31	0.50	58.44	54.9
63	1	5.08	50	135	2.331	27.331	117.5	0.5	0.30	0.49	58.29	42.0
64	1.5	5.08	50	45	1.317	26.317	92.5	0.75	0.30	0.61	70.34	71.1
65	1.5	5.08	50	90	1.824	26.824	105	0.625	0.29	0.50	70.17	57.2
66	1.5	5.08	50	135	2.331	27.331	117.5	0.5	0.29	0.74	69.99	44.6
67	0.5	5.08	75	45	1.824	26.824	117.5	0.5	0.33	0.63	42.68	43.5
68	0.5	5.08	75	90	2.331	27.331	130	0.375	0.33	0.54	42.56	42.7
69	0.5	5.08	75	135	2.838	27.838	142.5	0.25	0.33	0.50	42.41	28.9
70	1	5.08	75	45	1.824	26.824	117.5	0.5	0.30	0.55	58.36	57.5
71	1	5.08	75	90	2.331	27.331	130	0.375	0.30	0.53	58.19	57.2
72	1	5.08	75	135	2.838	27.838	142.5	0.25	0.30	0.13	57.99	48.0
73	1.5	5.08	75	45	1.824	26.824	117.5	0.5	0.29	0.29	70.09	79.3

Table 25 k and t50 prediction model in ELALR (continue)

Runs	Oil (g/l)	Diameter (cm)	Height (cm)	degree	Volume of DC	Total Volume	Head in Top DC	Diff Head	K Model	K Exp	t50 Model	t50 Exp
74	1.5	5.08	75	90	2.331	27.331	130	0.375	0.29	0.27	69.88	77.1
75	1.5	5.08	75	135	2.838	27.838	142.5	0.25	0.29	0.18	69.63	62.9
76	0.5	5.08	100	45	2.331	27.331	142.5	0.25	0.33	0.40	42.46	41.5
77	0.5	5.08	100	90	2.838	27.838	155	0.125	0.32	0.49	42.24	43.5
78	0.5	5.08	100	135	3.344	28.344	167.5	0.01	0.32	0.57	41.60	27.7
79	1	5.08	100	45	2.331	27.331	142.5	0.25	0.30	0.25	58.06	52.5
80	1	5.08	100	90	2.838	27.838	155	0.125	0.30	0.32	57.76	59.2
81	1	5.08	100	135	3.344	28.344	167.5	0.01	0.29	0.44	56.88	43.8
82	1.5	5.08	100	45	2.331	27.331	142.5	0.25	0.29	1.69	69.72	74.2
83	1.5	5.08	100	90	2.838	27.838	155	0.125	0.29	0.56	69.36	86.6
84	1.5	5.08	100	135	3.344	28.344	167.5	0.01	0.28	0.27	68.31	68.3

APPENDIX VI

CONTINUOUS SYSTEM AND RTD EXPERIMENTS

1. Continuous system in BCR and the best ELALR

Condition: Oil concentration 1 g/l
Distance between electrode 2.5 cm
Current density 100 A/m^2

ELALR configuration: Diameter 5.1 cm
Height 100 cm
Connector 135 °

Table VI. 1 Turbidity removal efficiency in continuous system

Time (minute)	BCR		ELALR	
	% turbidity removal	Sludge thickness	% turbidity removal	Sludge thickness
0	0	0	0	0
30	0.469	2	0	2
60	80.969	5	6.202	3
90	92.382	15	34.112	8
120	92.824	19	59.486	12
150	93.176	21	82.419	17
180	93.271	21	93.588	21
210	93.743	22	93.291	22
240	93.926	24	92.748	24
270	94.133	27	93.177	25
300	94.683	35	93.753	25

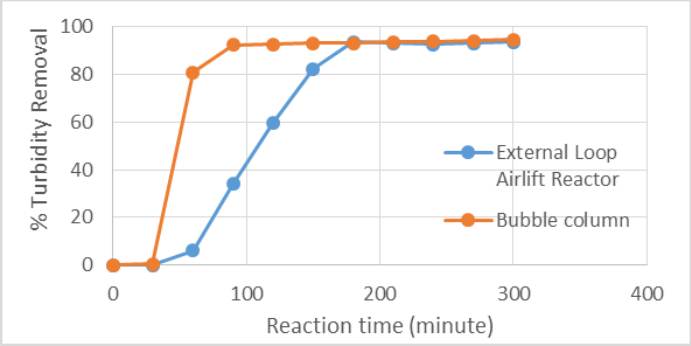

Figure VI. 1 Treatment efficiency in continuous system

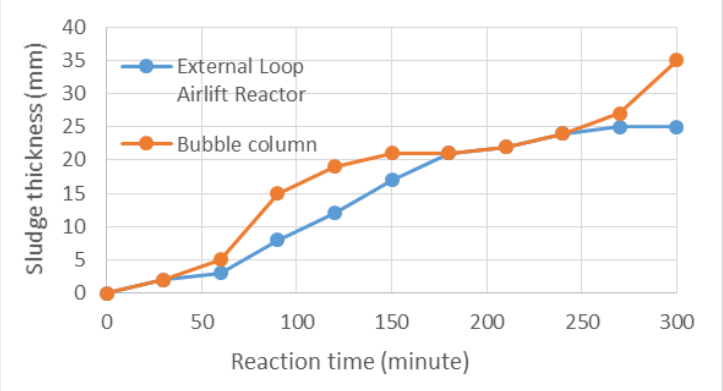

Figure VI. 2 Sludge generation in continuous system

2. Residence time distribution (RTD)

Table VI. 2 Standard curve of conductivity meter

NaCl concentration (g/l)	Conductivity meter No. 1 (ms)	Conductivity meter No. 2 (ms)	Conductivity meter No. 3 (ms)
0	0.348	0.347	0.342
1	2.21	2.16	2.07
5	9.5	9.17	9.01
10	17.43	16.93	16.58
15	26.4	26.1	22.8
20	34.4	34.3	29
25	41.8	41.7	35.3
30	48.8	48.8	41.5
35	55.5	55.6	46.6
40	61.6	62.4	52.5

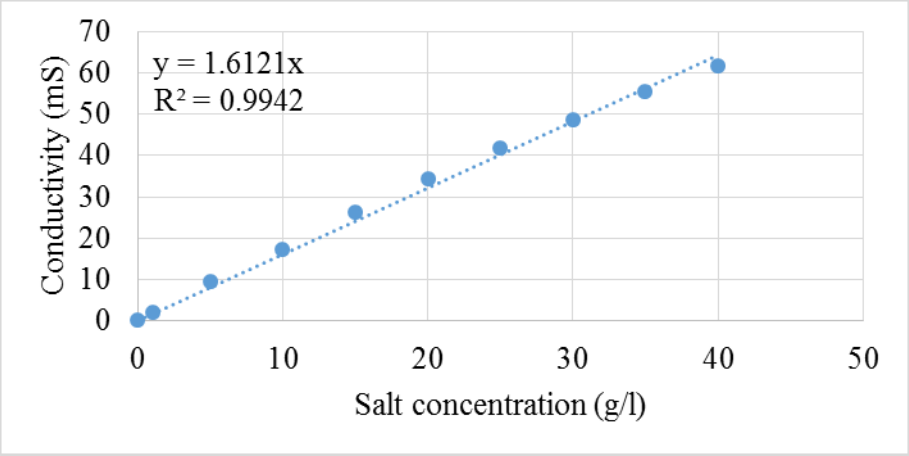

Figure VI. 3 Standard salt concentration to conductivity of conductivity meter No. 1

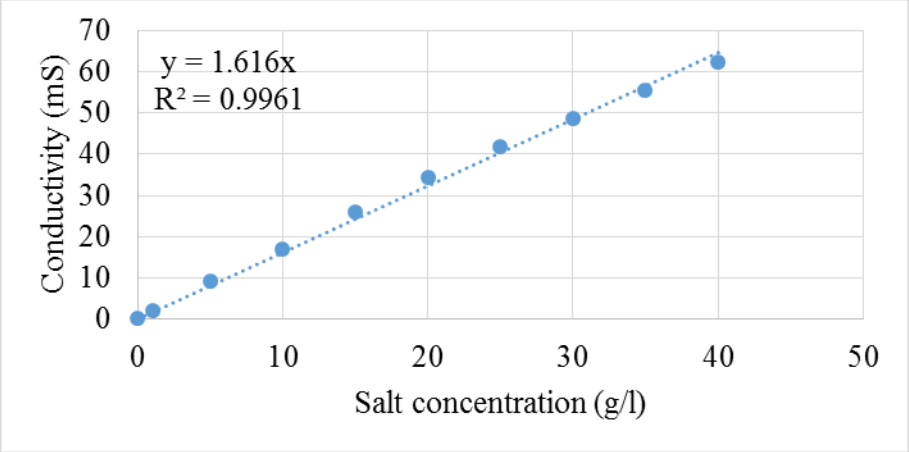

Figure VI. 4 Standard salt concentration to conductivity of conductivity meter No. 2

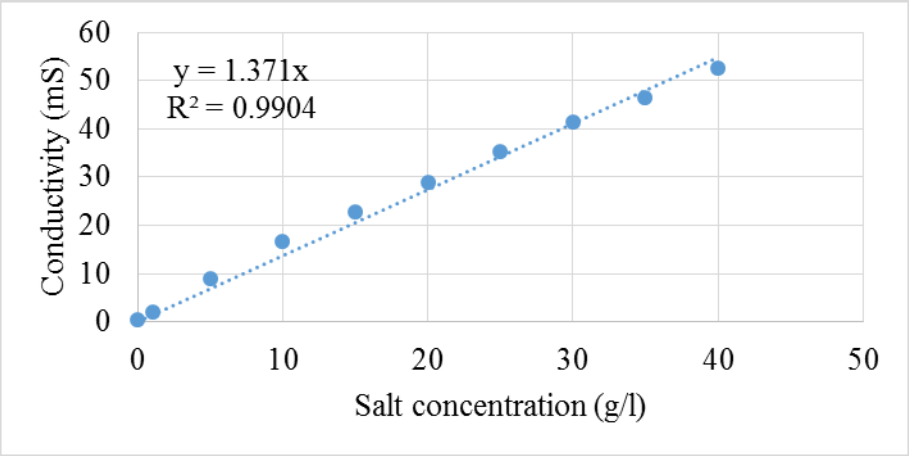

Figure VI. 5 Standard salt concentration to conductivity of conductivity meter No. 3

Bubble column

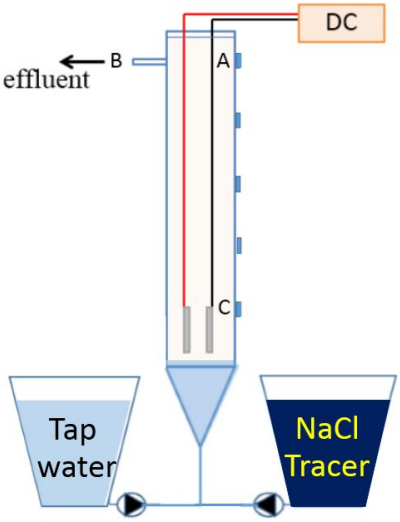

Figure VI. 6 Schematic diagram of conductivity meter in BCR

According to a large amount of data set, the salt concentration that shows in Figure 57 was provided. In order to calculation the E(t) function, the following equation was applied;

$$E(t) = \frac{C(t)}{\int_0^\infty C(t)dt} \qquad \text{(Eq.2.14)}$$

Where; E (t) = conductivity portion in specific duration t to t+dt

C (t) = conductivity (µS)

This equation was applied to both BCR and ELALR system as well.

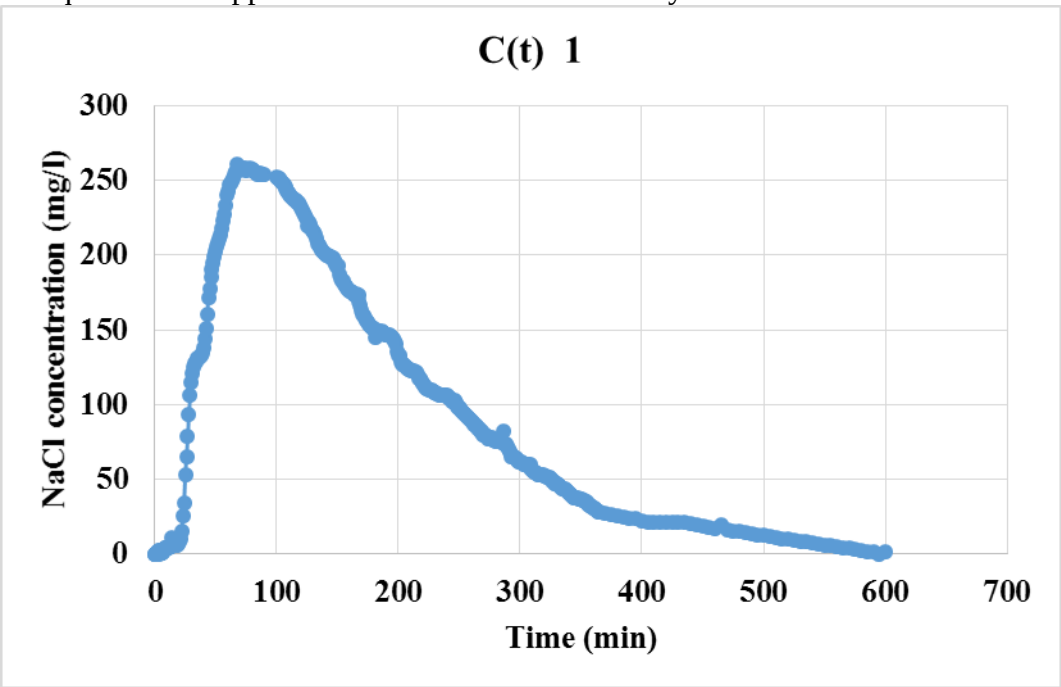

Figure VI. 7 Salt concentration from conductivity meter No.1

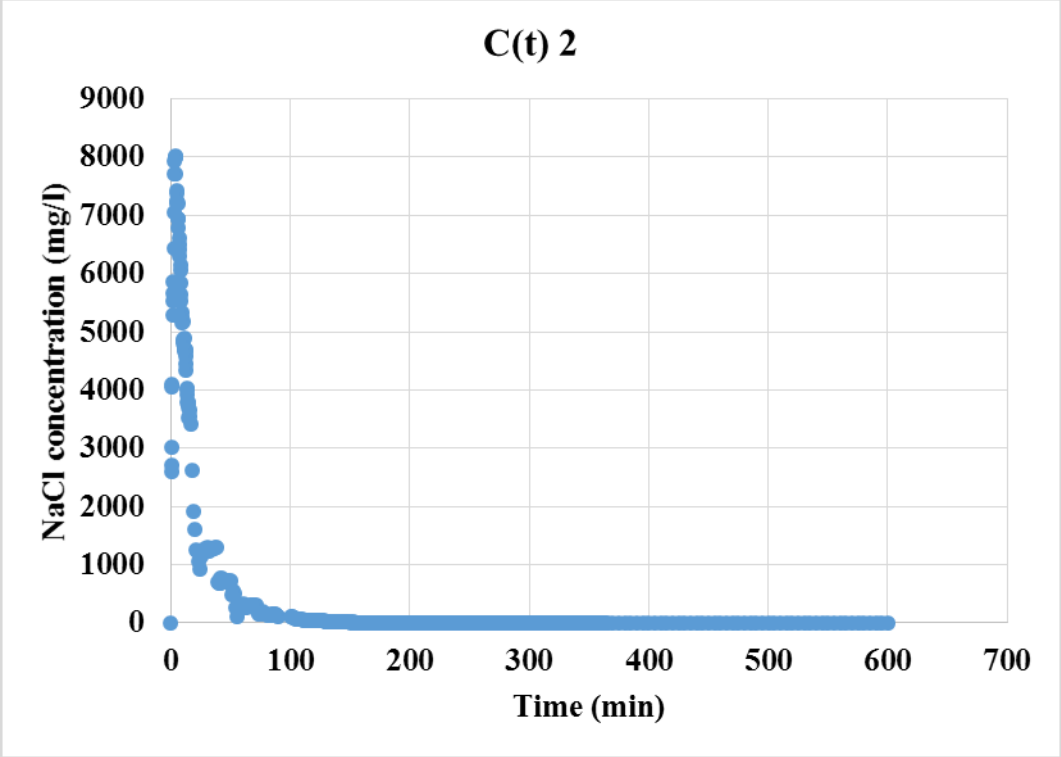

Figure VI. 8 *Salt concentration from conductivity meter No.2*

External loop airlift reactor

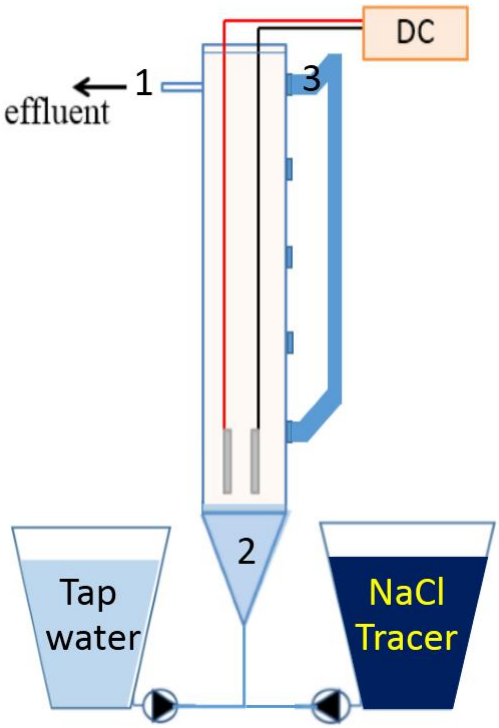

Figure VI. 9 Schematic diagram of conductivity meter in ELALR

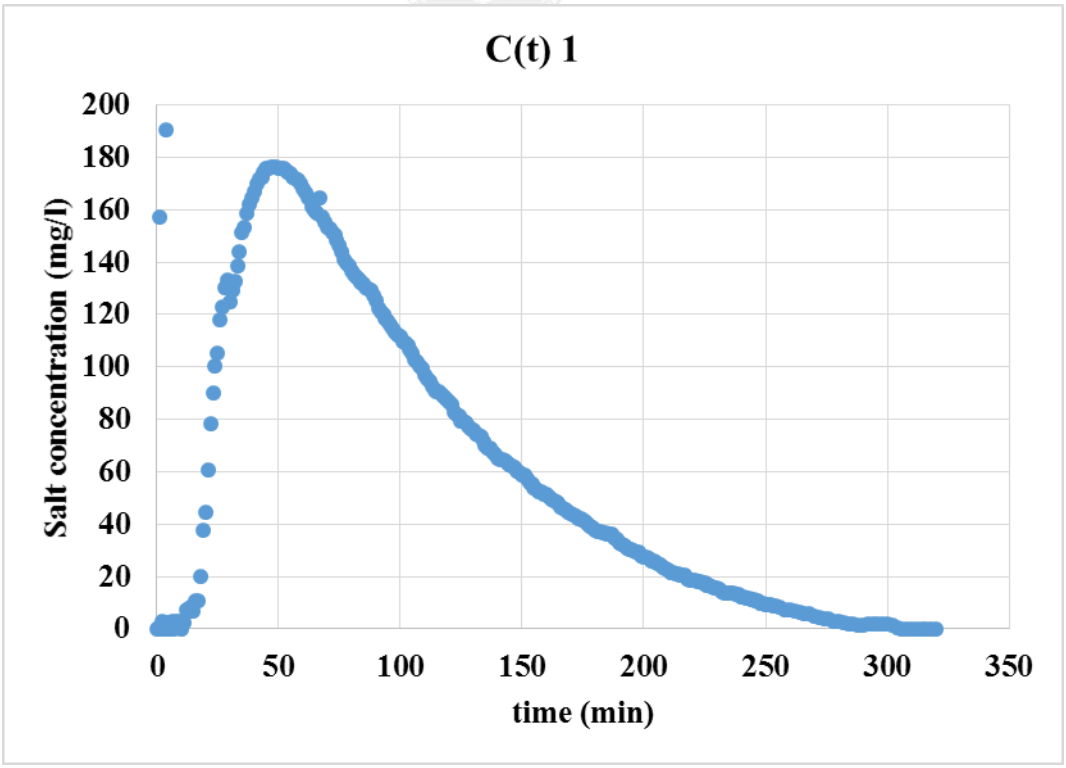

Figure VI. 10 Salt concentration from conductivity meter No.1

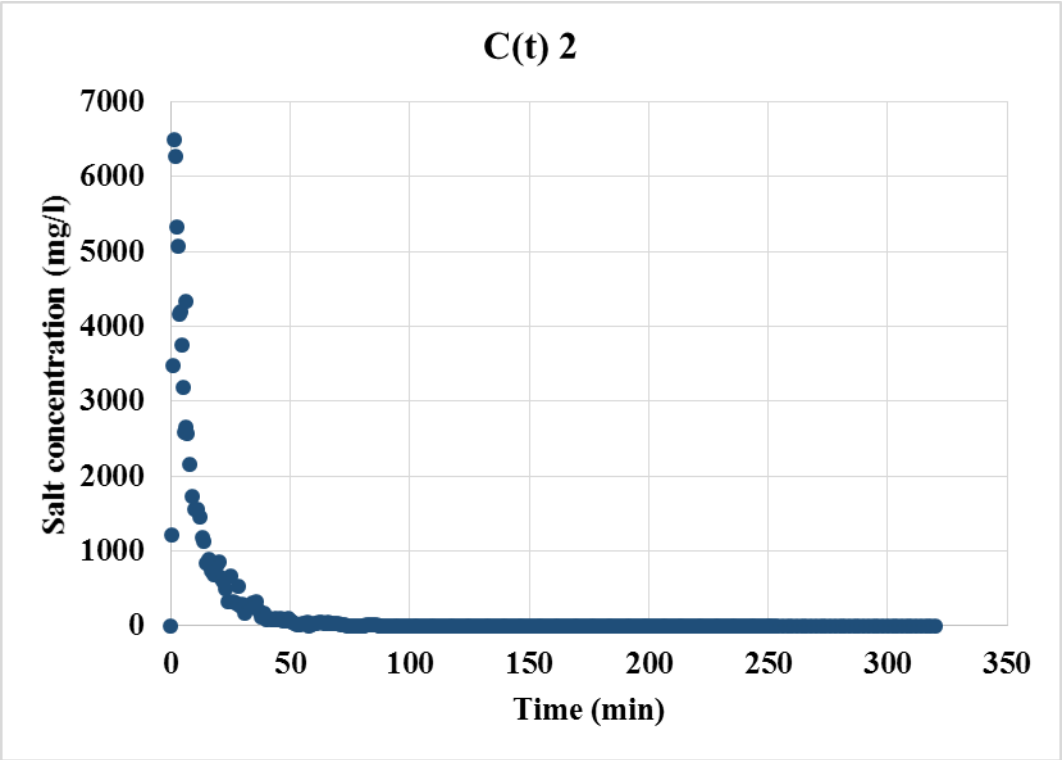

Figure VI. 11 Salt concentration from conductivity meter No.2

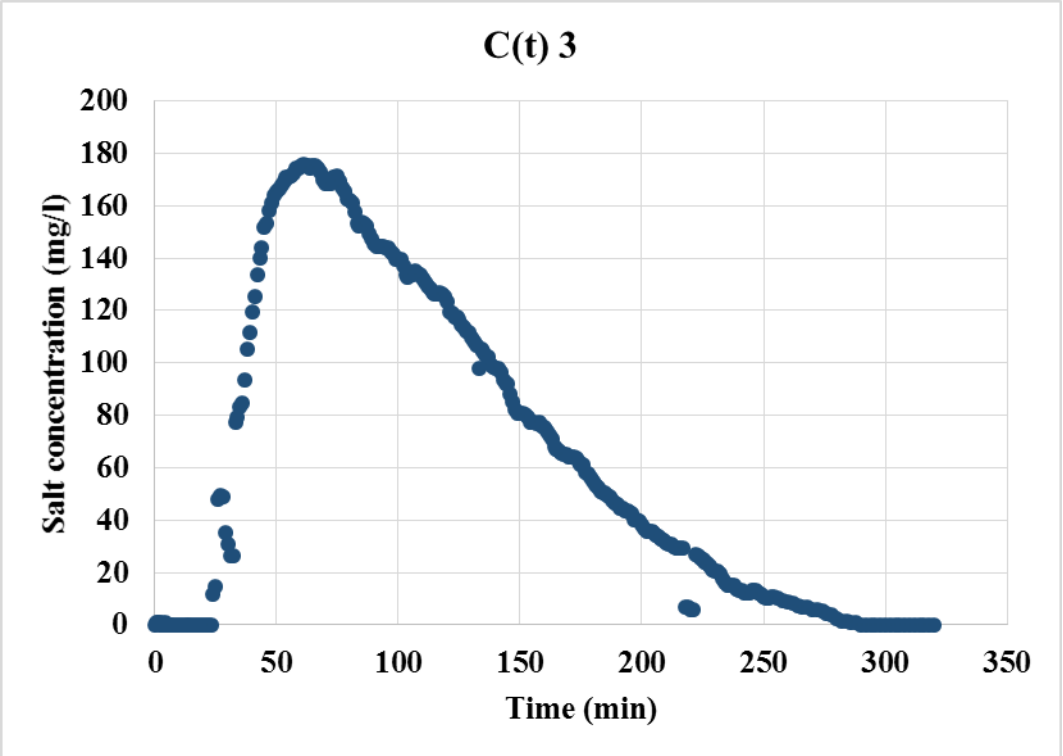

Figure VI. 12 Salt concentration from conductivity meter No.3

VITA

Miss Jittrapa Mongkolnauwarat was born on May 14th, 1991 in Bangkok, Thailand. Her academic background are listed as follow;

Bachelor degree: (B.Eng) Environmental Engineering, Faculty of Engineering, Chulalongkorn University, 2012

Master degree:(M.Sc) Environmental Management, Inter-Department of Hazardous Substance and Environmental Management, Graduate School, Chulalongkorn University, 2015